CHALMERS
UNIVERSITY OF TECHNOLOGY

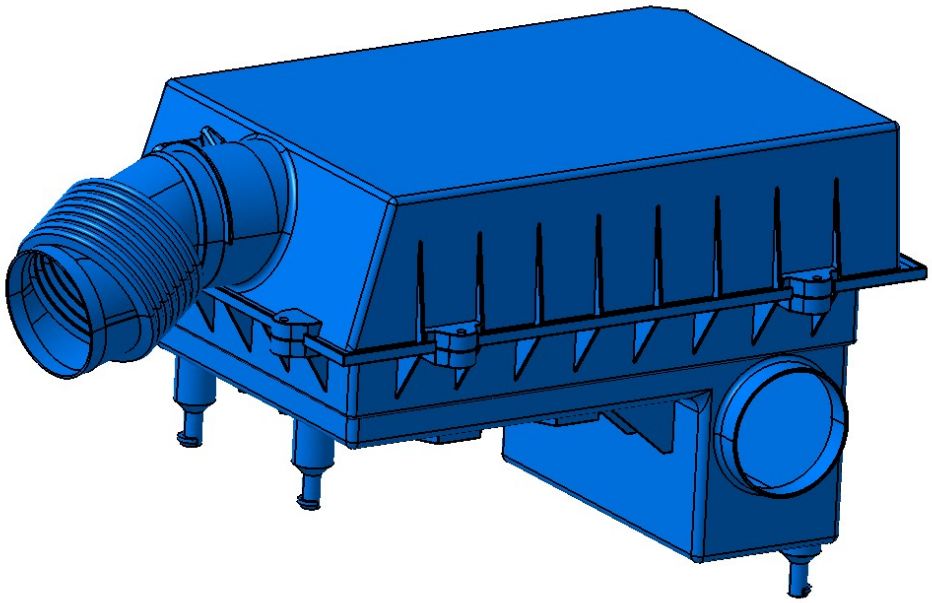

Design of air filter box and duct bellow for range extender engine in medium/heavy duty applications

Master's thesis in Product Development

LOUISE ANDERSSON
LINUS HERMANSSON

DEPARTMENT OF INDUSTRIAL AND MATERIALS SCIENCE
CHALMERS UNIVERSITY OF TECHNOLOGY
Gothenburg, Sweden 2023
www.chalmers.se

Master's thesis 2023

Design of air filter box and duct bellow for range extender engine in medium/heavy duty applications

LOUISE ANDERSSON
LINUS HERMANSSON

CHALMERS
UNIVERSITY OF TECHNOLOGY

Department of Industrial and Materials Science
Division of Product Development
Chalmers University of Technology
Gothenburg, Sweden 2023

Design of air filter box and duct bellow for range extender engine in medium/heavy duty applications

LOUISE ANDERSSON
LINUS HERMANSSON

Supervisor: System Responsible Petter Björsell, Aurobay
Supervisor: Group Manager Robert Mattans, Aurobay
Supervisor: PhD student Mohammad Arjomandi Rad, Product Development
Examiner: Professor Johan Malmqvist, Industrial and Materials Science

Master's Thesis 2023
Department of Industrial and Materials Science
Division of Product Development
Chalmers University of Technology
SE-412 96 Gothenburg
Telephone +46 31 772 1000

Cover: The final concept, a rectangular shaped air filter box with a flat filter, and a duct.

Typeset in LaTeX
(Gothenburg, Sweden 2023

Design of air filter box and duct bellow for range extender engine in medium/heavy duty applications

LOUISE ANDERSSON
LINUS HERMANSSON

Department of Industrial and Materials Science
Chalmers University of Technology

Abstract

This study focuses on designing an air filter box for REX (range extender) engine applications in medium/heavy duty trucks. The aim is to meet the technical requirements set by Aurobay and design an air filter box and duct bellow that fulfill the necessary criteria. The research questions addressed include identifying current designs and filters used in the automotive industry and establishing technical requirements. Along with exploring design possibilities, and evaluating how the new designs can meet and exceed expectations. By comparing existing designs, establishing requirements, and exploring design possibilities, this study provides a design for an air filter box and duct bellow that meet the requirements and can be produced. It also provides Aurobay with a foundation for future air filter box designs.

The study includes a literature review and benchmarking of existing air filter system designs in the automotive industry. Technical requirements are established through interviews, considering factors such as airflow, air quality, pressure drop, leakage, durability, and space constraints. CAD (Computer Aided Design) modeling and CFD (Computational Fluid Dynamics) simulations are conducted to evaluate the design parameters' impact. The results highlight the significance of inlet placement, inlet angle, guides, distance between the inner wall and filter, filter thickness, radius on the outlet, and inlet design on the air filter box's performance.

Two significant findings emerge from the study. The radius on the inlet and outlet are important factors that affects the UI (uniformity index) over the outlet and the air filter. Additionally, placing the bellows on the duct at a greater distance from the box improves uniformity over the MAF (mass flow sensor).

The recommended final concept is a rectangular air filter box with a flat-shaped filter. It incorporates a short duct bellow for cost benefits and the inlet is positioned near the top of the engine to create a shorter path for a dirty side duct. The air filter box is divided into two parts for optimal placement and replacement of the air filter and is securely fastened using screws. Hexagonal pattern ribs on the top lid and outer surface of the bottom part enhance structural integrity, while rounded corners and edges prioritize safety. The recommended concept fulfills the requirements and serves as a guide for Aurobay's future air filter box designs.

Keywords: Air filter box, air filter, duct bellow, limited space, CAD, CFD, REX

Acknowledgements

We would like to express our gratitude to everyone who has contributed to the completion of this master's thesis. A special thanks go to our supervisors at Aurobay, Group Manager Robert Mattans and System Responsible Petter Björsell, for their invaluable guidance, insights, and technical expertise. We would also like to extend our appreciation to our supervisor at Chalmers University of Technology, Ph.D. student Mohammad Arjomandi Rad, for his feedback and support throughout the master's thesis. Lastly, we would like to give special thanks to our examiner, Professor Johan Malmqvist, at the Department of Industrial and Materials Science, for his technical feedback and constructive criticism.

Louise Andersson & Linus Hermansson, Gothenburg, June 2023

Contents

List of Figures

List of Tables

List of Acronyms

Below is the list of acronyms that have been used throughout this thesis listed in alphabetical order:

AIS	Air Intake System
CAD	Computer Aided Design
CFD	Computational Fluid Dynamics
DHC	Dust Holding Capacity
FMEA	Failure Mode and Effects Analysis
ICE	Internal Combustion Engine
MAF	Mass Airflow Meter
NVH	Noise, Vibration, and Harshness
REX	Range Extender
RPN	Risk Priority Number
UI	Uniformity index

1
Introduction

In this chapter the background of the project will be presented, along with the aim, delimitations, reserach questions, and the outline of the report.

1.1 Background

Aurobay, a company that specializes in designing and producing engines for the automotive industry, is widening its potential customer base. As a result, applications beyond the regular scope of ICE (internal combustion engines) for passenger vehicles are becoming a possibility. Therefore, a study is needed to investigate a solution for an air filter box that can be utilized in REX (range extender) engine applications. Figure 1.1 depicts the initial stage of the AIS (air intake system), which includes an air filter box, an air filter, and a duct bellow.

Figure 1.1: Overview of a part of the AIS with the dirty side duct (1), air filter box (2), air filter (3), duct bellow (4), and Mass Airflow Meter (MAF) (5) [1]. With permission from Mann+Hummel.

The REX application differs from traditional car engines in terms of its usage as a large generator to charge a battery pack when additional energy is required. This approach enables the engine to operate at an optimized load, resulting in efficient consumption and reduced usage of the combustion engine. The vehicle is powered by the battery, while the combustion engine is used sparingly. The targeted applications for the REX are medium/heavy-duty trucks that operate in diverse environments, including construction sites where dust concentration levels are higher than those typically encountered by passenger cars.

The air filter box, which usually is located in the engine bay in front of the vehicle, takes the air from the atmosphere. The air is usually collected through high positioned ducts to avoid dirt and water from the outside environment. In the REX application, the engine will be installed in a box with a sub-frame which can be installed at a preferred location depending on the application, but still have the same geometry requirements. Usually, the air filter box is placed beside the engine in a car. However, for this REX application, the air filter box needs to be placed in the same sub-frame which creates a limited space constraint for the air filter box. The REX application can be placed wherever suits the customer, for this investigation, it would most likely not be placed in the front of the vehicle. This creates a new challenge to get fresh clean air into the filter box. The requested study should include a benchmark for air filter box options for the medium/heavy duty and construction sector to understand the design differences compared to light duty options.

The thesis involves establishing requirements for the air filter box and duct bellow, which give the company a deeper understanding for these components. Additionally, the thesis provides recommendations for air filter box and duct bellow designs for upcoming projects, helping the company understand the limitations that come with space constraints.

1.2 Aim

The aim of this project is to design and develop an air filter box, air filter, and duct bellow for use in dusty environments, optimized for the REX installation box. The project seeks to provide at least one concept that meets the new requirements and filters the air to a suitable level in the new working environment and placement. The design of the air filter box, air filter, and duct bellow solution also considers both cost and manufacturing feasibility.

1.3 Research questions

The research questions addressed in this thesis are important for the air filter design and are as follows:

- **What designs and different filters are currently used in the automotive industry?**
  To determine the most efficient air filter system designs currently in use, conducting a literature review and comparative benchmarking is necessary. This process helps to understand the standards of current filters and filter boxes.

- **What are the technical requirements for the designs of the air filter box and duct bellow?**
  In order to create a well performing air filter box and duct bellow, it is essential to establish specific requirements. These requirements encompass various aspects, including airflow. To investigate the required airflow, communication needs to be conducted with teams responsible for the affected components, such as the turbo team, who possess knowledge regarding the necessary airflow for turbocharging. Additionally, factors such as air quality after filtration, pressure drop, leakage, durability, and fit within space constraints needs to be established. To establish these requirements, a combination of internal interviews within Aurobay, external interviews, and the utilization of secondary data sources needs to be employed.

- **What design possibilities exist for the available space?**
  The available space comes with limitations on the possible designs. What are these limitations, and what possibilities for the design exist?

- **How can the new designs fulfill the requirements and exceed the desires?**
  The air filter box and duct bellow should consider all the factors mentioned above when creating the new design. How can the possibilities be utilized to fulfill the requirements?

1.4 Delimitations

- Since the master thesis is 30 ECTS, the project time is limited to five months.

- The study only considers materials that are currently in use for the air filter box and for the air filter and do not investigate the potential benefits or drawbacks of utilizing alternative materials.

- Physical testing of the air filter box and the duct bellow is not included. This would be too time consuming, and the flow rigs that need to be used are often booked.

- The design of the dirty side duct, through which the intake air enters the engine, is not included, but the theory and design guidelines related to it are explored. This is because the engine needs to be positioned according to the customer's requirements, necessitating custom made dirty side ducts for each engine placement.

1.5 Outline of report

This report consists of a theory section in Chapter 2 to give an insight into the AIS. Chapter 3 describes the research approach and the methods employed in the project. Thereafter, Chapter 4 presents the most significant findings from the literature review. This is followed by Chapter 5 which shows all the results from the project, including interview outcomes, requirement specifications, analysis of design possibilities, and the final design. Chapter 6 discusses the results from the previous chapter. Chapter 7 presents the project's conclusions and what future work that is recommended. Finally, the appendix is presented, which includes interviews, function-means trees, and the scaling for FMEA.

2

Structure of the air intake system

In this chapter a description of the AIS and its components will be provided. The way these components interact with each other will also be explained.

2.1 Air intake system description

The AIS, shown in Figure 2.1, starts with air entering through the dirty side duct and ends with the intake manifold. The "dirty side" consists of the dirty side duct and the bottom part of the air filter box. The dirty side duct serves as the entry point for the incoming air and prevents water and snow from entering the system. Next, the air flows into the air filter box and passes through the filter to the "clean side". Typically, a MAF (Mass Airflow Meter) is positioned at the outlet of the air filter box. At this stage, the air is clean and enters the duct below to reduce engine vibrations. Subsequently, it proceeds to a resonator, which reduces noise, before reaching the turbocharger.

The turbocharger compresses the air to high pressure, increasing its mass per unit volume. However, this also raises the air temperature. To decrease the temperature, either an air or water cooler is used. The water cooler uses a separate fluid to absorb the heat. The air is, at this point, cooled and high in pressure. The airflow is then controlled by a throttle which regulates the amount of air that enters the combustion chamber. Once the air passes through the throttle, it enters the intake manifold, where it is distributed to all cylinders and transferred to the combustion chamber. Inside the combustion chamber, the fuel is mixed with the cooled, compressed air and ignited by the spark plug. This initiates a combustion cycle that drives the engine and produces exhaust gas. A basic flow diagram of the system is illustrated in Figure 2.1 where the largest box (gray) includes the key components of this project.

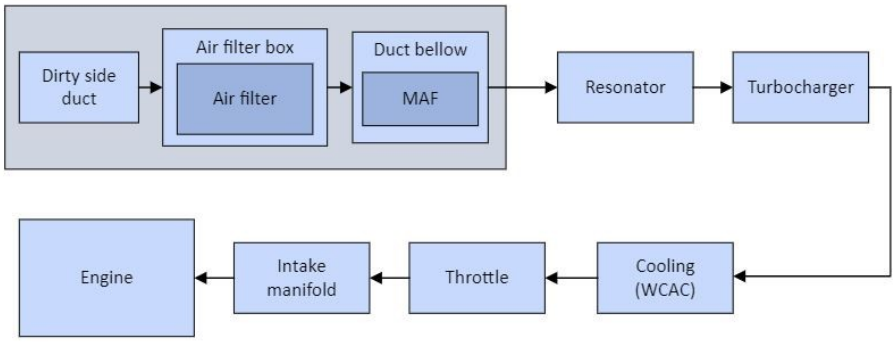

Figure 2.1: Flow diagram of the air passing through the system, from the dirty side duct to the combustion chamber.

2.2 Air intake system components

The components that are involved in the air getting into the system until it gets compressed are described below. This includes the dirty side duct, air filter box, air filter, duct bellow, MAF, resonator and turbocharger.

2.2.1 Dirty side duct

The dirty side duct serves as the entry point for the air into the engine. The dirty side duct transports the air from the environment into the air filter box. The primary purpose of the Dirty Side Duct is to prevent rain, water, and snow from entering the system [2]. An example of a dirty side duct is shown in Figure 1.1 as number (1).

2.2.2 Air filter box

The air filter box is a crucial component of an engine's AIS, providing a protective housing for the air filter and keeping it isolated from the external environment. It serves as a connection point between the Dirty Side Duct, the Air Filter, and the Duct Bellow. For optimal engine efficiency, the air filter box should ensure uniform air distribution and a minimal increase of pressure drop [3]. The air filter box not only affects engine efficiency, but also has an impact on the engine's NVH (Noise, Vibration, and Harshness) levels of the engine. An improperly designed or poorly maintained air filter box can result in increased engine NVH levels, negatively impacting the overall driving experience. Conversely, a well-designed and properly maintained air filter box can reduce NVH levels, contributing to a smoother and more comfortable driving experience. An example of an air filter box is shown as number (2) in Figure 1.1.

2.2.3 Air filter

Air filters play a critical role in engine systems, serving to protect the engine by removing dirt, dust, and other contaminants from incoming air [4]. In heavy duty

vehicles, air filters often consist of a paper element due to their high DHC (dust holding capacity) and ability to withstand sudden changes in air pressure [5]. Although air filters can be cleaned, excessive pressure during the cleaning process can enlarge the filter's pore size, diminishing its effectiveness. An example of an air filter is shown as number (3) in Figure 1.1.

2.2.4 Duct bellow

The duct bellow serves a dual purpose, both to transport the air and to reduce the vibrations that the intake air is causing. The structure of the duct bellow is made to absorb the vibrations. The duct bellow can be positioned either in front of the air filter box, on the dirty side, or after the air filter box, on the clean side [6]. An example of a duct bellow is shown as number 4 in Figure 1.1.

2.2.5 Mass airflow meter

The MAF is a sensor that measures the mass flow rate of air entering the engine. Its primary function is to detect variations in airflow, which may arise due to differences in density and viscosity [7]. An example of the placement of the MAF sensor is shown as number 4 in Figure 1.1. The placement is between the outlet of the air filter box and the duct bellow.

2.2.6 Resonator

The air that enters the engine generates noise. A resonator's main function is to reduce the sound levels of the intake air. A resonator creates an open space for the sound waves, resulting in a lower noise level [6].

2.2.7 Turbocharger

A turbocharger is usually located after the duct bellow in the AIS. Its primary function is to compress the air so that molecules of the oxygen gets more packed. An increase in air pressure makes it possible to add more fuel, resulting in an increase in the efficiency of the combustion engine [8].

3
Research approach

In this chapter the overall research approach is explained, providing information on why certain approaches were used and how they are related to each other. The approaches are divided into six different sections, Overall research approach, Information gathering, Information structuring, Concept development, Evaluation and Further development.

3.1 Overall research approach

Information gathering was first conducted, which included a literature review that utilized more than 25 different sources. Factors affecting performance, air filter configurations, pleat shapes, and previous work that optimized the designs for AIS were investigated. Next, a benchmarking study was conducted using A2MAC1 [9], a database that includes various car brands and allows for an investigation of certain components inside the cars. In this case, the air filter box, air filter, and duct bellow were analyzed. Additionally, two interviews with external experts were also conducted along with internal interviews. Furthermore, a study visit at Volvo Cars helped in gathering the information needed to establish a solid foundation for the mounting process.

The next step involved taking the gathered information and structuring it. Various approaches were used for structuring the information, function-means tree, requirement specification, and a design FMEA (Failure Mode and Effects Analysis). These methods facilitated a foundation of what to consider when designing the new air filter box, air filter, and duct bellow.

Once the information had been structured, the concept development phase began. This phase included identifying a suitable placement for the concept within the available space. Additionally, CAD models were prepared for conducting CFD simulations. These simulations were used to draw conclusions about various design parameters. The subsequent step involved the evaluation of concepts. Initially, CFD simulations were employed to evaluate individual design parameters. Next, it was decided to make a Pugh matrix to understand how the concepts performed relative to each other. After that two remaining concepts were compared using a Kesselring matrix to even further understand their advantages and to select a final concept. When the final concept had been selected, further development was made. This included attachment points, drainage, and structural integration, among other

design aspects. Furthermore, manufacturing feasibility and cost estimation were conducted. The layout of the approach is illustrated in Figure 3.1 where the dark blue boxes are the sections and the light blue boxes are subsections, performed in order following the arrows.

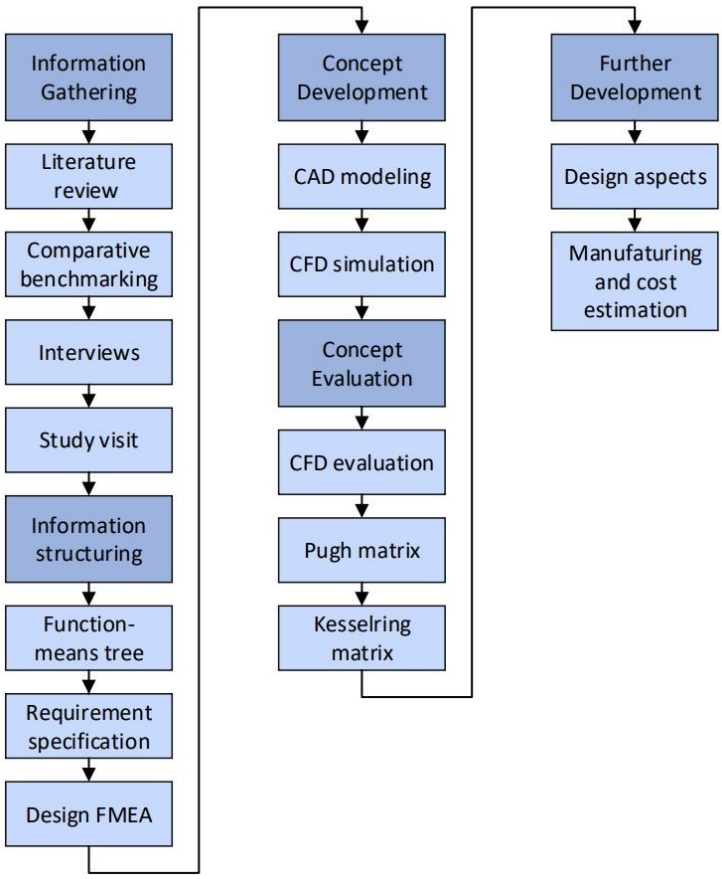

Figure 3.1: The process of the research approach.

3.2 Information gathering

In order to answer the research questions stated in Section 1.3, it was necessary to gather information on the relevant topics. Initially, a literature review was conducted to gain an understanding of the airflow field and the role that the air filter box, air filter, and duct bellow play in ensuring air quality. This literature review served as a foundation for understanding the essential requirements and the existing design options. Additionally, information was obtained through interviews conducted both internally within Aurobay and externally with experts in the field.

3.2.1 Literature review

Literature reviews could be described as a systematic way to collect and analyze previous research done on a specific topic. By conducting a well performed literature review, a great knowledge on the specific topic could be achieved. When using

multiple sources as a foundation, an overview of the area is gathered and could help the user find more relevant areas to investigate since further knowledge is achieved [10]. One of the most efficient ways to access published research is through digital sources. To optimize search results and enhance the relevance of literature, utilizing methods such as including keywords can be beneficial [11].

Google Scholar and Chalmers Library were utilized to find the sources used in the literature review. Literature reviews served as a tool to initially gain an understanding of the entire AIS. Once an overview had been gathered, more in depth research was conducted for each individual component. It started with an understanding of the function and purpose of each component within the AIS. Subsequently, benchmarking was performed to identify which designs existed for each component. To get an insight into which parameters affect the performance of the AIS, research papers that explored how these components could be optimized were reviewed. This examination allowed for an exploration to see how improvements could be made to the existing designs.

3.2.2 Benchmarking

Benchmarking is a method for investigating existing solutions and gaining insight into competitors' products on the market. By conducting benchmarking, companies can identify areas where their own products, system, or services could be improved. Depending on the project's focus, different types of benchmarking may be used.

This benchmarking research employed a technique to assess the performance and design parameters of air filter boxes, air filters, and duct bellows. A2MAC1, a database with numerous car models and their components, was used to benchmark how various car manufacturers had designed their AIS. A total of ten different cars were investigated. This analysis provided insights into which common solutions existed between car brands. Additionally, solutions for more heavy duty vehicles were also part of the benchmark, allowing for a comparison between trucks and cars, for example.

3.2.3 Interviews

The purpose of conducting interviews is to collect information on individuals' thoughts, beliefs, opinions, and experiences that cannot be observed or captured through other means. Interviews can be carried out face-to-face or online and serve as the primary data collection method. When formulating interview questions it is important to provide a structured framework that allows respondents to articulate their own interpretations using their preferred language. Interviews can be divided into different types, including structured, semi-structured, unstructured and informal conversational interviews. Structured interviews are easier to analyze and compare, while unstructured interviews are more suitable for exploratory studies. Six types of questions can be asked during interviews, including experience/behavior, opinion/belief, feeling, knowledge, sensory, and background/demographic [13].

Interviews during the thesis were conducted using various approaches. The most frequently employed method was through meetings and unstructured interviews internally at Aurobay. Aurobay has different departments for different systems, therefore, it was essential to gain an understanding of the requirements and needs for the respective departments. Discussions were held with relevant departments, such as the turbo team, simulation team, the project team that works with this engine and test engineers. Meetings and other means of communication such as E-mails were utilized for this purpose. External interviews were also conducted. One such interview was held with the former responsible for the air filter box at a car manufacturer, called "Expert 1" in this report. Two interviews with air filter box suppliers were also held, for this report they going to be referred as "Supplier 1" and "Supplier 2".

3.2.4 Study visit

A study visit was conducted at a Volvo Cars facility located in Gothenburg to gain firsthand insight into the installation process and to understand the function of the air filter box and duct bellow. This firsthand experience helped to enhance an understanding of the assembly process which would be difficult to obtain otherwise.

3.3 Information structuring

Once the information had been collected from the literature review, benchmarking, interviews, and the study visit, the information needed to be structured. This was achieved by creating a function-means tree in order to gain an understanding of the function of each part. Furthermore, the information obtained from the information gathering was synthesized to generate a requirement specification. Finally, the collected information helped to conduct a design FMEA.

3.3.1 Function-means tree

A product always has functions, some might not be as obvious as other functions. Function analysis is an approach to get an overview of the different components and their functions within a product. It involves breaking down the overall function of a product into smaller, more manageable sub functions [11].

A function-means tree was conducted in order to gain an overview of the different functions and their dependencies on the existing components. This analysis proved beneficial in providing an improved understanding of the system and giving guidance for the design of the air filter box, air filter, and duct bellow. The analysis initially focused on breaking down the air filter system, comprising of the dirty side duct, air filter box, air filter, and duct bellow. The function-means tree listed the various functions that an air filter system should fulfill and then identified the components that contribute to solving each function.

3.3.2 Requirement specification

The requirement specification is a method in the design and development process that involves documenting and analyzing the stakeholder's needs and expectations for a product, system, or service. The purpose of a requirement specification is to enable designers and product developers to meet the needs and expectations of the stakeholders. It helps to identify the necessary features and functions of the product, understand the user's needs, and the constraints that need to be considered. The outcome of requirement specification is documented in a specification document that serves as a reference point throughout the design and development process [14].

A requirement specification was created to gather the necessary requirements and desired attributes for the air filter, air filter box, and duct bellow. The categories in the requirement specification were created from a combination of inputs, including the literature review, external interviews and internal discussion within Aurobay. The specific data collected mainly originated from internal sources within different departments at the company. For instance, the data regarding the filter efficiency was provided by the turbo team.

3.3.3 Design FMEA

FMEA is a tool used by engineers in the design process to identify and mitigate potential failures before they occur. The primary objective of FMEA is to help improve the reliability and safety of products. The FMEA process typically involves a team of engineers and subject matter experts who analyze the potential severity, likelihood of occurrence, and likelihood of detecting it before it causes harm. Based on these factors, an RPN (risk priority number) is assigned to each failure mode, allowing the team to prioritize the most critical failure modes and develop strategies to prevent or mitigate them effectively [15].

One of the key benefits of using FMEA in the design process is the ability to identify potential failure modes early, enabling the development of more effective mitigation strategies. This may involve redesigning components, changing materials, or implementing additional safety measures. Additionally, involving a diverse team of experts in the FMEA process helps identify potential failure modes that may not be immediately apparent to individual engineers [15].

The FMEA methodology was employed to identify potential failures and associated risks associated to a new design for the air filter box, air filter, and duct bellow. The function and design intent was established for all three components. The design FMEA was based on earlier FMEA:s conducted on the AIS. The function analysis was employed to detect potential failure modes, their corresponding effects, and potential causes/mechanisms of failure. During the FMEA, a point scoring system was used to identify how severe the potential failure was, which is used at Aurobay.

3.4 Concept development

After the information had been structured, concepts were generated using CAD modeling. The CAD program was utilized to define the available space making it possible to create the concepts directly in the program. This approach proved to be time-saving since measuring the space would be time consuming because it had numerous uneven sections. Subsequently, CFD simulations were conducted to evaluate whether the generated concepts would meet the requirements for UI (uniformity index) and pressure drop specified in the requirement specification.

3.4.1 CAD modeling

CAD (Computer Aided Design) modeling is used to create a 3D model of a concept or idea. These models can range from a rather simple illustration to a more complex model. By creating a CAD model it is possible to test various functions, for instance, it allows for the evaluation of the model's weight and volume. [17].

In this project, Catia V5 [18] was utilized as the CAD tool. Initially, the CAD software was used to draw the available space for the air filter box and duct bellow. The drawn space served as a reference for developing concepts that could fit within the designed space. The concepts that were generated and designed consisted of three parts, the air filter box, the air filter, and the duct bellow.

3.4.2 CFD simulation

CFD (Computational Fluid Dynamics) simulation refers to the computational modeling of fluid flows using numerical methods. The CFD software employs computer algorithms to analyze and simulate the behavior of fluids, including liquids, gases, or mixtures, within different physical systems. The results of the simulation provide predictions for the behavior of the fluid flow, such as velocity, pressure, temperature, and other related parameters [19].

In order to compare different designs and verify that the concepts fulfilled the requirements, CFD simulations were conducted. The simulations aimed to assess various aspects, including pressure drop, UI over the filter and UI over the outlet (MAF sensor). Simulations were outsourced to the simulation department at Aurobay to verify that the concepts fulfilled the requirements. However, to compare the performance of different concepts against each other, simulations were also conducted by the project team. The simulation approach for both the project team and the simulation department at Aurobay is shown in Figure 3.2. For the CFD simulations, Ansys Discovery [20] was the simulation tool that was used by the project team. The CFD simulations were performed using the expected airflow for the REX engine. The resistance for the air filter was given by the simulation department.

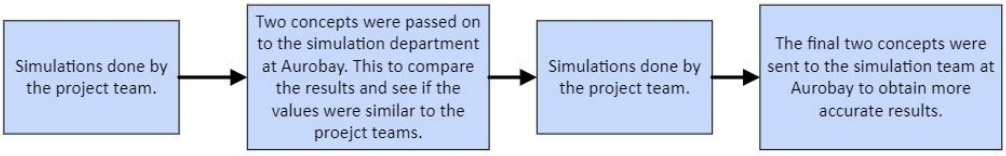

Figure 3.2: CFD simulation approach.

3.5 Concept evaluation

Evaluations of the concepts were conducted to find a final concept for the air filter box, air filter, and duct bellow. Evaluations of the results from CFD were used along with Pugh matrices to determine the areas where the concepts were superior and where they lacked in performance. Finally, the best performing concepts were evaluated in a Kesselring matrix.

3.5.1 CFD evaluation

Ansys Discovery was utilized as a CFD tool to evaluate adjustable parameters for the air filter box, air filter, and the duct bellow. The evaluations involved modifying a design parameter individually and testing various values for the selected parameter. The design parameters were evaluated based on pressure drop, UI over the MAF and UI over the filter. These evaluations were performed using an air filter box that fitted into the available space for the air filter box and the duct bellow. Following the testing of all design parameters, concepts with the most optimal design parameters were further developed.

3.5.2 Pugh matrix

The Pugh matrix is a technique to streamline the design process by eliminating less promising concepts and identifying the most suitable ones. The matrix involves comparing different concepts against each other based on user needs and requirements. To ensure a fair comparison, concepts are presented at the same level of detail, with a well-known existing product serving as a reference point. Each concept is rated based on how well it meets the selection criteria, resulting in a relative score that determines its ranking. Based on this ranking, decisions are made of the most suitable concepts for further consideration and development [11].

Pugh matrices were used to compare and evaluate the concepts against each other. The concepts were assessed using a "+" if they outperformed the baseline concept in fulfilling a criterion, a "-" if they performed worse, and a "0" if the two concepts were equal at fulfilling the criteria. The evaluation process included two separate Pugh matrices, one for evaluating flat filters and another for round/oval filters. Both matrices used the same criteria, the desires in the requirement specification. The Pugh matrices helped to identify the most suitable round/oval filter and the most suitable flat filter.

3.5.3 Kesselring matrix

The Kesselring matrix is a method utilized to assess and rank different solution proposals. It provides a more refined comparison than the Pugh matrix. The criteria for ranking can be similar to the Pugh matrix but with more detailed breakdowns. The weights for each criteria is determined through pairwise comparison, where all criteria are evaluated against each other to determine their relative importance. The scoring scale within the Kesselring matrix can vary based on the development team's needs. Once the criteria and corresponding scores are added to the matrix for each concept, the total score for each concept is calculated by multiplying the weights assigned to each criterion with the respective scores. The concepts can be improved and modified during the scoring process, and new rankings can be conducted accordingly [11].

The Kesselring matrix was utilized to make the final decision between the two remaining concepts. Prior to conducting the Kesselring, the two final concepts were sent to the simulation department at Aurobay. This step was taken to ensure a more accurate evaluation of the two final concepts, due to more detailed simulations. The Kesselring matrix utilized the same criteria as the Pugh matrices and assigned weighting grades on a 1 to 5 scale, which indicated the importance of each criterion. Each concept was evaluated on the same scale for every criterion and multiplied by its corresponding weighted value. Additionally, ideal values were determined by multiplying the criteria weight by 5. The total sum represented the maximum achievable value, indicating how well the concepts performed in relation to the criteria.

3.6 Further development

For further development, various design aspects, such as strength and safety, were taken into consideration. Additionally, an estimation of the concept's cost and feasibility was conducted.

3.6.1 Design aspects

The design aspects were obtained from the information gathering and information structuring. These were used as a foundation for the further development of the final concept. Aspects such as attachment points, drainage, structural integrity, and safety were included. There were also factors such as the connection between the air filter box and duct and the holder for the MAF sensor which were developed as well.

3.6.2 Manufacturing and cost estimation

The manufacturing feasibility and cost estimation of the final concept were conducted together with an individual referred to as "Expert 2" . "Expert 2" has experience in tool development and cost estimation.

4

Literature review

In this chapter, a literature review was conducted to explore and identify key factors related to the air filter, air filter box, and duct bellow. The review contains information about the filter performance and types, along with other studies which has been conducted to optimize the components.

4.1 Factors affecting the performance

This part of the literature review focused on two primary areas: filter performance and filter types.

4.1.1 Filter performance

The filter performance consists of several factors, including NVH level, filter efficiency, DHC (dust holding capacity), air restriction, pressure drop, filter environment & longevity, filter mechanisms, and filter area.

4.1.1.1 Noise, vibration, and harshness

The NVH is an important aspect of the automotive, as it directly influences the perceived quality of the vehicle's sound, vibration and comfort for the passenger. Creating a smooth and enjoyable driving experience requires designing an AIS that minimize the transmission of engine NVH into the passenger cabin. This can be achieved partially by placing the engine away from the passenger cabin, as in the case of some trucks. The AIS itself generates intake noise, usually below 600Hz, which is generated from the pipe radiation sound, surface radiation sound, and discharge noise. The noise from the intake system can contribute to 30% of the total noise of the entire vehicle [21].

4.1.1.2 Filter efficiency

The efficiency is determined by the filter's ability to pick up contaminates of a specific type or size [22]. It is influenced by several factors, including the size and type of contaminants, as well as the design and material of the filter itself.

Air filters can be designed to target specific types of contaminants, such as dust particles and other allergens. The filter's ability to remove contaminants depends on the filter material and its structure. For example, there are filters that have a

dense mesh of fine fibers to trap the particles, while other filters utilize electrostatic charges to attract and capture contaminants [23].

It is important to select an air filter with the appropriate efficiency for specific contaminants present in the air and also for the intended application. For example, high-efficiency filters could provide greater protection against specific contaminants, but they could result in increased pressure drop, which could reduce the efficiency in an engine's AIS [23].

4.1.1.3 Dust holding capacity

The capacity of a filter refers to the amount of contaminants it can absorb before becoming clogged and reducing the flow of air to an unacceptable level [22]. This capacity holds significant importance for air filters as it directly impacts the performance and longevity of the engine's AIS. When the air filter reaches its capacity for handling contaminants, the airflow gets restricted, leading to reduced engine performance. This restriction in airflow subsequently contributes to increased fuel consumption and reduced engine lifespan. Therefore it is crucial to select an air filter with an appropriate capacity that suits the specific operating condition. Factors such as the type and size of the contaminants, the environment in which the vehicle operates, and the frequency of filter replacement should all be taken into consideration [24].

In certain scenarios, high-capacity filters can be used to extend the time between filter replacements. However, in other situations, a lower-capacity filter with a finer mesh may be preferable. These filters provide a higher level of filtration, capturing smaller contaminants that could affect engine performance and efficiency. However, this also means that the filter will become clogged more quickly, leading to more frequent filter replacements. The DHC of a filter is directly related to the surface area of the filter paper. A filter with a larger surface area could handle more dust without the filter clogging [25].

4.1.1.4 Air restriction

According to the ISO 5011 standard, restriction is defined as, "static pressure measured immediately downstream of the unit under test" [27]. The restriction imposed on the airflow within the air filter system is a result of the combined effect of all its components. The primary sources of restriction in the AIS are the dirty side duct and form of the air filter box, rather than the air filter itself [28].

4.1.1.5 Pressure drop

The AIS of an engine has a vital role in supplying clean air to the engine, ensuring the appropriate pressure, density, and temperature. However, pressure drop is an undesirable occurrence that can happen to the air as it travels through the AIS toward the turbocharger. The extent of pressure drop is influenced by several

variables, such as the dust environment the vehicle operates in, the level of contamination on the filter elements, the type of filter and the air path. Pressure drop has a negative effect on the power of the engine, the fuel consumption and the airflow [24].

4.1.1.6 Filters longevity & environment

It is not recommended to clean an air filter, as it can reduce the filter's capacity by 20-40% [26]. Instead, it may be more cost-effective to choose a filter with a longer lifespan.

The particle size of dust on commercial roads generally falls within the range of 2-10 μm, while on construction sites, the particle size can be larger than 50 μm. The dust concentration on construction sites can vary, ranging from 0.001 to 10 grams per cubic meter [4].

4.1.1.7 Filter area

The filter area is inversely proportional to the pressure drop. Increasing the filter area for a given flow rate leads to a reduction in pressure drop. This is because the load of airflow per unit of the filter decreases when the filter area is increased. In order to determine the optimum surface area of the filter, two important parameters need to be defined: the required flow rate and the requirement for pressure drop [31]. Therefore, the filter shape should be dimensioned to have a large surface area since this lets more air in [32].

4.1.2 Air filters designs

In this section, the design and performance of air filters are presented, focusing on the configuration of filter media and the type of air filter media.

4.1.2.1 Configuration of filter media

Air filter media shapes can be broadly categorized into two types: pleated filters and non-pleated filters. Pleated filters, made from pleated impregnated paper, are one of the simplest types of air filters. They offer a large surface area and provide structural support due to the pleats [23]. In comparison to non-pleated filters, pleated air filters are generally more effective at capturing small particles [36].

By pleating or corrugating the paper, the surface area of the filter can be increased compared to non-pleated filters. These types of patterns are shown in Figure 4.1a and Figure 4.1b. As the incoming air passes through the filter, dust particles either stick to the filter's outer surface or settle to the bottom of the filter casing. These filters are most effective when flow rates are moderate, and it is recommended to maintain a pressure drop between 0.1-0.3 bar [36].

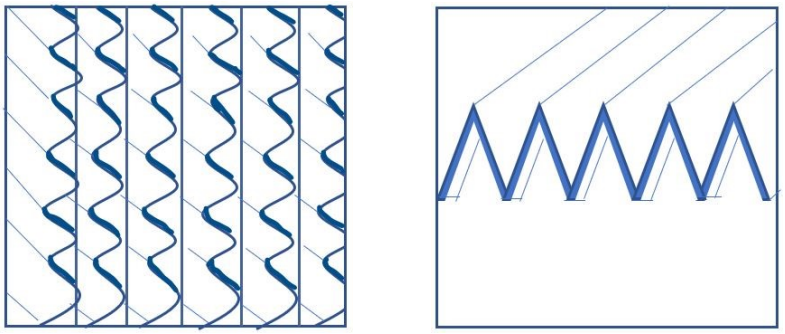

(a) Illustration of corrugating pattern

(b) Illustration of pleated pattern

Figure 4.1: Common pleat configurations [37].

4.1.2.2 Type of Air Filter Media

The most common filter media is paper since the material is cost-effective. However, paper filters are not suitable for dusty environments and require regular replacement. Another filter media is gauze filters, which has a longer lifespan compared to paper filters and can be cleaned. Foam filter is another filter media, but are typically for small engines. However, it is common to use foam wraps as an extra protection over the filter. This solution is both cost-effective and suitable for dusty environments [38].

For light duty applications, felt elements can serve as a suitable alternative to impregnated paper with similar capabilities. However, it usually requires wire mesh or other reinforcements to handle pressures of 7 bar [31]. Pleated paper filters, on the other hand, can withstand pressure without reinforcement. However, both types of filters may fail under higher pressure conditions. Fabric filters, which can be either woven or non-woven, can have significantly different designs than the pleated form. Heavy duty vehicles typically use fabric filters as they offer higher performance and durability compared to paper filters [31].

4.2 Previous work in design optimization

This section presents literature relevant to the optimization of parts design, including the air filter box, air filter, and duct bellow.

4.2.1 Duct bellow

NVH generated by the turbocharger is transferred to the beginning of the intake system. Therefore, a duct bellow is used to reduce the vibrations in the intake system and handle the engine movement. Depending on multiple of parameters, the duct bellow can be optimized for different purposes. The geometry of the duct bellow is specifically designed to absorb vibrations and improve the NVH performance for

the AIS [42].

Jung, H et al. [42] conducted an investigation into the optimal design parameters for the NVH performance of a duct bellow. The researchers examined eight different parameters, which are shown in Figure 4.2. Each parameter had either two or three different values. In total, 18 different duct bellow designs were simulated to analyze the NVH level. Among the parameters studied, the thickness of the hose performed most effectively at the thickest value tested, which was 3 mm. The optimal diameter of the hose was 70 mm, which was the middle of the values tested. Regarding the bellow's width and pitch, the optimal values were found at the highest value tested. In contrast to the width and pitch of the bellows, the gap between the bellows and the bottom width showed the opposite trend. The lowest value tested for the gap between the bellows was found to be the most favorable. These values were optimal to reduce NVH levels, however, Jung, H et al. also mentioned that there are more conditions to consider. Factors such as pressure drop and the space available in the target vehicle need to be considered.

Control Parameters	
A	Bellows Position
B	Thickness of Hose
C	Diameter of Hose
D	R Factor
E	Bellows Pitch
F	Bellows Top Width
G	Bellows Bottom Width
H	Bellows Number

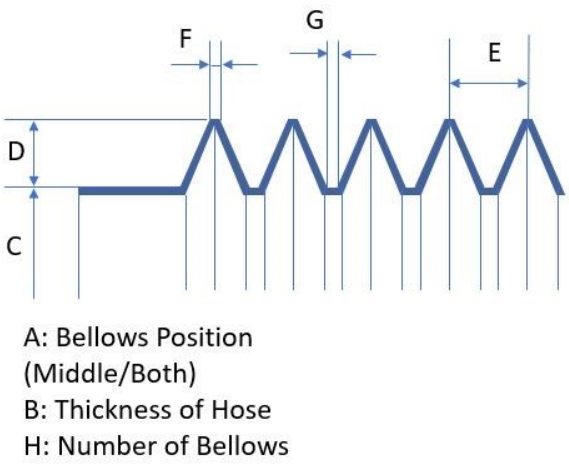

Figure 4.2: Parameters tested in [42] experiment.

Song, H et al. [43] conducted a study focusing on the effect of different parameters on pressure drop and velocity in the duct bellow. Their research aimed to minimize the losses when using a duct bellow. The study investigated the impact of two parameters on a duct bellow, the width of the bellows and the number of bellows. The simulations were performed under a single set of conditions which were tested on six different cases. The simulations conducted by Song, H et al. showed that the pressure drop increased with the number of bellows and a longer bellow width was shown to decrease the pressure drop. The width of the bellows had a greater influence on the pressure drop when more bellows were used. Regarding velocity, the bellows with the longer width had a more stable flow compared to thinner bellows. The number of bellows had a significant influence on the flow, an increasing number of bellows created a more centralized and unstable flow. A higher number of bellows made the duct bellow became more sensitive to the width of the bellows.

4.2.1.1 Restriction in the duct design

Any time the direction changes in an airflow path, it can lead to an increase in pressure drop which contributes to restriction of the system. While it is not always possible to avoid direction changes, minimizing them can significantly reduce restrictions. One example that can help illustrate restriction is blowing up a balloon with a straw. If the straw has a bend in it, it creates resistance and makes it more difficult to blow air into the balloon. Similarly, changes in the direction of airflow within a duct result in increased pressure drop and restriction, similar to the bend in the straw hindering the airflow. By reducing direction changes, similar to straightening the bend in the straw, the restriction in the intake system can be reduced, thereby enhancing its performance [33].

To ensure smooth changes in the direction of the airflow within a duct, ducts with a larger radius are preferred instead of sharp bends. According to Donaldson [33], a global manufacturer of filtration systems, a 30 degree bend has the least impact on restriction, while a 90 degree bend causes a significant increase in restriction. Even straight ducts can introduce some level of restriction. Additionally, straight ducts with a cut-off end can create greater restriction compared to ducts with a flared inlet. An illustration of the angles and flare is shown in Figure 4.3.

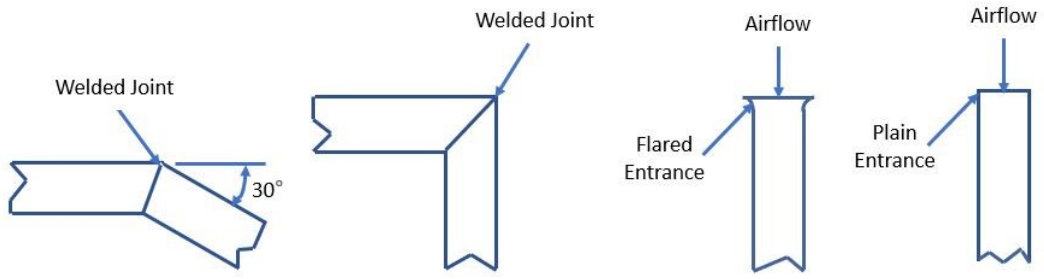

(a) 30 degrees angle **(b)** 90 degree angle **(c)** Flared entrance **(d)** Plain entrance

Figure 4.3: Illustration of duct configurations.

The length of a duct, along with its diameter, also contributes to the restriction. Donaldson has a graph that helps calculate the restriction based on the diameter of the duct and the length of a straight duct. To make the airflow rate stronger through the duct, it is recommended to have a larger diameter and maintain that diameter consistently throughout the system [33]. When two flows connect, the same principle as for the bends of the duct could be applied. In other words, the bend should be 30 degrees rather than 90 degrees to avoid turbulence. Additionally, it is important to ensure that the flows merge in the same direction [34].

4.2.2 Placement of inlet on cylindrical air filter box

Song, X et al. [44] explored the design and optimization of the air filter box for heavy-duty trucks. The main focus of the design optimization was to reduce the pressure drop and the deformation of the air filter. The filter used in the study was a pleated cylindrical air filter. To optimize the design, the study investigated the effects of different inlet positions. The tested positions are shown in Figure 4.4. Simulations showed that the optimal position is slightly below the center of the filter box. The position, shown in 4.4d, had the lowest pressure drop among the five tested intake positions. Additionally, it showed the lowest deformation in terms of both maximum and average deformation of the filter.

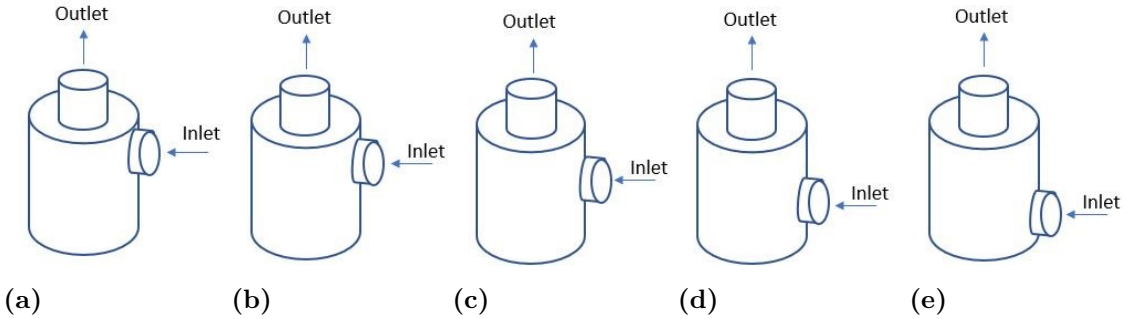

Figure 4.4: Tested inlet positions of a round air filter box with a round filter [44].

4.2.3 Air filter

The information found about air filter optimization is presented below and includes the difference between using cylindrical and flat pleated air filters.

4.2.3.1 Pleated shapes

Researchers S. Allam and A.M. Elsaid [39] conducted an investigation on different pleat shapes for air filters. These shapes included Flat-shaped, Sin-shaped, and V-shaped pleats, which are shown in Figure 4.5. The researchers varied several parameters during their investigation, including pleat spacing, pleat height, pleat shape, and filter medium thickness, among others. The study findings indicated that the sin wave-pleated air filter outperformed both the V-shaped and Flat-shape pleated filters in terms of lower pressure drop.

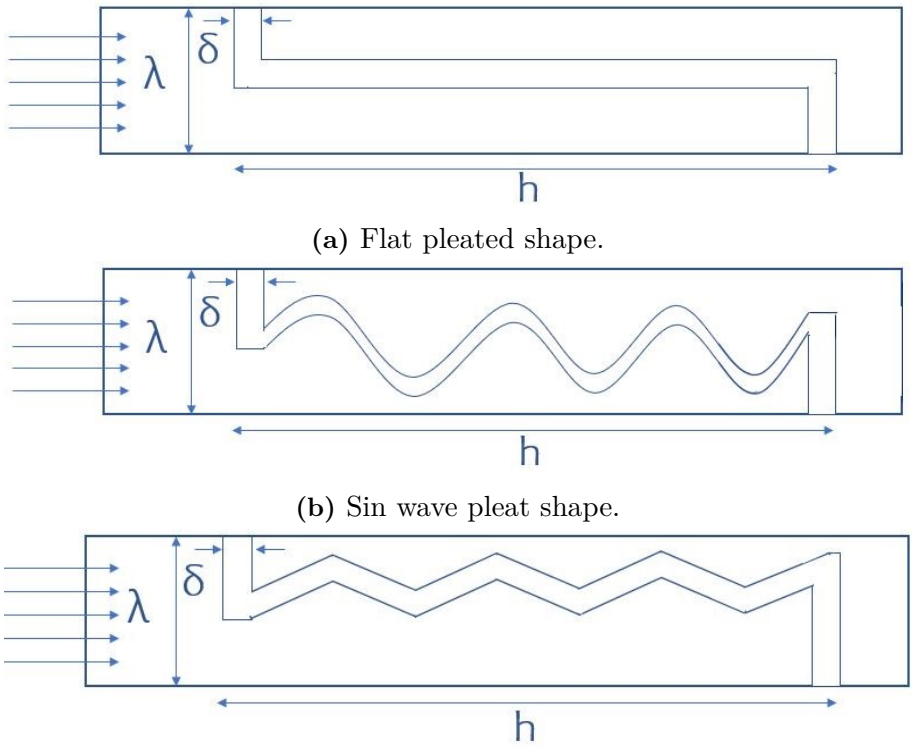

(a) Flat pleated shape.

(b) Sin wave pleat shape.

(c) V-pleat shape.

Figure 4.5: Three different pleat shapes: (a) Flat pleated shape, (b) Sin wave pleat shape, and (c) V pleated shape [39].

The article [40] conducted a test to compare the difference between V-shaped and U-shaped pleats and their impact on pressure drop, as illustrated in Figure 4.6. The study found that the V-shape pleats have an improved deposition of dust particles. However, it was observed that the bottom corner of the V-shaped pleats had an ineffective area since dust tends to be stored there. In terms of pressure drop, the study concluded that the U-shaped pleats outperformed the V-shaped pleats.

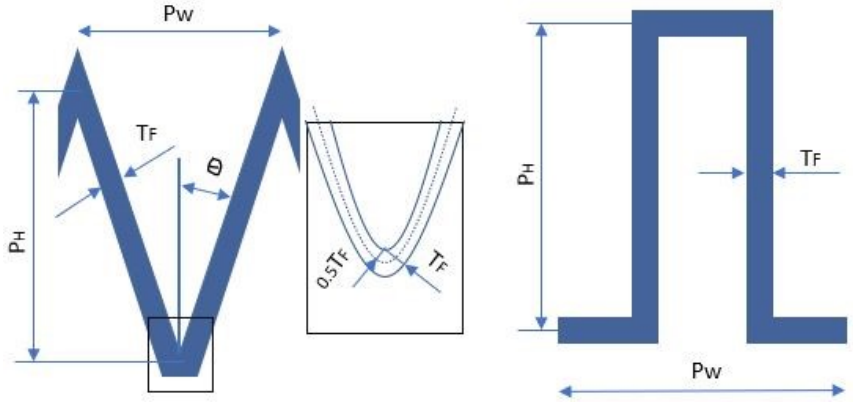

Figure 4.6: V- and U-shaped pleats.

Kang, J.-H et al. [41] utilized linear acoustic theory to evaluate the effectiveness of various air filter designs in terms of transmission loss. The research focused on flat air filters and employed linear acoustic theory to determine which designs exhibited superior performance. Several factors were taken into consideration, including the number of pleats, the length of the filter with plates, and the spacing between the pleats. The findings indicate that the design with few and longer pleats that offer high resistance achieved the best acoustical results.

4.2.3.2 Cylindrical vs flat pleated air filters

Saleh et al. [46] present a two-dimensional model for predicting the pressure drop and collection efficiency of circular pleated filters over time. The model uses average velocity profiles to estimate the flow field inside the filter and incorporates a dust-cake profile that grows as particles are collected. The model provides fast and approximate predictions, making it useful for the design and development of circular pleated filters. The study focuses on comparing the performance of circular pleated filters to their flat counterparts and explores the effects of geometric parameters on filtration performance. An illustration of the circular- and flat pleated filter is shown in Figure 4.7. The model is validated against computational fluid dynamics (CFD) simulations. The paper discusses the influence of pleat angle and inlet-to-outlet diameter ratio on particle deposition and cake formation inside the pleat channels.

The study's findings revealed that circular pleated filters with a larger inlet-to-outlet diameter experienced less pressure drop compared to their flat filter counterparts. This phenomenon occurs because when the inlet-to-outlet diameter is greater, the particles tend to penetrate deeper into the pleats, forming a thin layer of dust near the entrance of the pleats [46].

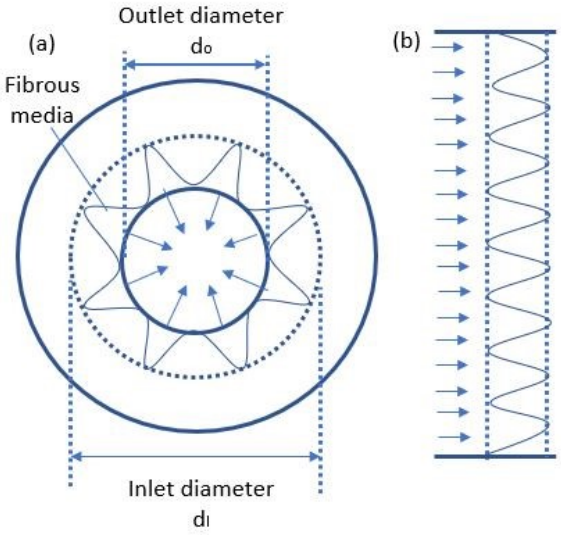

Figure 4.7: Circular pleated and flat pleated filter [46].

4.2.3.3 Cylindrical air filter

Song, X et al. [44] conducted an experiment to investigate the influence of the length of the cylindrical air filter and the number of pleats on both pressure drop and deformation of the air filter. The number of pleats varied from 60 to 100 and the pleat height varied from 250 mm to 300 mm. The results showed that increasing the number of pleats and filter height led to an increase in pressure drop, in a nonlinear way. The pressure drop increased significantly when the number of pleats exceeded 80. If only pressure drop was taken into consideration, both the number of pleats and the length of the filter would be as low as possible. However, this would mean that the filter area would become very small and therefore affect the volume of air in the engine. On the other hand, a high number of pleats and an increased filter length would make the filter more prone to deformation, negatively impacting the service life. The optimized design for pressure drop and minimized deformation was to reduce the number of pleats from 80 to 70 and reduce the length of the filter from 277 mm to 267 mm.

4.2.3.4 Flat air filter

Maddineni, A, K et al. [47] conducted tests to examine the impact several air filter parameters had on pressure drop. Firstly, different heights and pitches for the pleats were tested. The experiments showed that for the lowest height, 10 mm, the pressure drop decreased until the pitch reached 3 mm, but then it increased. For a height of 20 mm, the optimal pitch for pressure drop was between 3.5 mm and 4.5 mm, values below and above this range resulted in a higher pressure drop. For a height of 30 mm, the optimal pitch value was 4.5 mm. Thereafter, Maddineni, A, K et al. investigated how the inlet velocity influenced the pressure drop at different pleat pitches. The results showed that the optimal pleat pitch was 3 mm at the three different velocities that were tested, 1m/s, 2.5 m/s and 5m/s. However, the pleat pitch was less influential on the lower velocity compared to the higher ones. The final experiment was to investigate the impact of different pitch radius with various velocities on pressure drop. At a low velocity, the radius had minimal effect. As the velocity increased, it was observed that a higher pleat radius led to increased pressure drop.

The velocity distribution for different scenarios was also investigated. Firstly, how the pleat pitch affected the velocity at the top, flank and bottom of the filter pitch. The test used a pleat pitch of 2.5 mm and 5.5 mm. It was found that a low pleat pitch had a low velocity that approached the filter media due to the high filter surface. Additionally, the low pleat pitch also resulted in a non-uniform velocity distribution within the pleats. As expected, the velocity decreased as the airflow through the filter, with the lowest velocity at the bottom of the filter. Furthermore, the simulation also showed that a higher pleat pitch led to a lower velocity loss within the filter media compared to the lower pleat pitches [47].

In the study, experiments were also conducted to examine how different pleat heights affected the velocity. Higher pleats resulted in that the approaching velocity being

lower due to the increased pleat area. This effect became more pronounced at lower pleat pitches, which also increased the pleat area. The velocity was also influenced by the pleat radius, and the experiment showed that the velocity was higher at a smaller pleat radius. This can be due to that the pleats were more narrow which caused an acceleration of the airflow in the pleat channels [47].

4.3 Benchmarking

This section presents the benchmark of existing air filters, the surface area, filter efficiency, and longevity along other aspects.

4.3.1 Mann+Hummel air filter

Mann+Hummel has developed an air filter for heavy duty vehicles that is designed to fit in tight spaces. The filter design, shown in Figure 4.8, is thin while still providing a filtration surface area of 5700 $cm^2/(m^3/min)$. The airflow direction is from the outside of the filter to the inside. The filter has a volume flow of 8.8 m/s on the clean side. According to Rieger, M et al. would a round filter, that has the same filtration surface area, have to increase the height with 60% [48].

Figure 4.8: Mann+Hummel air filter for heavy duty trucks in tight spaces [48].

To maximize the service life and still perform well in terms of pressure drop, the airflow should follow a longitudinal axis along the filter elements. In the designed air filter by Mann+Hummel, the airflow is directed towards the end of the filter to achieve an even distribution of air in the filter. This offers several benefits. Firstly, it results in a low airflow velocity that is distributed evenly. Secondly, the dirt will be evenly distributed across the filter. These two benefits contribute to increasing the service life of the filter [48].

4.3.2 Volvo Trucks genuine air filter

Volvo Trucks uses pleated filter media with frames at the ends which is embedded in Polyurethane (PUR) foam to support the air cleaner housing elements. To handle the force generated by the airflow, an additional plastic tube is employed for extra support. The Volvo genuine air filter has a service interval of 2 years. However, there is no available data on how the filter efficiency is affected after this time period. The filter should either be replaced after 2 years or when the dashboard in the truck indicates that it should be changed. A new genuine filter from Volvo

has a filter efficiency of 99.9% which almost reaches 100% efficiency after collecting dust during use. The air filter should not be cleaned since this damages the filter. To maintain the dust capacity, the filter element has glue beads to ensure proper spacing between media pleats. The air filter area can reach up to 17.5 m^2. The filter paper is fixed with the help of adhesive strings placed on the outer case, which prevent the paper from folding when vibration occurs. The filter paper is fire resistant and Volvo uses Polyurethane as sealing for the air filter. The use of glue lines enhances the design's robustness, minimizing the impact of vibrations [25].

4.3.3 Pall Corporation filter

Pall Corporation, a filtration provider, has introduced a new design for hydraulic filters. Instead of using a traditional V-shaped pleat design, as shown in Figure 4.9a, a curved structure is utilized, as shown in Figure 4.9b [49]. The primary objective behind this new design is to increase the surface area. By reducing the gap in the middle of the cylinder while maintaining the same outer diameter, the curved structure achieves a larger filtration area. The V-pleated element has higher flow resistance at the top of the pleats, resulting in uneven dirt loading which could lead to shorter service life of the filter. In contrast, the curved-pleated element provides uniform resistance throughout the pleats, making the dirt loading uniform and extending the service life [49]. However, the curved-pleated design does result in a slightly higher pressure drop than the V-pleated design. This could be compensated with the larger surface area. The flow distribution for the V-pleated and curved-pleated shapes are also illustrated in Figures 4.9a and 4.9b [49].

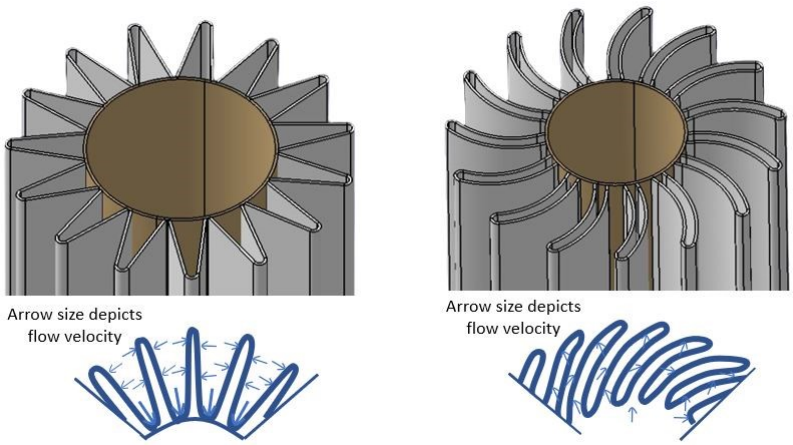

(a) V-pleat shape [49] **(b)** Curved-pleat shape [49]

Figure 4.9: V-pleated design, curved-pleated design, and flow distribution of both designs.

4.4 Conclusion of literature review

The literature review started with information about various factors influencing filter performance. Regarding NVH, it was found that minimizing NVH is desirable to avoid disturbance to the surroundings and passengers. Additionally, it was found that the AIS had a significant impact on the overall noise level of the vehicle. Understanding filter efficiency provided insights into how it is measured. Furthermore, it gave insights into the capacity of different filters to handle contaminants based on their structure and the trade-off between higher efficiency and lower pressure drop. The measurement of DHC is also explained, along with potential airflow restriction caused by the air filter becoming clogged, affecting the performance of the vehicle. The difference between high-capacity filters and low-capacity filter were also investigated. Another parameter that was investigated was the air restriction, revealing that most restriction is caused by the dirty side duct and air filter box, rather than the air filter itself. Pressure drop was contributed by all components, and it has a negative effect on the performance of the vehicle. The longevity of the filter depends on both the operating environment and whether the air filter is cleaned or not. It was recommended to select a filter with a longer life span rather than trying to clean it, as cleaning could harm the filter. The particle size for a general construction site was also found. Moreover, it was found that the filter area is affecting the pressure drop and that a larger surface area is preferred to allow an even distribution of air passing through the filter.

Regarding air filter materials, the literature review indicated that paper filters are the cheapest. However, they need to be changed regularly when operating in dustier environments. Vehicle operating in high dust concentrating environments are typically using fabric filter since the performance and durability is superior.

The previous research on the design optimization for the duct bellow focused on two main aspects, NVH and pressure drop. The findings showed that optimizing the bellows design involved a trade-off between these two factors. A design with smaller and shorter bellows results in lower pressure drop while a larger and longer bellows design would be preferable for NVH. Furthermore, it was found that the duct design could be modified to minimize air restrictions. The optimal design would be to have the duct straight with a flared end. However, if the duct needs to be angled, the best constellation would be to have the duct angle of 30 degrees.

The study on circular air filter boxes investigated the optimal positions for the inlet and outlet in terms of pressure drop and filter deformation. The findings indicated that the best position for the inlet was slightly below the center of the filter box when the inlet was placed on the side and the outlet was placed on the top of the filter box.

Optimizing air filters involves various factors and considerations. One study found that pleating the filter offers a larger surface area compared to non-pleated filters. They are also generally more efficient in capturing small particles. These filters are most efficient when the airflow rate is moderate. The pleated shape also affects the

performance of the air filter. It was found that V-shaped pleats have a uniform deposition of particles, while U-shaped pleats caused lower pressure drop. A study found that circular pleated filters that had a high inlet-to-outlet diameter had less pressure drop compared to the flat filter equivalent. Furthermore, a study about cylindrical air filters found that the number of pleats and the filter length affected the pressure drop and deformation. A higher number of pleats and an increased length of the filter would lead to easier deformation and decrease the longevity of the filters. The impact of pleat height on velocity was investigated as well. It was found that higher pleats result in lower approaching velocity due to the increased pleat area. The velocity was also depending on the pleat radius, smaller radius resulted in higher velocity.

During the benchmarking, the air filters examined had a filter efficiency of around 98-99.9%. Glue was commonly used in filters to strengthen the filter pleats to protect against deformation and maintain the DHC. Additionally, the glue beads ensure that the media pleats proper spacing. It was found that an oval filter would be beneficial when it comes to saving space since the height could be lower without sacrificing the surface area. Another design feature that can improve the surface area of air filters is to use curved pleats instead of V-pleats. The V-pleated air filters were found to have an uneven distribution of dirt as mentioned in 4.2.3.1 while the curved design is superior in this aspect. However, the curved design creates a slightly increased pressure drop.

5

Results

This section provides the results from the benchmarking, interviews, study visits, detailed study of Volvo Cars' air filter box, function-means tree analysis, requirement specification, and design FMEA. Along with CAD modeling, CFD simulation, Pugh and Kesselring matrices, further development stages, the final concept, manufacturing considerations, cost estimation, and verification of requirements.

5.1 Benchmarking

The findings from the benchmark provided a guideline for what customers could expect regarding the performance of the air filter box, duct bellow, and air filter. The study found that customers could expect the air filter to have a filter efficiency ranging from 98-99.9%. Additionally, it was also found that the air filter needs to be protected from snow and water. This could be achieved by either applying glue to protect the pleats or positioning the air filter higher up in the air filter box so that water and snow cannot reach it.

By investigating the different AIS, using the database A2MAC1, it was found that most air filter boxes, air filters, and duct bellows followed the same principles, these principles are listed in Table 5.1.

It was observed that 90% of the investigated air filters were placed horizontally. Furthermore, the placement of the air filter box was relatively close to the resonator for all investigated AIS:s. For the duct bellow, 90% of the AIS:s placed it between the air filter box and the resonator, with one placed before the air filter box. Notably, all of the bellows on the ducts were placed on a straight part of the duct. 90% of the air filter boxes had a flat filter and 10% had a round filter. Additionally, all of the air filter boxes had drainage holes in the bottom of the box. The air filter boxes were also strengthened with ribs, 100% had ribs on the outside of the box and 80% had ribs inside the box.

Table 5.1: Most common ways to orientate the air filter box, air filter, and duct bellow.

Principle (Most common)	
Placement of filter	Horizontally
Placement of filter box	Close to resonator
Placement of duct bellow	Connected to resonator and air filter box
Placement of bellows	Not placed on curved surfaces
Type of filter	Flat
Drainage	Holes in the bottom of box
Durability	Ribs for extra strength

Furthermore, it was found that filters are customized to fit inside the air filter box, as the air filter boxes themselves are customized to fit in the available space. The length of the ducts was primarily adjusted based on the distance to the resonator. In a few instances, a net was placed on the clean side right before the MAF sensor.

5.2 Interviews

Based on the interviews, it was determined that the noise level generated by the filter box is dependent on its size; a larger filter box results in less noise. Additionally, a larger box is necessary to prevent snow and water from making the air filter wet. As discussed in Section 5.1, the air filter should be placed out of reach of water and snow. Furthermore, the dirty side duct could be installed at a higher position to prevent dust from the ground from entering the system and to minimize the amount of water and snow that can enter it.

According to "Expert 1", round filters are more expensive than flat filters but offer a larger surface area in proportion to the space they occupy. "Supplier 1" explains that the size of the filter is determined by the requirements of DHC and the airflow. Additionally, "Supplier 1" notes that for round filters, airflow can occur in both directions, from the outside to the inside and vice versa, visualized in Figure 5.1. However, if the airflow is directed from the inside to the outside, the DHC is 15% lower. By allowing airflow from the outside, the filter's area is also larger. DHC is estimated by conducting a dust test, the filter is weighed before and after the test, and the test is finished when the allowed pressure drop is reached.

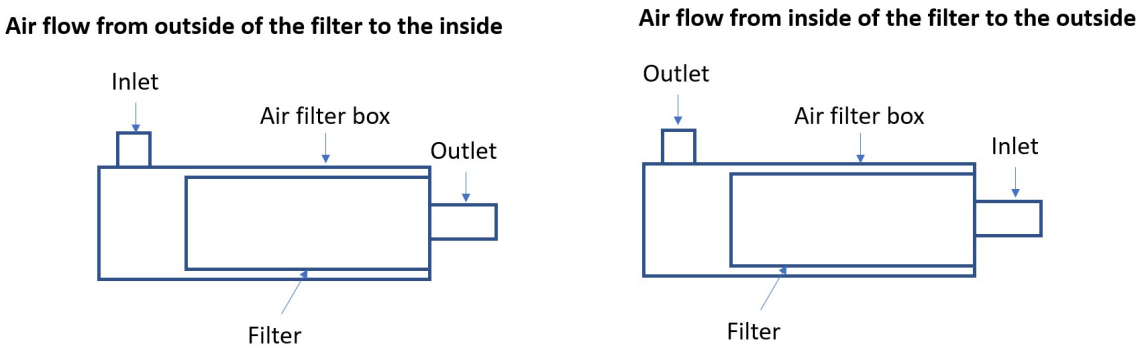

Figure 5.1: Directions of airflow for oval and round air filter boxes.

To maintain consistent filter efficiency throughout the lifespan of the filter, nanofiber can be used at the bottom of the filter. Nanofiber is shown in Figure 5.8, and it makes the air filter more resistant to water and flame.

To prevent the air filter box from leakage, a minimum of six screws are necessary, as recommended by "Expert 1". The locations of these screw holes are shown in Figure 5.2.

The MAF sensor should be placed before the outlet of the air filter box, but the placement is more critical for the flow inside the duct bellow than for the air filter box. The placement is visible in Figure 5.2.

The interview with "Expert 1" provided insights into the design requirements for drainage and snow accumulation rates. These requirements were subsequently included in the requirement specification found in Section 5.6.

All the interviews are presented in Appendix A.

5.3 Study visit

During the study visit, the primary focus was given to the mounting of the components and their interconnections. For example, it was observed that the duct bellow and the filter box were secured using clips and hose clamps. Additionally, the visit provided an opportunity to see where the attachment points of the air filter box were located to improved stability. The key findings from the visit are found in Table 5.2.

Table 5.2: Main takeaways from the mounting process.

Investigation	Takeaway
The connection between duct bellow and resonator	The connection was made by hose clamp.
The connection between the air filter box and duct bellow	The connection was made by hose clamp.
The connection between the bottom and top part of the filter box	Either with screws or clamps
The mounting of the air filter box	Using two holes and screwed onto body.

5.4 Study of Volvo's air filter box

An investigation was conducted on the air filter box and filter design to gain an understanding of the different components and their respective functions even further. The key findings from the study are presented in this section.

A top view with both the top part and bottom part of the air filter box is presented in Figure 5.2. The red arrow shows the placement of the MAF sensor. The MAF sensor is placed at the end of the filter box to measure the mass flow rate. The green circle shows the two attachment points for the air filter box. They are placed to

make the air filter box more steady and not move around. The blue arrow presents the six thread screw holes, located on the top part and on the bottom part. They are placed to keep the top part and bottom parts together. The yellow arrow points at the frame on the bottom part which makes a slot for the top part. The frame makes the top part and bottom part stick together horizontally.

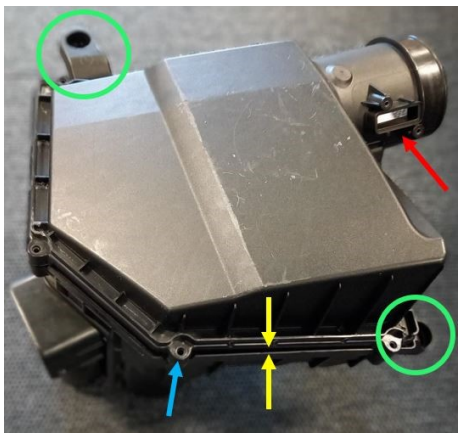

Figure 5.2: Takeaways from the study of the air filter box, top view.

An inside view of the top part of the air filter box is shown in Figure **??**. The red arrow in the figure points at the part near the outlet, which does not have any ribs. Having a ribbed part near the outlet could lead to a disturbance of the airflow. The blue arrow points at the ribbed part of the air filter box. The ribs increase the durability of the air filter box, placed inside the box due to aesthetics.

Figure 5.3: Takeaways from the study of the air filter box, inside view of top part.

A top view of the inside of the bottom part of the air filter box is presented in Figure 5.4. The red arrow in the figure shows the drainage holes. They remove the water and snow that enters the air filter box.

Figure 5.4: Takeaways from the study of the air filter box, top view of the bottom part of the air filter box.

Figure 5.5 presents the bottom part of the air filter box, but it turned 180 degrees. The red arrow in the figure points to a hollow space for a nut. If the thread inside the air filter box gets worn out. It is possible to use a nut to secure the screw (It does not cost anything extra to have this in the design).

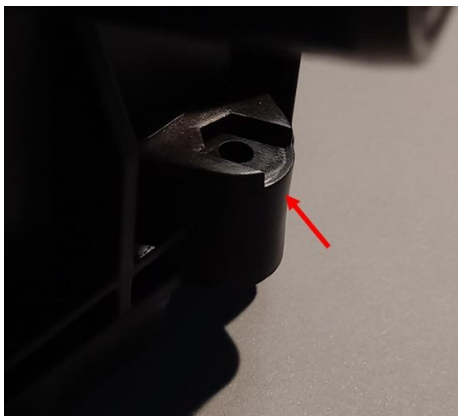

Figure 5.5: Takeaways from the study of the air filter box, bottom part turned 180 deg.

A top view of the inside of the bottom part of the air filter box is presented in Figure 5.6. The red arrow points at a square hole that is placed in both the top and bottom parts of the air filter box. The hole is placed there to be able to see that an air filter is inside the box. The green arrow points at the Inlet to the air filter box from the dirty side duct. The inlet has a rounding on the corners, shown by the blue arrows. The rounding is placed on the inlet to create less restriction on the airflow [33].

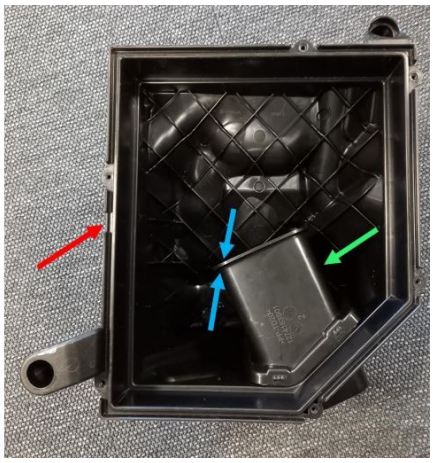

Figure 5.6: Takeaways from the study of the air filter box, top view of the bottom part of the air filter box.

A top view of the air filter is presented in Figure 5.7. The red arrow shows that one of the edges is angled, which is due to the limited space in the engine room. The blue arrow points at a glue line, which strengthens the pleats. The frame of the air filter, shown by the green arrows, also strengthens the pleats but also prevents leakage.

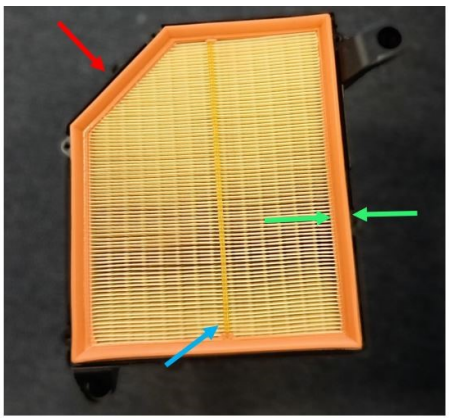

Figure 5.7: Takeaways from the study of air filter, top view.

Figure 5.8 shows a bottom view of the air filter. The red arrow points at a layer of white nanofiber. An air filter box has lower filter efficiency when it is new and higher when it has been used. The nanofiber increases the filter efficiency even when it is new.

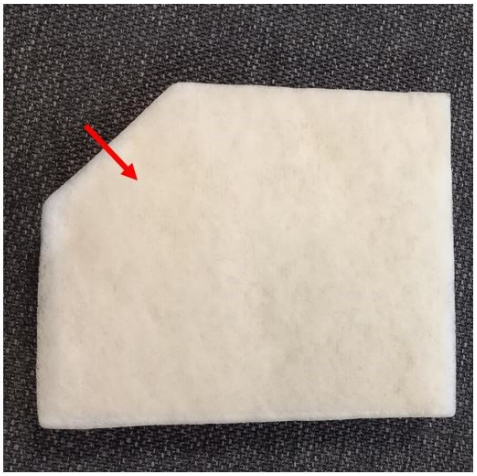

Figure 5.8: Takeaways from the study of air filter, bottom view.

A side view of the air filter is presented in Figure 5.9. The red arrow points at the air filter pleats. They capture the contaminants that enter through the dirty side duct.

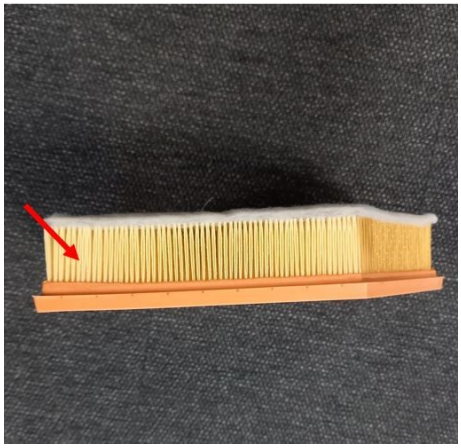

Figure 5.9: Takeaways from the study of air filter, side view.

5.5 Function-means tree

The function analysis can be found in Figure 5.10. The main function of the system was set to transport clean air to the engine, accomplished through the mean of using an air filter system. Thereafter, several functions were listed and linked to the components which influence the outcome of the function. As shown in Figure 2.1 the air filter system can be divided into four different components, dirty side duct, air filter box, air filter and the duct bellow.

According to "Expert 1", it is important to achieve an even and laminar flow of air within the AIS. This applies to every component of the air filter system. Each component needs to transport the air to the next components in a laminar flow.

According to "Expert 1", the air filter boxes usually have a large volume to minimize the NVH levels. A larger volume could allow a reduction in the number of resonators needed. Jung et al explained that duct bellows are used to reduce the NVH levels of the AIS [42].

The main function of an air filter is to trap dirt particles, thereby preventing dirty air to flow into the engine [24]. Both "Expert 1" and "Supplier 1" mentioned that the air filter's service life is determined by the amount of dust it can hold while still reaching the airflow requirements.

According to "Expert 1", the dirty side duct should prevent dirt particles and big size contaminates to enter the air filter box. Placing the dirty side duct as high as possible helps accomplish this. Furthermore, a high placed dirty side duct also prevents water from entering the air filter box. When water enters the air filter box, it is important to have proper drainage in place to prevent the air filter from becoming wet. This is also shown in the benchmark.

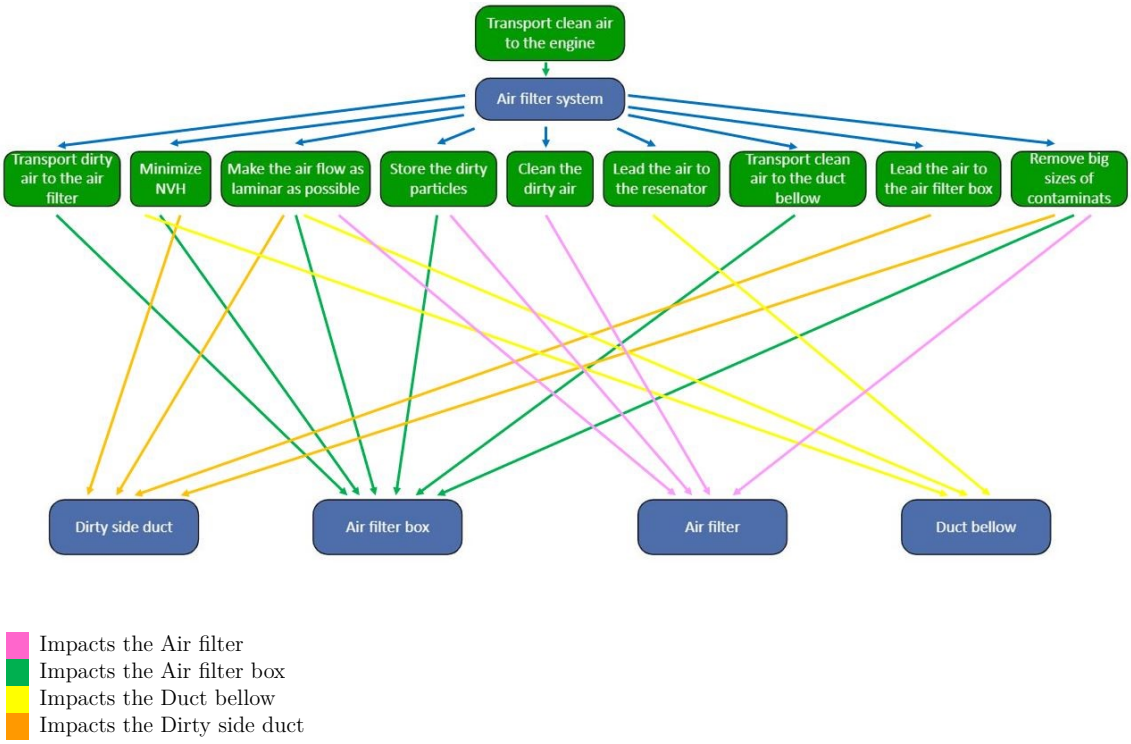

Figure 5.10: Function-means tree of the air filter system, including the dirty side duct, air filter box, air filter, and duct bellow.

Following the analysis of the main function, each individual component underwent further function analysis in order to gain a more comprehensive understanding. A detailed breakdown of these individual component analyses can be found in Appendix A.

The detailed function analysis revealed that the size and depth of the air filter, filter material and shape of the filter all contribute to achieving laminar airflow, collecting

particles, reducing the NVH levels and lower pressure drop. Particle size and the size of the filter media also contributed to collecting particles.

The geometry of the air filter box contributed to maintaining laminar airflow, reducing the NVH levels and lower pressure drop. To measure the airflow, a MAF sensor was placed on the outlet of the air filter box, which could affect the laminar flow. The air filter box functioned as the entry point for air from the dirty side duct, transporting air through the filter and forward air to the duct bellow.

The duct bellows main function was to transport the air from the air filter box to the resonator. It helped to maintain a laminar airflow, minimize NVH levels and lower pressure drop with its geometry and shape.

The primary function of the dirty side duct was to collect air from the environment and lead it to the air filter box. Both the geometry and the placement of the dirty side duct were important to maintain laminar airflow while ensuring the supply of air.

5.6 Requirement specification

The space allocated for the installation of the air filter box, air filter, and duct bellow has been identified as limited. Another requirement was that the duct bellow needs to be connected to the resonator. The available space, illustrated in light gray, and the placement of the engine and resonator are shown in Figure 5.11.

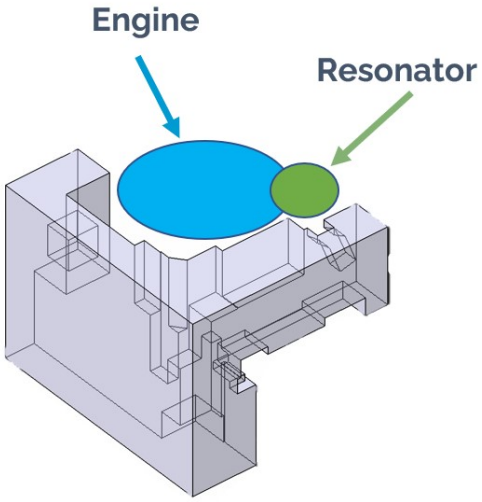

Figure 5.11: Installation space for air filter box, air filter, and duct bellow.

The rate of water discharge from the air filter box was a requirement, validated through physical testing. The conducted test can be found in Section 5.13.2. Due to the potential for water and snow infiltration through the dirty side duct into the

air filter box, it is essential for the water to exit the box in order to prevent any disruption to the airflow. Furthermore, the ability of the air filter box to withstand a specific applied force prior to failure was also a requirement. This requirement was established due to the necessity for the air filter box to exhibit durability throughout both the installation and maintenance processes. Specifically, when undergoing air filter replacement, thereby ensuring its continued functionality and longevity.

In addition to the established requirements, several desires were identified. One of these desires was that the air filter box and filter should be easy to install. Similarly, it was desirable for the air filter to easily be replaced, as a difficult replacement could lead to unnecessary costs. Additionally, although there was no specific budget for the project, it was desirable for the cost of the air filter box, air filter, and duct bellow to be as low as possible while remaining competitive with other air filter boxes on the market. The NVH levels should also be minimized. The requirement specification can be found in Figure 5.3 while the specific marginal values and ideal values were hidden since these values are confidential.

Table 5.3: Requirement specification.

No.	Requirement/Desires	Unit	Marginal Value (Requirement)	Ideal value (Desire)	Justification	Verification
1	Airflow	g/s			Test	CFD
2	UI over MAF				Supplier req.	CFD
3	Pressure drop	Kpa			Turbocharger req.	CFD
4	Service life air filter	h			Project req.	Calculations with required airflow and chosen environment
5	Service life air filter box and duct bellow	Km			Project req.	Future testing
6	Dimensions installation space	mm*mm*mm			Project req.	CAD
7	Drainage of water in air filter box	l/s			Carry over	Physical testing
8	NVH level	Dba			Disturbance of environment and driver	Simulation/Calculation
9	UI index over filter area				Service life	CFD
10	Cost	SEK			Project req.	Cost analysis
11	Dust removal capacity	kg			Service life	Numerical analyze
12	Weight	Kg			Project req.	CAD
13	Handle forces	N			Handle driving conditions	NVH/FEM Simulations/Calculations
14	Initial filter efficiency				Turbocharger/exhaust req.	Numerical analyze
15	Overall filter efficiency				Turbocharger/exhaust req.	Numerical analyze
16	The air filter must not be placed in a way were it will be in direct contact with water	Binary			Wet air filters are less efficient	Placed over water wading
17	Ability to operate in different environmental conditions (high humidity, high dust concentration, extreme temperatures, etc.)	Binary			The engine should be able to operate in different environments	Dust concentration calculation and future work for real-world testing
18	Ease of installation and maintenance	Binary			Ergonomic work environment	CAD

5.7 Design FMEA

The result from the design FMEA for the air filter box, air filter, and duct bellow is presented down below. All design FMEA used the scale presented in Appendix C.1.

5.7.1 Design FMEA air filter box

The FMEA for the air filter box is shown in Table 5.4. One potential failure mode identified for the air filter box was a low airflow, which could lead to reduced performance as less air would be available for combustion. The severity of this potential failure mode was rated as 7 on a scale of 1-10, indicating that it would degrade the primary function of air transportation, but the vehicle would still be operable with a reduced level of performance. To prevent such failures at an early stage, CFD simulations were conducted, Section 5.9, to visualize the airflow behavior for the air filter box design, and modify the design accordingly. The occurrence, in this case, was also set as a 7, considering the uncertainties surrounding the potential changes in the new air filter box design compared to previously tested designs. The detection of the failure mode was set to a 6 since it could be identified by CFD simulations, which was the closest available action that this project could reach. However, it was suggested that a future flow rig test should be conducted to obtain more accurate results.

Another potential failure mode with the same effect was if the connection between the dirty side duct and the air filter box failed to seal. In this case, the severity rating was determined to be 6, as the air is not yet cleaned at this stage and the failure does not pose a significant risk of contaminants getting into the turbocharger. However, the connection between the air filter box and the duct bellow, where the air is cleaned and could potentially contain dust from the engine room, was assigned a severity rating of 7. The occurrence rating was set to 5 in both cases, as it is relatively easy to check the connection during the installation and compare it to the existing connection designs. However, the detection was rated as 8 since there was no way that the potential leakage could be checked in this project. Therefore, it was recommended to conduct a flow rig test in the future as well.

There was also a risk of too high pressure drop, which could result in reduced performance for the same reason as previously explained, with a similar cause of failure. Additionally, sharp corners inside the air filter box could also lead to pressure drop. Therefore, it was assigned the same severity but a lower occurrence since it was easier to evaluate the impact of corner roundness on pressure drop with existing designs and CFD simulations. The detection rating was set to a 6 since the airflow of a new design could be tested in a post-design freeze stage using CFD simulations. Additionally, a flow rig can be used in the future.

A potential risk was that the UI over the air filter could be too low, which could result in a reduced service life for the air filter. This failure mode could be caused

by unevenly distributed air over the filter area. The severity rating was given a 6 since it affects the secondary function leading to a less optimal solution. It would be preferred to have a long service life of the air filter, which indicates that it would be a minor inconvenience to change the filter more often.

In the case of a too low UI over the MAF sensor, caused by the airflow being unevenly distributed, leading to a sub-optimal air-to-fuel ratio for combustion. The severity rating was set as a 7 since it gives a reduced level of performance of the combustion. The occurrence rating was set as a 7 as well, considering the uncertainty associated with the new design. Similarly, the risk of the MAF sensors not being placed properly and air not being filtered.

Furthermore, there could be a potential failure relating to water and snow entering the air filter box. If the dirty side duct or air filter box becomes filled with snow, the air path gets blocked which could lead to no air reaching the combustion chamber. This severity was rated as an 8 since it causes loss of primary function which is to transport the air. Although the vehicle would be inoperable, it still would be safe. The occurrence rating was set to 4 since there will be physical testing conducted to verify the drainage requirement. The detection was set to 6 since it can be detected at an early stage of the design freeze by verifying that the drainage test fulfills the requirement. Additionally, there could be secondary effects if water enters which would be that the engine would be damaged. This also has a severity rating of 8 since this impacts the driving operation and the air filter box losses its primary function.

Two potential factors that could lead to failure of the air filter box system were excessive noise levels and high vibration levels. Excessive noise could disturb both the surrounding environment and the vehicle's passengers. This may be caused by a small air filter box volume. The severity of this issue was rated as a 3, as it is unlikely to cause a significant disturbance. The occurrence was rated as a 4, as the new design can be compared to existing designs. However, the detection rating was set at 8, as the noise level cannot be fully verified within this project and requires further testing.

High vibration levels may damage the air filter box if it is not designed to withstand the forces involved. This may result in air leakage, which could impact the primary function of the air filter system. The severity rating for this potential failure was set at 7. The occurrence rating was set at 4, as the thickness and material of existing air filter boxes can be examined. The detection rating was set at 5, as the design will be tested to assess its ability to withstand the applied force prior to the design freeze.

Improper placement of fasteners has the potential to cause excessive vibration and damage to the air filter box. The severity rating for this potential failure was set at 5, as it does not directly impact the primary function of the vehicle, but could cause additional noise and damage. The occurrence rating was set at 5, as vibration levels differ for each design and engine, but other designs could be examined to obtain

an overview of the required design aspects. The detection rating was set at 8, as validation will be performed in future work using a flow rig and NVH simulation.

Table 5.4: Design FMEA for the air filter box.

No	Item/Object	Function/ Design Intent	Potential Failure mode	Potential Effect(s) of failure	Severity	Potential Cause(s)/ Mechanism(s) of failure	Current Design Control			Detection	RPN	Recommended action
							Prevention	Occurrence	Detection			
1	Air filter box	Transport gas, mass flow, keep filter in place	Too low flow	Reduced performance	7	Filter box not designed for flow, air is bouncing back	-Design review -CFD	7	- CFD	6	294	- Flow rig (future work)
					7	Air filter box is not totally sealed, air is leaking	-Design review	7		8	392	- Flow rig (future work)
					6	Connection between dirty side duct and air filter box not sealed	-Design review - Check when installing	5		8	240	- Flow rig (future work)
					7	Connection between duct and air filter box not sealed	-Design review - Check when installing	5		8	280	- Flow rig (future work)
			Too high pressure drop	Reduced performance	7	Filter box not designed for flow, air path is too long	-Design review -CFD	7	- CFD	6	294	- Flow rig (future work)
					7	Too sharp corners inside the air filter box	-Design review, -CFD	5	- CFD	6	210	- Flow rig (future work)
			Too low UI over air filter	Reduced service life for air filter	6	Air path not evenly distributed over air filter	-Design review -CFD	7	- CFD	6	252	- Flow rig (future work)
			Too low UI over MAF	Not optimal air to fuel ratio	7	Air path not evenly distributed over MAF	-Design review -CFD	7	- CFD	6	294	- Flow rig (future work)
			MAF sensor not placed properly	Not optimal air to fuel ratio	7	Air path not evenly distributed over MAF	-Design review -CFD	7	- CFD	6	294	- Flow rig (future work)
			Air not filtered by air filter	Dust is transported to turbocharger	7	Gap between air filter and air filter box	-Design review	7		5	245	- Flow rig (future work)
				Damage of compressor wheels and turbine blades	7	Large contaminants gets into the turbocharger	-Review filter efficency	7		8	392	- Flow rig (future work)
			Water/snow is transported to turbocharger/engine	The turbocharger inlet gets blocked	8	No air into the combustion chamber	- Required drainage - High air filter volume dirty side	4	-CAD geometry	6	192	- Flow rig (future work)
				Engine is damaged	8	Water is not drained fast enough	Required drainage	3	-Physical test	5	120	
			Too high noise level	Distubing outside environment and passengers	3	Too low volume of air filter box	Make it as large as possible	4	-CAD geometry	8	96	- Flow rig (future work)
			Too much vibration	Damage of air filter box	7	Low strenght of the air filter box	-Design review	4		5	140	- NVH-simulation -FEM analysis
					5	The fasteners are not properly placed		5		8	200	- Flow rig (future work) - NVH-simulation

5.7.2 Design FMEA air filter

The design FMEA for the air filter is shown in Table 5.5. The main function of the air filter is to remove dust and contamination. One potential failure mode was the excessive transportation of dust into the turbocharger, which could be caused by a low efficiency of the air filter. This could result in an impact on the emissions and potential damage to the turbocharger. The severity rating was set to a 7 since it could lead to loss of the primary function of filtering the air to a required level, but the car would remain operable. To prevent this, the efficiency of the filter needs to be reviewed. The occurrence was set to a 5 since the risk of a low-efficiency air filter causing too much dust transported into the turbocharger can be mitigated through careful design and testing. The efficiency of the filter could be reviewed by conducting lab tests or real-life testing in various driving conditions. By ensuring that the air filter has high efficiency, the risk of this failure mode occurring can be reduced. Detection was set to a 6, as the air filter needs to be tested in a laboratory or in real life setting before its launch.

Another potential failure mode was that the air is not filtered by the air filter. This could lead to damage of the turbocharger since it can not handle large contaminants. The severity rating was set to a 7 since the primary function of filtering the air would be lost, but the car would remain operable. This failure mode could occur if there was a gap between the air filter and the air filter box. The occurrence was set to a 7, considering the uncertainties surrounding potential changes in the new air filter design and higher dust concentration environment compared to earlier developed air filters. However, testing could be conducted in other projects which might lower the occurrence rating. The detection was set to 7 for the same reason as for the occurrence.

Another mechanism that could lead to that unfiltered air entering the turbocharger was if the air filter became wet. In this case, it would have the same severity rating as before, 7, but a lower occurrence, 3, since the physical drainage test. The detection was set to 5 since there is no easy way to detect if the air filter becomes wet.

In very rare cases, an air filter could catch fire, for example, if a cigarette would enter the dirty side duct. In this case, the severity rating was set to be a 10 since the engine could catch fire and the primary function would be lost since the car wouldn't work and potentially harm people since the fire would be near flammable fluids. The occurrence was set to a 2 since the possibility of this happening would be extremely rare and could be prevented by using flame resistant material for the air filter. The detection was set to a 9 since there is almost nothing that could be done if the engine would catch fire.

Another potential failure mode could be too high pressure drop due to the air filter geometry which could lead to reduced performance. The severity rating was set to a 5 since this leads to a reduced level of performance and impacts the secondary function, which leads to a decreased performance of the vehicle. The occurrence rating was set to a 7 since there is going to be a trade off between the DHC and

the lifespan of the filter when considering the pressure drop. The detection was set to a 6 since the air filter size and how pressure drop would be impacted could be analyzed by CFD simulation. The same reasoning could be used for the air filter material which had the same ratings of severity and occurrence but a rating of 8 when it comes to detection. The material needs to be reviewed by experts such as "Supplier 1", but it was outside the scope of this project.

If the UI over the air filter would be too low, it could lead to decreased service life. The severity was set to a 5 since an air filter could easily be replaced and that the primary function would not be affected. The occurrence was also a trade off between pressure drop and service life and set to 7. The detection was set to 6 since this could be detected in CFD simulations, but not in real-world testing. The same reasoning is done when the DHC is affected.

Another potential failure mode was if the vehicle operates in an environment where the dust concentration would be higher than the air filter was estimated to handle. The occurrence was set to a 5 since the air filter often could handle these environments. However, it could lead to a decreased service life of the air filter but the users were not expected to be in such dusty environment for long. The detection was set to 8 since it would be difficult to know how much it would impact the air filter without doing tests.

Table 5.5: Design FMEA air filter.

No	Item/Object	Function/ Design Intent	Potential Failure mode	Potential Effect(s) of failure	Severity	Potential Cause(s)/ Mechanism(s) of failure	Current Design Control			Detection	RPN	Recommended action
							Prevention	Occurrence	Detection			
2	Air filter	Remove dust and contamination	Too much dust is transported to the turbo	-Emissions - Affect turbocharger negatively	7	Too low air filter efficiency	-Review filter efficiency	5		6	245	- Flow rig (future work)
			Air not filtered by air filter	Dust is transported to turbocharger	7	Gap between air filter and air filter box		7		7	392	- Flow rig (future work)
			Air not filtered by air filter	Dust is transported to turbocharger	7	Air filter gets wet	- Design air filter box high -Required drainage	3	-Physical test of drainage - Air filter box placed over water wading line in CAD	5	105	
			Engine catch fire through the intake manifold	Air filter catch fire	10	Air filter burns up	Flame resistant material	2		9	180	
			Too high pressure drop	Reduced performance	5	Air filter geometry	CFD	7	- CFD	6	294	- Flow rig (future work)
					5	Air filter material	Material review	5		8	280	
				Decreased service life of air filter	5	Low UI over air filter	CFD	7	- CFD	6	294	- Flow rig (future work)
					7	Low DHC		7		6	294	- Flow rig (future work) -Calculate DHC and design to increase service life
					7	Vehicle used in a more dust concentrated environment than intendent	Set service life depending on usage	5		8	280	-Flow rig with different dust concentration (future work)

5.7.3 Design FMEA duct bellow

The FMEA for the duct bellow is shown in Table 5.6. The duct has the functions of transporting air, keeping a laminar flow, and reducing NVH levels. One potential failure mode was if the noise levels were too high which could disturb the surrounding environment and its passengers. This could be caused by the bellows geometry. The severity was set to be a 3 since this could cause some disturbing noise but would not affect the primary function of the duct bellow. However, it would reduce the convenience for the people nearby. The bellows material is another factor that could create unwanted noise which set a severity rating of 3 as well. The occurrence of both potential failures were set to a 5 since the noise would be relatively low. The detection was set to an 8 in both cases since NVH simulations would be needed, which was not covered in this project.

The duct bellow geometry and duct angle could lead to increased pressure drop and reduced performance. This failure mode had a severity rating set to 5, the occurrence set to a 7, and the detection set to a 6 using the same reasoning as before.

The connections should be sealed, both between the duct bellow and the air filter box, and the connections between the duct bellow and the resonator. If not, it could lead to reduced performance which does not affect the primary function but the secondary function would be affected.

Table 5.6: Design FMEA duct bellow.

No	Item/Object	Function/ Design Intent	Potential Failure mode	Potential Effect(s) of failure	Severity	Potential Cause(s)/ Mechanism(s) of failure	Current Design Control			Detection	RPN	Recommended action
							Prevention	Occurrence	Detection			
3	Duct bellow	Transport gas, mass flow, reduce NVH	Too high noise level	Disturbing outside environment and passengers	3	Bellow geometry		5		8	105	- Flow rig (future work) -NVH simulations
					3	Bellow material	Material review	5		8	120	-NVH simulations
			Too high pressure drop	Reduced performance	5	Bellow geometry	CFD	7	- CFD	6	294	- Flow rig (future work)
					5	Angle of duct	CFD	7	- CFD	6	294	- Flow rig (future work)
			Too low flow	Reduced performance	5	Connection between duct bellow and air filter box not sealed	-Design review - Check when installing	5		8	280	- Flow rig (future work)
					5	Connection between duct bellow and resonator not sealed	-Design review - Check when installing	5		8	280	- Flow rig (future work)
					5	Duct bellow geometry	CFD	7	- CFD	6	294	- Flow rig (future work)

5.8 CAD modeling

After investigating the available space for the air filter box, air filter, and duct bellow, concepts were developed. By utilizing the measurements from the available space, some simple shapes with either flat- or round filters were developed. The five shapes in Figure 5.12 were used. These shapes were selected since they took up the most amount of the available space. The shapes were round 5.12a, oval 5.12b, rectangular 5.12c, tube 5.12d, and half tube 5.12e shapes. Inspiration for the oval filter shape was taken from Section 4.3.1. The width and height of the available space were already very limited, therefore it would be difficult to develop shapes that would occupy lesser space. Furthermore, as mentioned in Section 5.2, a larger air filter box would lower the NVH level and could also fit a filter with a larger surface area. An increasing surface area leads to a reduction in pressure drop [31].

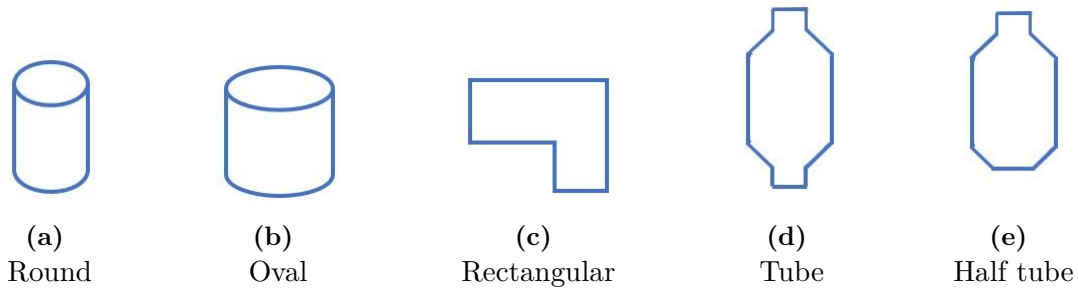

Figure 5.12: Shaped that was used for CFD simulation.

The shapes were placed in different positions to see how the dimensions could be maximized for the available space. Depending on the placement of the air filter box, the inlet and outlet positions had to be adjusted to fit each position. For the round and oval filters, this also meant that the airflow could either go from the inside and exit on the outside or enter the air filter box on the outside and exit on the inside. This was mentioned in the interview Section 5.2 and a visualization of this is shown in Figure 5.1.

Furthermore, the diameter, length, inlet position and outlet position depended on where the air filter box was placed. Inlet and outlet diameter as well as the limited space were the only two design parameters that were fixed. The other design parameters, listed in Table 5.7, needed to be tested to confirm how the design could meet the set requirements for airflow, UI over the outlet, UI over the filter, and pressure drop. These requirements were established in Section 5.6.

Table 5.7: Design parameters investigated in CFD.

Design parameters investigated
Placement of filter
Inlet angle
Inlet placement
Outlet placement
Inlet radius
Filter thickness
Oultet angle
Oultet radius
Guiding vanes
Inlet inside box
Length of box

5.9 CFD simulation

The simulations were performed with the expected airflow for the REX engine, a flow rate of XX g/s (not disclosed due to being a company secret), applied at the inlet. For the outlet, 0 pressure, 0 Pa, was applied. The fluid used in the simulations was air, with a density of 1.16 kg/m^3. The mesh used for the simulations can be found in Figure 5.13.

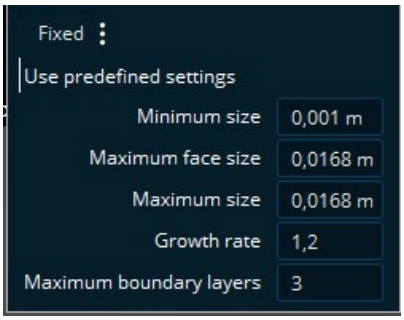

Figure 5.13: Mesh values for CFD simulations.

The output values examined in the CFD simulations were pressure drop, UI over the filter, UI over the MAF sensor, UI over the outlet of the duct bellow and velocity. The results from the CFD simulations for concepts on the air filter box and the duct bellow are presented below.

5.9.1 Round and oval shaped filters

The diameter and length of the air filter box remained constant during the simulations to get an understanding of how different parameters affected the outcome. The parameters that were experimented with for round and oval air filter boxes are found in Table 5.7. The values of the simulations in this phase were only used for comparative purposes to assess the impact different parameters had on the outcome, whether it improved or worsened. An illustration of a round shaped air filter box can be found in Figure 5.14.

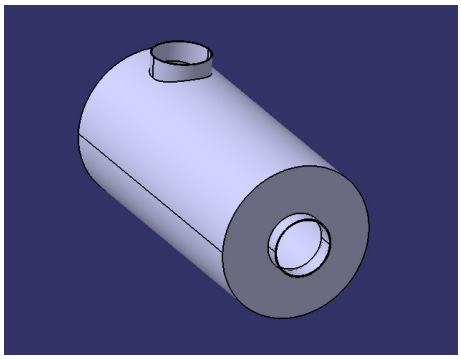

Figure 5.14: Round shaped air filter box.

An illustration of an oval shaped air filter box can be found in Figure 5.15

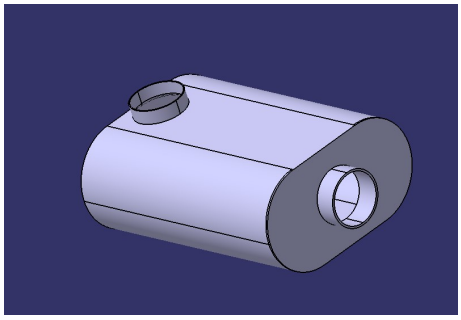

Figure 5.15: Oval shaped air filter box.

5.9.1.1 Oval shaped filter

The first parameter investigated was the inlet angle, shown in Figure 5.16. Three different angles were tested to evaluate their impact on pressure drop and UI. The results indicated that the UI for both the outlet and the filter was greatest at a 70-degree angle, as shown in Figure 5.16b. An angle of 60 degrees, shown in Figure 5.16a, resulted in the lowest pressure drop. The values from the CFD simulations are shown in Figure 5.8. The green boxes in the table represent the best performance for each output value.

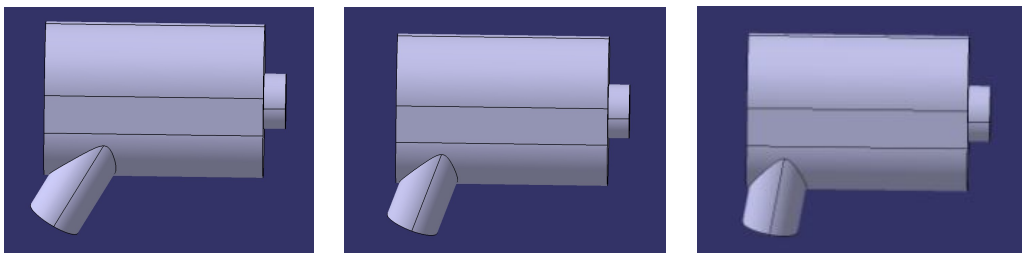

(a) 60 degrees **(b)** 70 degrees **(c)** 80 degrees

Figure 5.16: Angle of inlet.

Table 5.8: Test of different angles on the inlet.

	Test of angle on inlet		
Output value	**80 degrees**	**70 degrees**	**60 degrees**
Max. Velocity [m/s]	60.7	61.7	60.8
Avg Static Pressure [Pa]	2280	2310	2260
Vel. UI Outlet	0.813	0.822	0.814
Pressure drop [Pa]	1930	1930	1920
Vel. UI Filter	0,596	0.599	0.587

The other parameters listed in Figure 5.7 were tested in a similar way. The distance between the wall and the filter was investigated next, shown in 5.17.

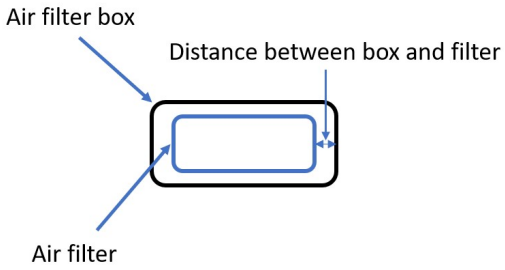

Figure 5.17: Cross section of air filter box showing the distance between the wall and the filter.

The longer the distance, the greater value of UI over the filter. However, the UI over outlet was found to be greatest when the filter was positioned 10 mm from the wall, which was the shortest distance. At a distance of 20 mm, the UI over filter was the lowest. The pressure drop was almost the same for all the different distances, with the 10 mm and 30 mm distances even yielding the same pressure drop. The results from the CFD simulations suggest that a longer distance between the wall and the filter is the best for UI over the filter, however, this would mean that the filter area would be lower. UI for the outlet, UI for the filter, pressure drop and filter area all need to be considered for the design to fulfill all the requirements. The values from the CFD simulations are shown in Figure 5.9.

Table 5.9: Values of the different distances between wall and filter for oval shaped air filter box.

	Distance of filter from the outer wall with 70 degrees on inlet		
Output value	**30 mm**	**20 mm**	**10 mm**
Max. Velocity [m/s]	62.5	61.6	61.7
Avg Static Pressure [Pa]	2330	2270	2310
Vel. UI Outlet	0.816	0.813	0.822
Pressure drop [Pa]	1930	1890	1930
Vel. UI Filter	0.622	0.616	0.599

The next parameter to be tested was different ways of guiding the airflow. The simulations were conducted with an inlet angle of 70 degrees and a distance between the wall and filter of 20 mm. The various guiding methods are illustrated in Figure 5.18. The objective of guiding the airflow was to achieve an improved UI for both the outlet and filter. Therefore, a ramp was placed in the inlet to direct the airflow

toward the inner wall of the air filter box to see how it affected the airflow distribution across the whole filter. Several variants of this ramp were developed, including adjusting the height, placing the ramp in different positions and including holes in the ramp. These ramp guides were developed due to that the airflow had previously been hitting the wall on the opposite side of the inner wall, instead of following the wall directly. A description and names for all simulated guide concepts are shown in Table 5.10.

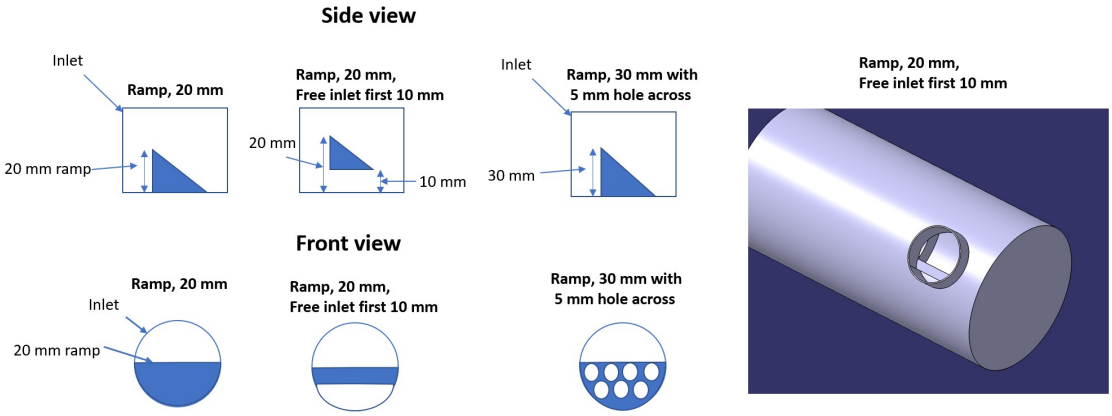

Figure 5.18: Visualization of guiding.

Table 5.10: Guide concepts.

Concept description	Concept number
No ramp	**1**
ramp, 10 mm	**2**
ramp, 20 mm	**3**
ramp, 20 mm, Free inlet first 10 mm	**4**
ramp, 20 mm, Free inlet first 15 mm	**5**
ramp, 10 mm, Free inlet first 5 mm	**6**
ramp 30 mm with 5 mm holes across	**7**
ramp 40 mm with 5 mm holes across	**8**
Ramp 40 mm, Free inlet first 20 mm	**9**
Ramp 40 mm,Free inlet first 20 mm with 5 mm holes	**10**
Ramp on the left side 10 mm	**11**
Ramp on the right side 10 mm	**12**
Ramp on the right side 10 mm with 5 mm holes	**13**

The results from the test are shown in Table 5.11. It was observed that a guide in the inlet increased the pressure drop compared to the case without any guidance. However, the UI for both the outlet and the filter improved with the use of guidance. Achieving an even distribution of airflow while minimizing pressure drop posed a challenge. For round and oval filters, the airflow gets into a "swirl" motion. Therefore, a combination of direct entry and entry through different locations of the filter was needed. This was tested by placing a ramp in the inlet with different heights. The result showed that a higher ramp increases pressure drop but improved UI. To reduce the pressure drop, holes were placed across the whole ramp or by positioning the ramp slightly above the bottom of the inlet. Additionally, a ramp on the left side was also tested which resulted in most of the air going to the end of the air filter

box. A similar test was conducted with a ramp on the right side and the result was worse for UI over the outlet compared to both the left side and the bottom. Both the left side and the right side resulted in a lower pressure drop without decreasing the UI significantly. As stated before, the lowest value for pressure drop was obtained without any guidance and the greatest value for UI was with a 40 mm ramp but the bottom 20 mm had a free inlet.

Table 5.11: Values of different guidance on the inlet oval shaped air filter box.

	Test of guiding				
Output value	**1**	**2**	**3**	**4**	**5**
Max. Velocity [m/s]	61.6	63.2	104	75.5	129
Avg Static Pressure [Pa]	2270	3220	6300	3350	3920
Vel. UI Outlet	0.813	0.825	0.858	0.831	0.837
Pressure drop [Pa]	1890	2800	5920	3000	3540
Vel. UI Filter	0.616	0.601	0.614	0.62	0.626
Output value	**6**	**7**	**8**	**9**	
Max. Velocity [m/s]	148	84.6	84.3	65.6	
Avg Static Pressure [Pa]	4770	5290	3480	2920	
Vel. UI Outlet	0.845	0.86	0.831	0.828	
Pressure drop [Pa]	4420	4910	3100	2530	
Vel. UI Filter	0.631	0.631	0.627	0.628	
Output value	**10**	**11**	**12**	**13**	
Max. Velocity [m/s]	58.3	61.1	65.2	90.1	
Avg Static Pressure [Pa]	2400	2530	2740	2520	
Vel. UI Outlet	0.836	0.821	0.817	0.821	
Pressure drop [Pa]	2110	2170	2340	2150	
Vel. UI Filter	0.606	0.618	0.622	0.609	

The next test was conducted to investigate the difference between if the inlet was free, the filter started above the inlet, and if the filter covered the whole air filter box. A visualization of this is shown in Figure 5.19.

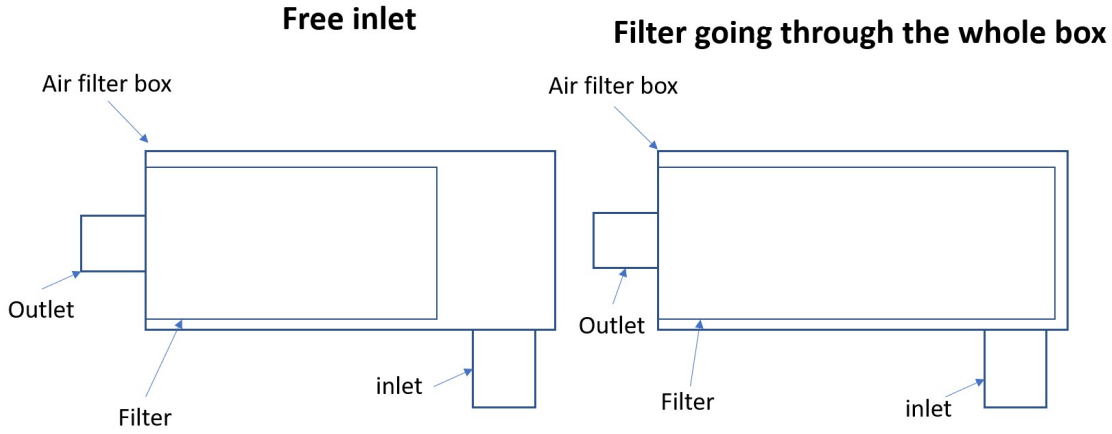

Figure 5.19: Free inlet and filter going through the whole box.

The results showed a difference in how the UI behaved. When the inlet angle was low, the air tends to not going to go through the filter near the inlet. UI for the

outlet and pressure drop behaved similarly to when the inlet was free from the filter. For angles above 90 degrees, the air was hitting the wall close to the inlet. The result showed that an angle of 90 degrees had the greatest UI for the filter but the greatest pressure drop and a low UI for the outlet. The greatest UI for the outlet could be found at an angle of 70 degrees, while both 80 and 100 degrees inlet were very close. The pressure drop was lowest at 70 and 100 degrees. All the values from this test are shown in Figure 5.12.

Table 5.12: Values of different angles for oval shaped air filter box with filter going through the whole box.

	Test of angle on inlet when the filter is going the whole box				
Output values	**70 degrees**	**80 degrees**	**90 degrees**	**100 degrees**	**110 degrees**
Max. Velocity [m/s]	59.8	59.1	60.4	57.5	59,4
Avg Static Pressure [Pa]	2320	2410	2570	2250	2380
Vel. UI Outlet	0.827	0.826	0.807	0.824	0.803
Pressure drop [Pa]	2000	2110	2250	2010	2070
Vel. UI Filter	0.626	0.638	0.642	0.629	0.629

To investigate how the UI for the filter could be improved when the filter was the full length of the air filter box, tests of guidance were conducted. There were only a few tests, mainly because of the conclusions that were made in the earlier testing of guides. The tests included simulation without a guide and then simulations of those that showed promising results in previous guide tests. Unsurprisingly, the test without guidance had the lowest pressure drop and also had the greatest UI for the filter. However, the UI for the outlet had a lower value compared to the larger ramps. The smaller ramp had a similar UI as the one without guidance but had a higher pressure drop. The greatest value for UI over the outlet was the one with a 40 mm high ramp but the first 20 mm was free. However, it had the highest pressure drop. To lower the pressure drop, holes were put in the ramp which improved the UI for the filter but it also resulted in a lower UI for the outlet. The test results are shown in Table 5.13.

Table 5.13: Values of different guidance for oval shaped air filter box with filter going through the whole box.

	Test of guiding, 90 degrees inlet, filter 20 mm from wall filter the whole box			
Output values	**Without guide**	**ramp, 20 mm, Free inlet first 10 mm**	**Ramp 40 mm, Free inlet first 20 mm**	**Ramp 40 mm, Free inlet first 20 mm, 5 mm holes**
Max. Velocity [m/s]	60.4	69.2	80.9	78.9
Avg Static Pressure [Pa]	2570	3290	4790	3590
Vel. UI Outlet	0.807	0.806	0.851	0.824
Pressure drop [Pa]	2250	2960	4540	3250
Vel. UI Filter	0.642	0.64	0.627	0.634

5.9.1.2 Round filter

The first parameter tested was the placement of the inlet. There were two different positions were investigated, in the middle of the cylinder and 50 mm away from the middle, shown in Figure 5.20.

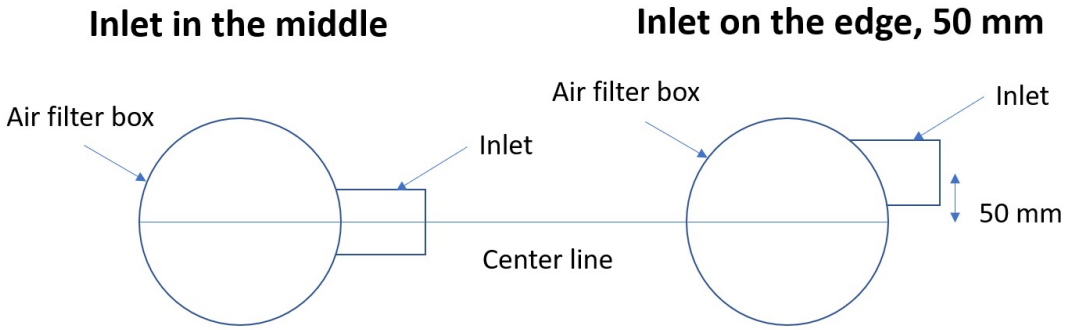

Figure 5.20: Inlet placements.

The inlet was significantly better when the inlet was positioned away from the middle. This was in terms of the pressure drop, UI for the outlet and UI for the filter, shown in Table 5.14.

Table 5.14: Test of Inlet placement for round filters.

	Inlet in the middle	Inlet on the edge, 50 mm from middle
Max. Velocity [m/s]	63,7	61.7
Avg Static Pressure [Pa]	2790	2560
Vel. UI Outlet	0.782	0.816
Pressure drop [Pa]	2340	2160
Vel. UI Filter	0.587	0.645

The next parameter that was tested was the angle of the inlet, similar to the oval shape shown in Figure 5.16. The results aligned with those for the oval shaped filter. With a lower angle, the pressure drop became lower. The angle with the best result for the UI for both outlet and filter was 70 degrees for the round filter as well. The result is shown in Table 5.15.

Table 5.15: Values of different angles for round shaped air filter box.

Output values	60 degrees	70 degrees	80 degrees
Max. Velocity [m/s]	56.2	56.8	56.6
Avg Static Pressure [Pa]	915	961	1000
Vel. UI Outlet	0.849	0.854	0.844
Pressure drop [Pa]	1840	1900	1950
Vel. UI Filter	0.599	0.604	0.599

The distance between the wall and the filter were tested, visual representation shown in Figure 5.17, with the inlet angle of 70 degrees. The results were similar to the oval filter. The pressure drop was almost the same but the UI on both outlet and filter were improved when the distance between the wall and the filter increased. The filter area needs to be considered here as well, a higher distance results in a lower filter area. The test was only conducted for two different distances, 10 mm and 30 mm, and the results are shown in Table 5.16.

Table 5.16: Values of different distance between wall and filter for round shaped air filter box.

Output values	Distance wall/filter 10 mm	Distance wall/filter 30 mm
Max. Velocity [m/s]	81.6	79.6
Avg Static Pressure [Pa]	1930	1910
Vel. UI Outlet	0.858	0.863
Pressure drop [Pa]	2860	2850
Vel. UI Filter	0,609	0.649

The air could either enter from the outside and exit on the inside of the filter or the other way round. The next test was, therefore, to switch places for the inlet and the outlet, as is shown in Figure 5.1. Additionally, different guides were used, as shown in Figure 5.21.

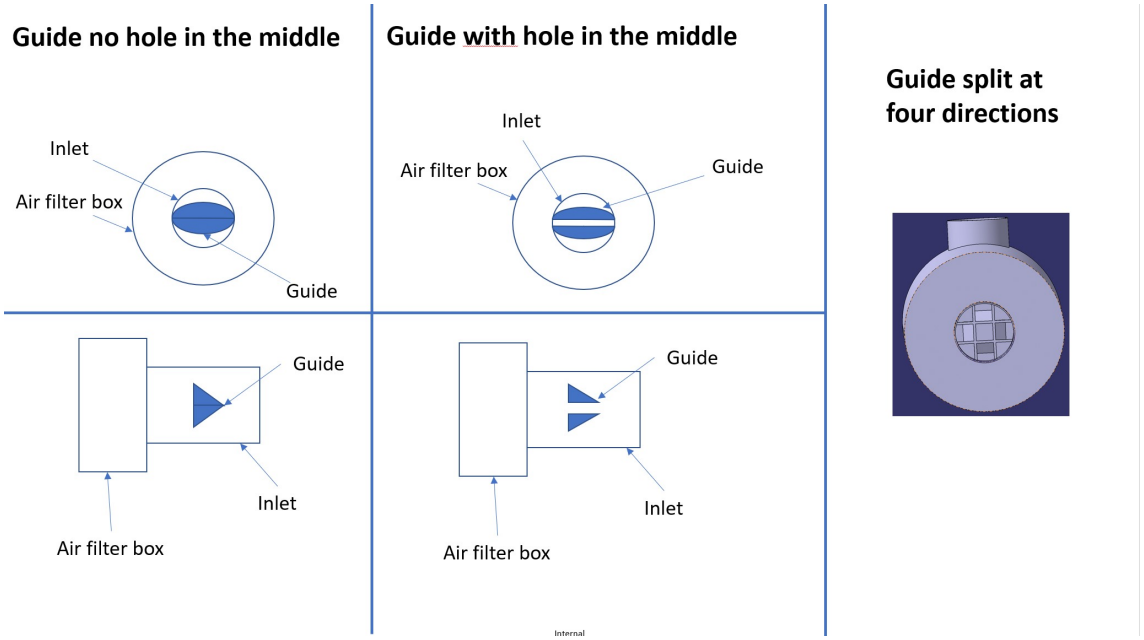

Figure 5.21: Inlet on the inside with guides for round shaped air filter box.

The first test was conducted without any guidance which resulted in a low UI for the filter because the air went directly to the outlet and almost bypassed half of the filter. As stated before, when using a guide in the inlet the pressure drop increases. Three different kinds of guides were tested with the aim of evenly distributing the airflow over the whole filter area. The second and third tests were a guide with a sloping surface, with the only difference being that the third test had a hole in the middle of the guide. The result showed that it had a lower pressure drop and higher UI for the outlet but it was inferior for the UI over the filter. The fourth and final test had four sloping surfaces in four different directions, which proved to improve values on UI but resulted in a high pressure drop. Values for the test can be found in Table 5.17

Table 5.17: Values of Inlet on the inside with guides for round shaped air filter box.

Output values	No guide	No hole in the middle	Hole in the middle	Guide split at four directions
Max. Velocity [m/s]	79.8	107	69	76.5
Avg Static Pressure [Pa]	4100	9140	4050	5040
Vel. UI Outlet	0.799	0.847	0.876	0.88
Pressure drop [Pa]	2020	8840	3850	4720
Vel. UI Filter	0.562	0.642	0.62	0.658

The filter thickness was also a parameter that was tested, visualized in Figure 5.22. To investigate how the thickness impacted the UI and pressure drop, the round air filter box had a filter the full box length with a filter thickness that varied between 40 mm and 20 mm. The air filter box used for testing had an inlet angle of 70 degrees, a distance of 10 mm between the wall and the filter and no guides. The tests showed that a higher filter thickness resulted in a higher pressure drop because the air had to travel a longer distance in the resistance from the filter. Additionally, a higher filter thickness resulted in a higher UI for both the outlet and the UI for the filter. The values for the test are shown in Table 5.18.

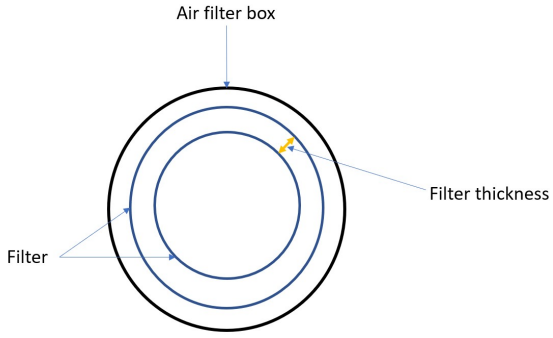

Figure 5.22: Filter thickness.

Table 5.18: Values of different filter thicknesses for round shaped air filter box.

	Test of filter thickness wall/filter distance 10 mm, 70 degree inlet		
Output values	40 mm	30 mm	20 mm
Max. Velocity [m/s]	72	70.6	67.4
Avg Static Pressure [Pa]	4090	3950	3680
Vel. UI Outlet	0.819	0.801	0.797
Pressure drop [Pa]	3850	3950	3400
Vel. UI Filter	0.627	0.612	0.616

The radius of the outlet had in previous simulations been zero, so the next test aimed to investigate how it impacted the outcome, visualized in Figure 5.23. The first simulation was conducted without a radius, resulting in a majority of the airflow did go toward the middle. Subsequently, two different radius were tested, 5 mm and 10 mm. These helped the distribution of the airflow to be more evenly spread over the outlet. It also decreased the pressure drop significantly. The radius of 5 mm and 10 mm were very close in most of the outcome values, but the larger radius performed slightly better, shown in Table 5.19.

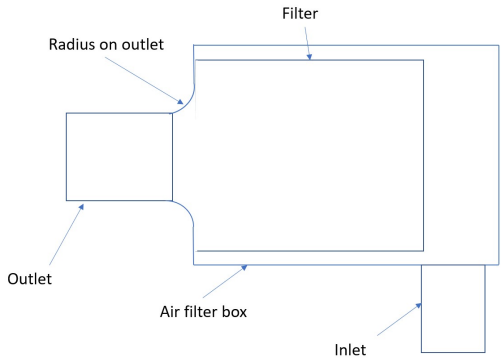

Figure 5.23: Radius on outlet.

Table 5.19: Values of different outlet radius for round shaped air filter box.

	Testing of raidus on outlet with 40 mm + distance wall/filter (10 mm), no ramp, inlet free		
Output values	**No radius**	**5 mm radius**	**10 mm radius**
Max. Velocity [m/s]	58.1	54.7	47.3
Avg Static Pressure [Pa]	2410	1530	1510
Vel. UI Outlet	0.81	0.964	0.966
Pressure drop [Pa]	2160	1530	1500
Vel. UI Filter	0.691	0.687	0.684

Depending on the placement of the air filter box, the outlet may be needed to have an angle to ease the airflow of the duct bellow. Therefore, different outlet angles were tested to see how they impacted the outcome, visualized in Figure 5.24. As shown in Table 5.20, the UI and the pressure drop were the best without an angle. The angle that affected the outcome the least was a small angle, 20 degrees, that pointed towards the inlet. In Figure 5.24 the inlet is placed to the right and the outlet is angled to the right as well, and the outlet point towards the inlet. Higher angles resulted in an airflow that was minimal after the sharp corner which made the outlet UI lower, it also increased the pressure drop.

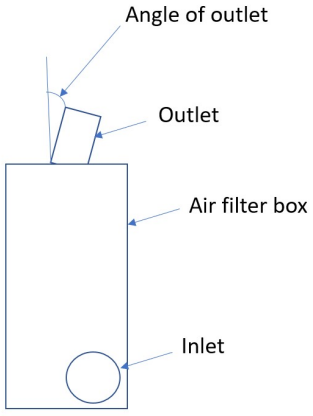

Figure 5.24: Angle of outlet.

Table 5.20: Values of different outlet angles for round shaped air filter box.

	Testing of outlet angle with 40 mm + distance wall/filter (10 mm), no ramp, inlet free, radius 10 mm on outlet			
Output values	**20 degrees same direction as inlet**	**20 degrees opposite direction as inlet**	**40 degrees same direction as inlet**	**No angle on outlet**
Max. Velocity [m/s]	56.5	58.2	71	47.3
Avg Static Pressure [Pa]	1700	1730	2420	1510
Vel. UI Outlet	0.961	0.949	0.825	0.966
Pressure drop [Pa]	1620	1650	1960	1500
Vel. UI Filter	0.666	0.667	0.665	0.684

In the previous tests, the inlet of the air filter box had stopped at the inner diameter of the air filter box. However, upon observing the current air filter box, it was seen that the inlet went inside the box as shown in Figure 5.6. Therefore, it was investigated how that impacted the UI and pressure drop. The result from this test can be found in Table 5.21. The result showed that the UI is almost identical but the pressure drop decreased significantly when the inlet continued into the box.

Table 5.21: Values of inlet going inside air filter box for round shaped air filter box.

	Test of inlet that go into the box	
Output values	**Stopping at the box**	**Going inside the box**
Max. Velocity [m/s]	49.7	49.3
Avg Static Pressure [Pa]	1600	1250
Vel. UI Outlet	0.969	0.967
Pressure drop [Pa]	1600	1240
Vel. UI Filter	0.666	0.667

The observations showed that the inlet had rounded corners on the inlet, as shown in Figure 5.25. The literature review also highlighted, in Section 4.2.1.1, that a pipe design with a flared end would result in less restriction compared to a design without one. This was therefore investigated to see the impact. The rounding of the inlet lowered the pressure drop compared to without any rounding. The UI for both outlet and filter were similar in both cases. All output values from the test are shown in Table 5.22.

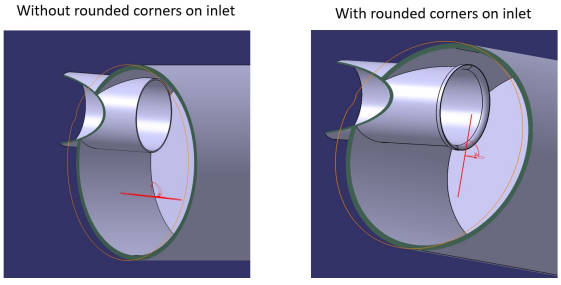

Figure 5.25: Inlet rounded corners.

Table 5.22: Values of inlet have round corners for round shaped air filter box.

	Test of rounded corner on inlet	
Output values	**No rounded corner**	**4 mm round corner**
Max. Velocity [m/s]	47.8	47.5
Avg Static Pressure [Pa]	1410	1240
Vel. UI Outlet	0.966	0.966
Pressure drop [Pa]	1410	1230
Vel. UI Filter	0.674	0.679

In the final test, the best performing parameters for the round shaped filter, from the previous tests, were compared to concepts that used different parameter combinations. The goal was to see if combining different parameters could improve the result compared to the individual best performing parameters. Some of the parameters had "locked" values, shown in green, and the reason for this was that these parameters significantly outperformed other values in previous tests. For the other parameters, the interesting values were those that performed on the higher scale or had both benefits and drawbacks. The concepts and values that were tested are shown in Table 5.23. The concepts called "Chosen parameters" had the best performing parameters for the previous tests. From the test, it can be seen that "Chosen parameters" also performed best in two categories, UI over the filter and the pressure drop. "Concept 2" did however perform best for the UI over the outlet. One drawback with this solution was that it had a high pressure drop compared to "Chosen parameters". For "Concept 2" the UI over the filter was a bit lower, but it compensated for it with a larger filter area. A challenge for "Concept 2" would be that with a full length filter, it would be difficult to drain water without the filter getting wet. This test confirmed that the "Chosen parameters" concept still outperformed the other concept.

Table 5.23: Other combinations of parameters for round shaped air filter box.

Parameter	**"Chosen parameters"**	**Concept 1**	**Concept 2**	**Concept 3**	**Concept 4**	**Concept 5**
Inlet placment	45 mm from middle, edge	Middle	Middle	45 mm from middle, edge	45 mm from middle, edge	45 mm from middle, edge
Inlet angle	70 degrees	90 degrees	110 degrees	110 degrees	90 degrees	110 degrees
Filter placement from wall	10 mm	20 mm	10 mm	10 mm	20 mm	10 mm
Filter length	Free inlet	Free inlet	Full lenght	Full lenght	Full lenght	Free inlet
Guiding	No Guide	No Guide	No Guide	40 mm ramp, free inlet first 20 mm, 5 mm holes	40 mm ramp, free inlet first 20 mm, 5 mm holes	No Guide
Inlet inside of box	Yes	Yes	No	No	No	Yes
Outlet inside or outside	Inside	Inside	Inside	Inside	Inside	Inside
Inlet radius	4 mm	4 mm	4 mm	4 mm	4 mm	4 mm
Outlet radius	5 mm	5 mm	5 mm	5 mm	5 mm	5 mm
Filter thickness	40 mm	40 mm	40 mm	40 mm	40 mm	40 mm
Outlet angle	No	No	No	No	No	No
Max. Velocity [m/s]	47.7	324	66.6	94.5	93.5	54.6
Avg Static Pressure [Pa]	1260	1360	3370	3470	2900	1510
Vel. UI Outlet	0.966	0.927	0.969	0.965	0.919	0.963
Pressure drop [Pa]	1260	1340	3360	3450	2850	1500
Vel. UI Filter	0.683	0.63	0.62	0.625	0.61	0.671

5.9.2 Summary of CFD simulations for round and oval air filter boxes

The summary for both round and oval air filter boxes were merged into one list because the results were very similar for the two shapes.

- The output value for the pressure drop was low and the UI for filter and outlet had the best output values when the inlet was placed on the edge as shown on the right in Table 5.20.

- The inlet angle had an impact on pressure drop, 12%. The 70 degree angle had a low pressure drop and great values on the UI for the outlet and over the filter. This can be found in Table 5.12
- As shown in Table 5.11, the placement of a guide near the inlet was found to improve the UI for the filter and the outlet. However, it increased the pressure drop significantly.

- Placing the inlet on the inside of the filter, shown in Table 5.17, resulted in a lower UI for the filter. Guides increased the UI over the filter but decreased the pressure drop.

- The distance between the inner wall of the air filter box and the outer diameter of the air filter had an impact of 7% on the UI over the filter. A higher distance created a greater UI over the filter, which is shown in Table 5.16.

- A higher thickness of the air filter gave a higher UI on both the outlet and the filter, shown in Table 5.18. However, it increased pressure drop.

- A radius on the outlet generated a greater UI over the outlet and also decreases the pressure drop for the air filter box, shown in Table 5.19.

- An angle on the outlet increased the pressure drop and decreased the UI on the outlet, shown in Table 5.20.

- The pressure drop was reduced when the inlet was going inside the air filter box instead of stopping at the inner diameter of the box, shown in Table 5.21. It was reduced even more when the inlet had a rounded corner, shown in Table 5.22.

The test results have been summarized in Table 5.24. The colors represent how much each parameter impacted the outcome in pressure drop, UI over the outlet and UI over the filter. The green boxes impacted the outcome 15% or more, yellow 10%, orange 5% and the red 1% or less. As shown, there were many factors that impacted the pressure drop significantly. For the UI over the outlet, the parameters that influenced the most were outlet placement and outlet radius. The inlet placement and outlet angle impacted it to some amount. UI over the filter had the outlet placement as the most important parameter and the inlet placement as the second most important parameter.

Table 5.24: Color-scheme of impact of different parameters for circular and oval shapes.

Circular/oval filters			
Tested parameters	**Pressure drop**	**UI outlet**	**UI filter**
Inlet placement (middle or edge)			
Inlet angle			
Filter placement from wall			
Guiding			
Inlet inside box			
Outlet placement (Inside or outside of filter)			
Inlet radius			
Filter thickness			
Outlet angle			
Outlet radius			

Scale	1.15	1.1	1.05	1.01
Color				

5.9.3 Flat shaped filters

Various types of flat air filters were simulated and evaluated in different configurations. These included a rectangular-shaped box with a rectangular flat filter, a tube-shaped air filter box with a circular flat filter, and a cylinder with an inlet on the side and a tube-shaped outlet.

5.9.3.1 Rectangular air filter box

The testing of flat filters began with a rectangular-shaped box that was not representative of the actual available space for this project. Rather, it was used to test different inlet and outlet positions since the available space did not allow for a wide variety of positions. These results could be applied to other projects with larger spaces. The tested inlet and outlet positions are illustrated in Figure 5.26.

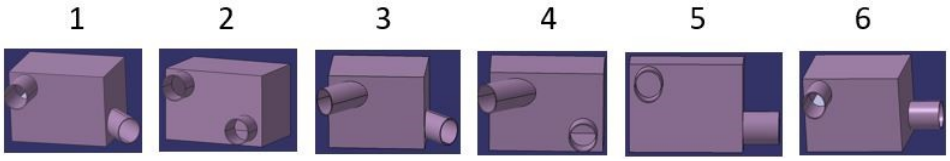

Figure 5.26: Concept 1, 2, 3, 4, 5, and 6.

Upon reviewing Table 5.25, it can be observed that there were variations in the performance of the different configurations. For instance, Concept 3 had the highest max velocity and average static pressure, while Concept 6 had the lowest pressure drop. In terms of velocity UI, Concepts 1 and 2 had the greatest UI at the outlet, while Concept 6 had the greatest UI over the filter.

Table 5.25: Inlet & outlet placement and the values from CFD.

Concept number	**1**	**2**	**3**	**4**	**5**	**6**
Max. Velocity [m/s]	64.3	65.2	70.8	68.5	63.6	62.5
Avg Static Pressure [Pa]	2320	2560	3430	2920	2310	2170
Vel. UI Outlet	0.873	0.828	0.785	0.786	0.863	0.883
Pressure drop [Pa]	2190	2260	2990	2520	2120	2020
Vel. UI Filter	0.741	0.7605	0.602	0.6995	0.7545	0.694

The next step in the testing of flat filters involved designing a box that was as large as possible given the available space. Due to the limited space, an L-shaped box was designed. The first aspect tested was the shape of the drainage area where air enters the filter box, referred to as the "Shape of drainage". The concepts are illustrated in Figure 5.27.

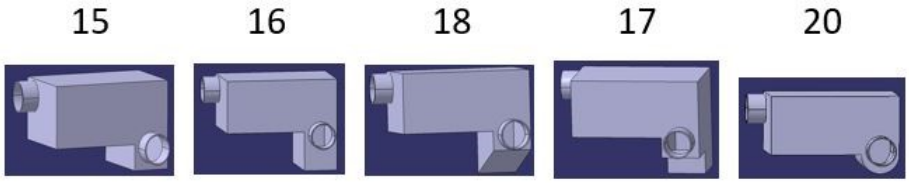

Figure 5.27: Concept 15, 16, 18, 17, 20.

The test results revealed that the maximum velocity and UI at the outlet were nearly identical for all five cases as shown in Table 5.26. However, the pressure drop appeared to increase as the length of the drainage area increased, as observed for Concepts 16 and 18. Concept 17 had the lowest pressure drop, which could be attributed to its shorter length at the beginning of the drain. However, it also had the lowest UI over the filter. Concepts 15 and 20 performed similarly in all measurements.

Table 5.26: Shape of drainage and used default settings.

Concept number	**15**	**16**	**18**	**17**	**20**
Shape of drainage	**Normal**	**Shorter**	**Slope**	**Stair**	**Rounded**
Max. Velocity [m/s]	64.9	65.4	65.6	64.9	64.5
Avg Static Pressure [Pa]	2580	2730	2680	2470	2580
Vel. UI Outlet	0.835	0.836	0.832	0.84	0.833
Pressure drop [Pa]	2270	2390	2340	2190	2250
Vel. UI Filter	0.813	0.787	0.79	0.773	0.8

As the length of the drainage area was found to have the greatest impact on filter performance among the drainage shapes tested, the placement of the inlet along the z-axis was investigated for the lengths of 50 mm and 100 mm. Concept 15, as shown in Figure 5.27, was used as the baseline for this test except for the inlet and outlet lengths which varied. An illustration of the distance between the inlet and outlet along with the length of drainage is shown in Figure 5.28.

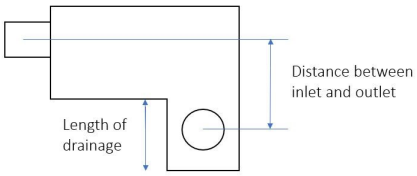

Figure 5.28: Illustration of parameters changed for the rectangular shapes drainage.

The test results indicated that a shorter length of drainage (50 mm) with the outlet placed 100 mm from the inlet resulted in the lowest pressure drop and had the highest UI over the filter. However, for the longer drainage shape, the UI over the filter decreased as the distance between the inlet and outlet increased. On the other

hand, the pressure drop decreased as the inlet and outlet lengths increased, except for when the length of the drainage shape was 50 mm.

Table 5.27: Distance between inlet and outlet (fixed inlet) and the values from CFD.

Inlet fixed while outlet change distance	**Length of drainage shaped**	
Middle of the inlet to middle of outlet, 100 mm.	**50 mm**	**100 mm**
Max. Velocity [m/s]	66,6	66,2
Avg Static Pressure [Pa]	2670	2760
Vel. UI Outlet	0,828	0,835
Pressure drop [Pa]	2300	2410
Vel. UI Filter	0,796	0,784

Middle of the inlet to middle of outlet, 115 mm.		**100 mm**
Max. Velocity [m/s]		65.8
Avg Static Pressure [Pa]		2770
Vel. UI Outlet		0.835
Pressure drop [Pa]		2410
Vel. UI Filter		0.786

Middle of the inlet to middle of outlet, 130 mm.		**100 mm**
Max. Velocity [m/]s		66.1
Avg Static Pressure [Pa]		2730
Vel. UI Outlet		0.839
Pressure drop [Pa]		2380
Vel. UI Filter		0.764

Middle of the inlet to middle of outlet, 145 mm		**100 mm**
Max. Velocity [m/s]		64.8
Avg Static Pressure [Pa]		2520
Vel. UI Outlet		0.829
Pressure drop [Pa]		2200
Vel. UI Filter		0.722

The next parameter that was investigated was the placement of the filter. Using Concept 15 as a basis, the filter was placed near the outlet, near the inlet, and in the middle of the inlet and outlet, as illustrated in Figure 5.29.

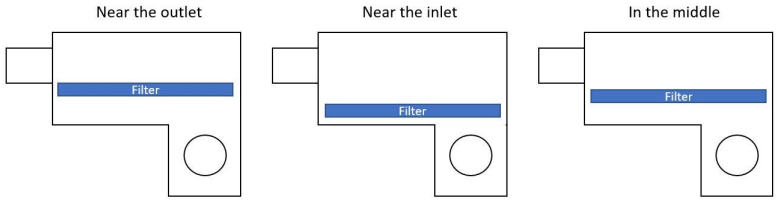

Figure 5.29: Illustration of various filter placements for rectangular box.

The results showed that the filter placed in the middle had the lowest pressure drop, as well as the greatest UI over the outlet and highest UI over the filter, as presented in Table 5.28.

Table 5.28: Three different filter placement and the values from CFD.

Filter placement	**Near the outlet**	**Near the inlet**	**In the middle**
Max. Velocity [m/s]	65.7	65	64.9
Avg Static Pressure [Pa]	2810	2870	2580
Vel. UI Outlet	0.822	0.827	0.835
Pressure drop [Pa]	2440	2520	2270
Vel. UI Filter	0.784	0.746	0.813

Furthermore, the impact of utilizing various filter thicknesses, as illustrated in Figure 5.30, for the filter box was investigated.

Figure 5.30: Illustration of various filter thickness sizes.

This was accomplished by simulating five different filter thicknesses, using Concept 15 once again as the basis. The results showed that the UI over outlet was greatest when using a 10 mm filter and lowest when using a 7 mm filter. The pressure drop was also found to be lowest with the 10 mm filter. However, the UI over filter was found to be greatest for the 3 mm and decreased as the filter thickness increased. Table 5.29 presents the simulation results.

Table 5.29: Six different filter thicknesses and the values from CFD.

Filter size [mm]	**3**	**5**	**7**	**10**	**15**	**40**
Max. Velocity [m/s]	64.9	63.8	64.8	63.7	63.2	63.9
Avg Static Pressure [Pa]	2580	2590	2520	2550	2530	2960
Vel. UI Outlet	0.835	0.849	0.829	0.858	0.844	0.833
Pressure drop [Pa]	2270	2310	2200	2310	2250	2620
Vel. UI Filter	0.813	0.736	0.722	0.69	0.672	0.512

To further explore additional parameters, the outlet position was tested in two new locations, to the right and in the middle. Placing the outlet further down was not considered as it would hinder airflow through the filter. Additionally, the impact of having an angled filter and rounded corners inside the air filter box was investigated and is shown in Figure 5.31.

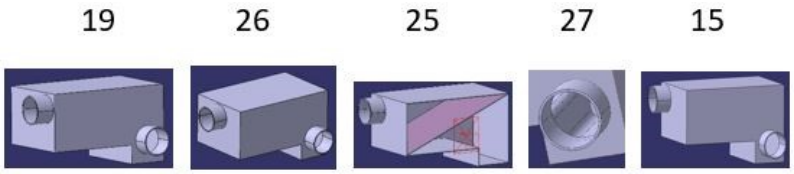

Figure 5.31: Concept 19, 26, 25, 27, and 15.

Despite testing these parameters, Concept 15 remained the top-performing configuration in terms of pressure drop and UI over the filter. It also had the second highest value in terms of UI over the outlet, as shown in Table 5.30. Note that in Concept 27 the inlet corner and outlet corner were not rounded.

Table 5.30: Other parameters and the values from CFD.

Concept number	**19**	**26**	**25**	**27**	**15**
Other paramets	**Outlet to the right**	**Outlet in the middle**	**Angled filter**	**Rounded corners**	**Normal**
Max. Velocity [m/s]	67.2	66.2	65.4	65.5	64.9
Avg Static Pressure [Pa]	2790	2810	2640	2780	2580
Vel. UI Outlet	0.816	0.824	0.837	0.824	0.835
Pressure drop [Pa]	2370	2450	2310	2390	2270
Vel. UI Filter	0.782	0.753	0.71	0.778	0.813

New concepts were developed by combining parameters that showed the potential to yield great values. Five new concepts with varying filter sizes were made. An illustration of the changed parameters is found in Figure 5.32.

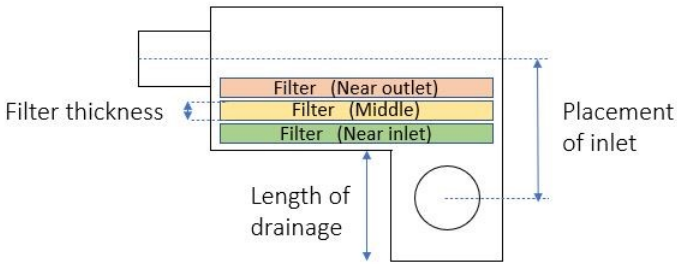

Figure 5.32: The different parameters for the rectangular concept.

Concept 33 emerged as the top performer, incorporating the most successful aspects of drainage shape, filter placement, filter size, and other relevant parameters. Notably, this concept achieved the highest UI over the filter by a significant margin. Meanwhile, Concept 32 boasted the highest UI over the outlet, while Concept 31 exhibited the lowest pressure drop. The results can be found in Table 5.31.

Table 5.31: Different parameters together and the values from CFD.

Concept number	**28**	**29**	**30**	**31**	**32**	**33**
Filter size	3 mm	5 mm	7 mm	10 mm	15 mm	3 mm
Length of drain shape	100 mm	50 mm	100 mm	100 mm	50 mm	50 mm
Placement of inlet	115 mm	100 mm	100 mm	145 mm	100 mm	100 mm
Filter placement	Near inlet	Near outlet	Middle	Near outlet	Middle	Middle
Placement of outlet	Middle	To the left	To the right	To the left	Middle	To the left
Rounded corners	Yes	No	No	Yes	No	No
Max. Velocity [m/s]	67.7	64.9	67.4	71.7	65.1	65.9
Avg Static Pressure [Pa]	2760	2760	2720	2510	2500	2680
Vel. UI Outlet	0.818	0.837	0.825	0.828	0.871	0.838
Pressure drop [Pa]	2390	2440	2360	2130	2320	2330
Vel. UI Filter	0.717	0.698	0.71	0.699	0.644	0.821

Upon realizing that the filter sizes used in the previous tests were unrealistically low, a more accurate test was conducted. As a result, a 40 mm filter thickness was employed to achieve a more accurate representation of the filter sizes commonly found in vehicles. Interestingly, the test results revealed that the filter size had a significant impact on the outcomes. However, the larger filter size required placement between the inlet and outlet, which eliminated alternative positions that were feasible with smaller filter sizes. Consequently, the test results were modified after implementing the 40 mm filter thickness, and these findings are presented in Table 5.32.

Table 5.32: Different parameters together with fixed filter size and the values from CFD.

Concept number	**28**	**29**	**30**	**31**	**32**	**33**
Filter size	40 mm	40 mm	40 mm	40 mm	40 mm	40 mm
Length of drain shape	100 mm	50 mm	100 mm	100 mm	50 mm	50 mm
Placement of inlet	115 mm	100 mm	100 mm	145 mm	100 mm	100 mm
Filter placement	Near inlet	Near outlet	Middle	Near outlet	Middle	Middle
Placement of outlet	Middle	To the left	To the right	To the left	Middle	To the left
Rounded corners	Yes	No	No	Yes	No	No
Max. Velocity [m/s]	66.5	64.7	64.8	73.8	64.7	65.4
Avg Static Pressure [Pa]	2500	2820	3080	2650	2620	2840
Vel. UI Outlet	0.867	0.819	0.831	0.821	0.849	0.818
Pressure drop [Pa]	2290	2450	2720	2290	2350	2440
Vel. UI Filter	0.512	0.529	0.503	0.572	0.536	0.56

The next test was connected to Section 4.2.1.1 where the restriction of pipe design was described. The literature review highlighted, in Section 4.2.1.1, that a pipe design with a flared end would result in less restriction compared to a design without one. Therefore, it was of interest to see the impact of rounded ends on both the UI and pressure drop. This is illustrated in Figure 5.33.

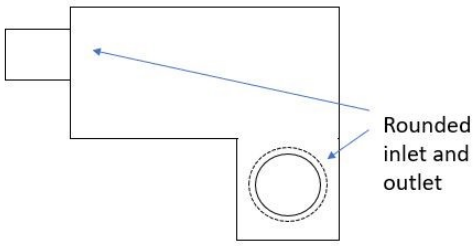

Figure 5.33: Illustration of rounded corners.

Table 5.33 presents the result from the simulations and clearly showed that the pressure drop was the main difference between the tests. Additionally, the UI over the outlet was also affected. Using a rounded corner on the outlet affect the UI over the outlet and the pressure drop decreased drastically by using the fillet on both outlet and inlet. Consequently, it could be assumed that all cases would benefit from using rounded corners in these places.

Table 5.33: Rounded and non-rounded inlet and outlet and the values from CFD.

Fillet corners	None	Only outlet	Both inlet and outlet
Max. Velocity [m/s]	67.9	71.6	74
Avg Static Pressure [Pa]	2550	1730	1460
Vel. UI Outlet	0.852	0.976	0.976
Pressure drop [Pa]	2310	1650	1380
Vel. UI Filter	0.525	0.523	0.55

5.9.3.2 Circular filter - Tube filter box

A tube-shaped concept, Concept 7, was developed with a round flat filter placed in the middle as the default setting. Although the pressure drop was low and the UI over the outlet was great, the UI over the filter could be improved. To achieve this Concept 8, shown in Figure 5.34), was created which included a ramp. This lead to a more even flow distribution over the filter.

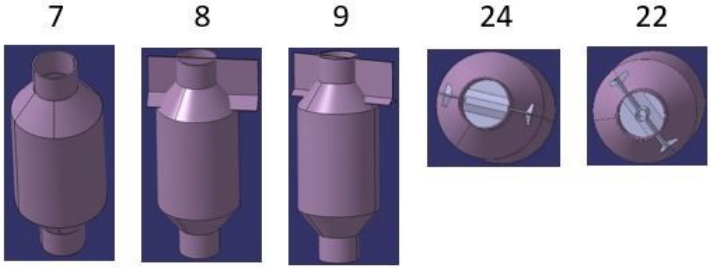

Figure 5.34: Concept 7, 8, 9, 24, and 22.

However, this came with a drawback, a significant increase in pressure drop. To mitigate this, Concept 9 was developed by reducing the edge of the ramp. This modification improved the UI over the filter, while simultaneously reducing the pressure drop as shown in Table 5.34.

Table 5.34: Tube formed box and the values from CFD.

Concept number	**7**	**8**	**9**	**24**	**22**
Tube formed	**Tube formed without ramp**	**Tube formed with ramp**	**Tube with smaller edge of ramp**	**Ramp with squared hole**	**Ramp with circular hole**
Max. Velocity [m/s]	49.8	68.7	56.9	50.1	60.1
Avg Static Pressure [Pa]	1100	1680	1390	1150	1470
Vel. UI Outlet	0.967	0.965	0.966	0.963	0.964
Pressure drop [Pa]	1070	1630	1350	1130	1430
Vel. UI Filter	0.7685	0.797	0.833	0.772	0.764

Then the placement of the filter was investigated for Concept 7, which was the default setting. An illustration of the placement of the filter within the air filter box is shown in Figure 5.35.

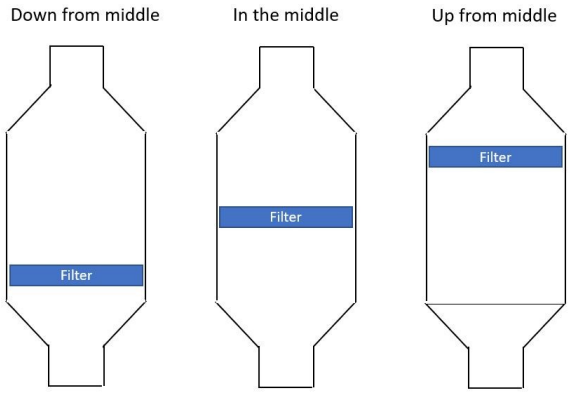

Figure 5.35: Illustration of various filter placements for tube formed box.

It was discovered that placing the filter in the middle of the air filter box yielded a higher UI over the filter compared to other placements. However, the UI over the outlet remained constant for all placements, and the pressure drop was nearly identical across all configurations. Further details regarding these findings are provided in Table 5.35.

Table 5.35: Filter placement for the tube formed box and the values from CFD.

Filter placement	**Filter placed 50 mm down from middle**	**In middle**	**Filter placed 50 mm up from middle**
Max. Velocity [m/s]	51,6	49.8	52
Avg Static Pressure [Pa]	1040	1100	1140
Vel. UI Outlet	0,967	0.967	0,969
Pressure drop [Pa]	1010	1070	1110
Vel. UI Filter	0,705	0.7685	0,715

The length of the box from the top to the bottom of the angled parts of the tube was examined as the next parameter. An illustration of this parameter is shown in Figure 5.37.

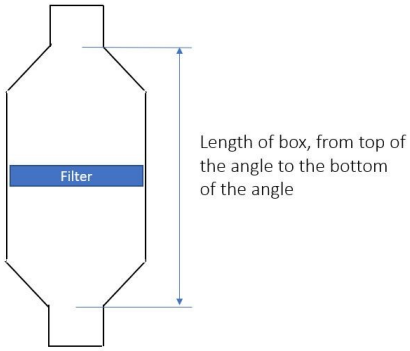

Figure 5.36: Illustration of length of the tube formed box.

Three different lengths were tested, as shown in Table 5.36. The simulation yielded similar UI over the outlet for all lengths, and the pressure drop was also relatively consistent. However, the longest concept had the highest UI value over the filter. It was also observed that the pressure drop decreased with increasing length. Surprisingly, the 250 mm length had a slightly lower UI value over the filter compared to the 200 mm length.

Table 5.36: Length of box to angle and the values from CFD.

Length of box to top of angle to bottom of angle	**300 mm**	**250 mm**	**200 mm**
Max. Velocity [m/s]	49.8	52.9	50
Avg Static Pressure [Pa]	1100	1130	1120
Vel. UI Outlet	0.967	0.969	0.962
Pressure drop [Pa]	1070	1090	1100
Vel. UI Filter	0.7685	0.669	0.712

Another parameter that was investigated was the length of the angle, illustrated in Figure 5.37.

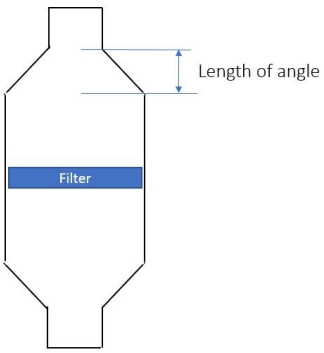

Figure 5.37: Illustration of the length of angle for the tube fromed concept.

Four cases were evaluated. The results, as shown in Table 5.37, indicated that a length of 50 mm resulted in a greater UI over the outlet, with the UI decreasing when the length decreased. Similar observations were made for the UI over the filter. However, the pressure drop was found to be lowest for the shortest angle length.

Table 5.37: Length of angle and the values from CFD.

Length of angle	50 mm	35 mm	25 mm	15 mm
Max. Velocity [m/s]	49.8	53.8	54.6	56.2
Avg Static Pressure [Pa]	1100	1230	1380	734
Vel. UI Outlet	0.967	0.957	0.947	0.914
Pressure drop [Pa]	1070	1180	1320	679
Vel. UI Filter	0.7685	0.708	0.692	0.531

For the final test, the filter size was kept fixed to observe changes in the other parameters. Simulations were conducted using parameter values that were expected to give greater results in terms of UI and lower pressure drop. An illustration of the parameters is shown in Figure 5.38.

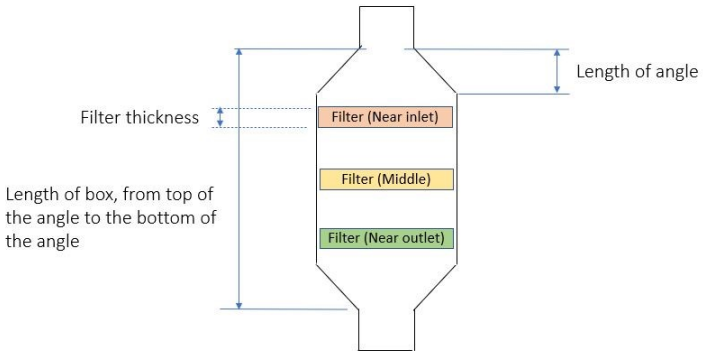

Figure 5.38: The different parameters for the tube shaped concept.

It showed that Concepts 36 and 38, which had the same angle length and the same tube length performed almost equally. As expected, Concept 38 had a higher pressure drop due to the ramp, but it also created a more even airflow through the filter. On the other hand, Concept 36 had a higher UI over the outlet, even though it was almost the same as that of Concept 38. The values from the simulation are shown in Table 5.38.

Table 5.38: Different parameters together and the values from CFD.

Concept number	34	35	36	37	38	39
Filter size	40 mm	40 mm	40 mm	40 mm	40 mm	40 mm
Length of angle	35 mm	25 mm	50 mm	15 mm	50 mm	50 mm
Filter placement	Middle	Up	Down	Middle	Up	Middle
Length of tube to angle end	250 mm	200 mm	300 mm	250 mm	300 mm	300 mm
Include ramp	Yes	Yes	No	No	Yes	Yes
Max. Velocity [m/s]	56.5	60.7	51.5	56.7	55.9	55.9
Avg Static Pressure [Pa]	2800	3460	1970	2690	2300	2370
Vel. UI Outlet	0.947	0.921	0.966	0.863	0.963	0.962
Pressure drop [Pa]	2750	3390	1950	2560	2270	2340
Vel. UI Filter	0.623	0.61	0.643	0.631	0.684	0.629

5.9.3.3 Circular filter - Half tube filter box

A half tube shape was also considered and tested on the configurations shown in Figure 5.39.

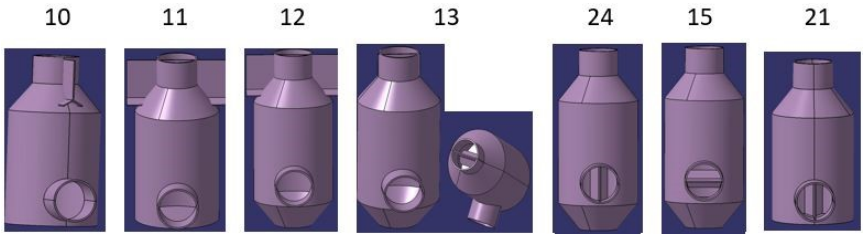

Figure 5.39: Concept 10, 11, 12, 13, 24, 15, and 21.

The half tube concept was approached differently due to time limitations. It was decided to alter one variable at a time. Initially, Concept 10 was developed, featuring a ramp facing the same direction as the outlet. Subsequently, Concept 11 was created with the ramp positioned opposite to the outlet. Upon comparing these two concepts, it was observed that Concept 10 yielded the highest UI over the filter, along with the lowest pressure drop and highest UI over the outlet. Furthermore, Concepts 14 and 15, which differed solely in the direction of the ramp, exhibited similar results. The concept with the ramp aligned with the outlet (Concept 14) performs optimally across all three measurements.

Concepts 10 and 21 differed in their inlet and outlet placements. It was observed that the inlet placement for Concept 10 achieved a higher UI over the filter and a lower pressure drop, while Concept 21 had a higher UI over the outlet. The difference between Concepts 11 and 12 was that Concept 12 was longer and had an angle. Concept 12 performed slightly better in terms of UI over the outlet, pressure drop and UI over the filter. Concept 13, which had the ramp rounded at the corners, performed best in terms of pressure drop and UI over the filter. Furthermore, it had one of the highest UI over outlet as shown in Table 5.39.

Table 5.39: Half tubed formed concepts and the values from CFD.

Concept number	**10**	**11**	**12**	**13**	**14**	**15**	**21**
Max. Velocity [m/s]	59.9	61.4	61.6	58	76.2	113	123
Avg Static Pressure [Pa]	2060	2160	2270	1210	2110	2180	2270
Vel. UI Outlet	0.856	0.783	0.839	0.965	0.97	0.961	0.968
Pressure drop [Pa]	1820	1860	1990	1180	2020	2130	2220
Vel. UI Filter	0.796	0.77	0.79	0.82	0.742	0.713	0.773

5.9.4 Summary of CFD simulations for flat filters

A summary for the simulations of the flat air filter boxes is presented below.

5.9.4.1 Rectangular filter box with rectangular filter

- The initial test, shown in Table 5.25, which was conducted by changing outlet position showed that placing the outlet further from the inlet resulted in a higher UI over the filter, less pressure drop, and higher UI over the outlet.

- When the inlet position was adjusted along the z-axis, the UI over the outlet varied slightly. The pressure drop varied more, although not significantly and

the UI over outlet varied slightly, as shown in Table 5.26.

- The filter placement in the middle was performing best when it came to UI over the filter, pressure drop, and UI over the outlet. The less successful placements were near the outlet and had the worst pressure drop and UI over the filter, as shown in Table 5.28.

- When different filter sizes were tested, shown in Table 5.29, the factor that varied the most was the UI over the filter, it increased as the filter size decreased.

- The rounded corners on the outlet and inlet lead to a significant difference in terms of pressure drop, shown in Table 5.31. The rounded corners on the outlet also contributed to less pressure drop.

Table 5.40 was created to get an overview of which parameters had the most impact on pressure drop, UI for the outlet, and UI over the filter. The colors represent how much each parameter impacted the outcome.

Table 5.40: Color-scheme of impact of different parameters for the rectangular concept.

Rectangular shape			
Tested parameters	**Pressure drop**	**UI outlet**	**UI filter**
Inlet position in z-axis			
Outlet position in x-axis			
Shape of drainage			
Filter placement			
Filter size			
Fillet corners outlet			
Fillet corners inlet			

Scale	**1.15**	**1.1**	**1.05**	**1.01**
Color				

5.9.4.2 Tube filter box with flat circular filter

- The tube shaped concept without a ramp gave a higher value for UI over the outlet and also a lower pressure drop. Meanwhile, adding a ramp to the concept resulted in that the pressure drop increased significantly but the UI over filter became much higher. This is shown in Table 5.34

- When investigating the filter placement, shown in Table 5.35, the UI over the filter was significantly higher when placing the filter in the middle. However, the UI over the outlet and pressure drop did not change much.

- The length of the box, investigated in Table 5.36, from the top of the angle to the bottom of the angle, gave the best result for UI over the filter when it was the longest. It also resulted in a small decrease in pressure drop while the UI over outlet was similar for all tested lengths.

- The test for the length of the angle showed that the UI over the filter and UI over the outlet got higher when the length increased. However, the pressure drop did not have a clear correlation to the length. This is shown in Table 5.36.

- The final test of concept showed that the pressure drop increased when a ramp was included, shown in Table 5.38. The test also showed that the UI over the filter was highest with the concept with the longest angle. It also had low pressure drop at the longest angle.

Table 5.41 was created to get an overview of the parameters that had the most impact on pressure drop, UI for the outlet, and UI over the filter. The colors represent how much each parameter impacted the outcome.

Table 5.41: Color-scheme of impact of different parameters for the tube formed concept.

Tube shape			
Tested parameters	**Pressure drop**	**UI outlet**	**UI filter**
Using ramp (7 & 9)			
Filter placement			
Length of box			
Length of angle			

Scale	**1.15**	**1.1**	**1.05**	**1.01**
Color				

5.9.4.3 Half tube filter box with circular filter

- The initial test showed that placing the ramp along the z-axis gave better output values compared with placing it along the x-axis, see Concept 14 and 15 in Table 5.39 as reference.

- By having a longer part with an angle near the outlet slightly improved the output values, which is presented in Table 5.39.

- Adding rounded corners to the ramp resulted in that the values of UI over the outlet and the filter increased while the pressure drop decreased, also shown in Table 5.39.

Table 5.42 was created to get an overview of the parameters that had the most impact on pressure drop, UI for the outlet, and UI over the filter. The colors represent how much each parameter impacted the outcome.

Table 5.42: Color-scheme of impact of different parameters for the half tube formed concept.

Half tube shape			
Tested parameters	**Pressure drop**	**UI outlet**	**UI filter**
Rounded instead of flat at one end (11 & 12)			
Ramp in different directions (10 & 11)			
Inlet and outlet are reversed (12 & 15)			
Rounded ramp (12 & 13)			

Scale	**1.15**	**1.1**	**1.05**	**1.01**
Color				

5.9.5 Developed Concepts

Based on the parameters that resulted in the best outcome for UI and pressure drop in the simulations, one concept was developed for each of the following shapes: round, oval, rectangular, tube, and half tube. The placement of the air filter boxes was chosen by identifying the location within the available space that provided the largest volume for the given shape. Figure 5.40 shows the round filter placement that used the largest volume, which used the "Chosen parameters" presented in Table 5.23.

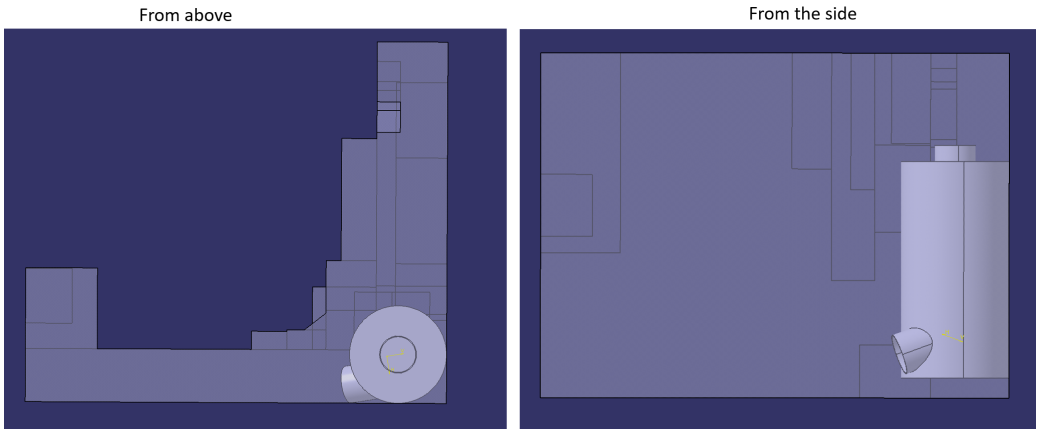

Figure 5.40: Concept round air filter box.

The placement for the oval shaped air filter box was different, shown in Figure 5.41. The same values for the simulated parameters were used, "Chosen parameters" presented in Table 5.23. The round concept had a larger volume for both the air filter box and the air filter compared to the oval shaped concept. However, the oval filter had a shorter way to the resonator and the inlet was placed higher. To evaluate these concepts further, the duct bellow needed to be taken into consideration.

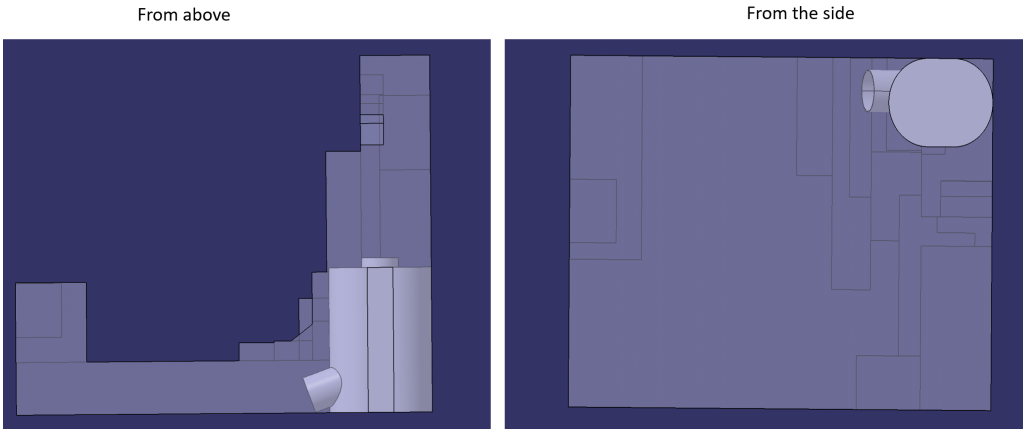

Figure 5.41: Concept oval air filter box.

The placement for the rectangular shaped concept is shown in Figure 5.42. The rectangular shape had a limitation in height since the available space didn't allow it to be longer in the z-axis. However, it could be wider compared to the tube- and half tube concepts.

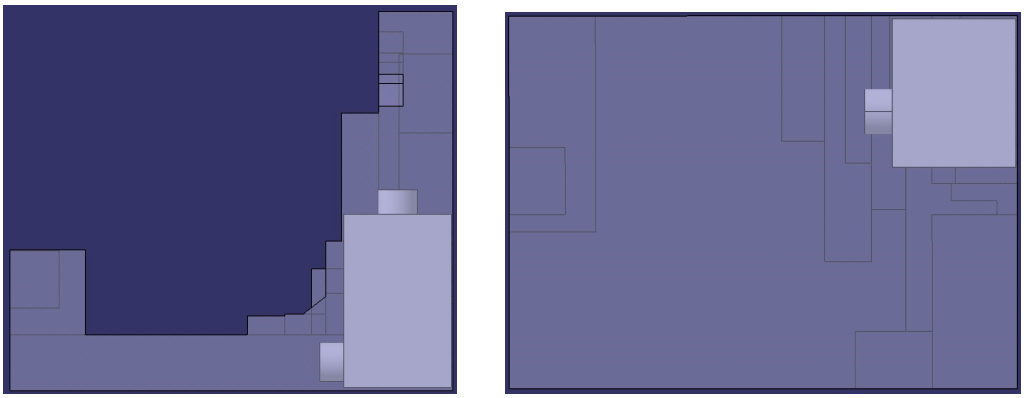

(a)
Top view rectangular concept.

(b)
Side view rectangular concept.

Figure 5.42: Rectangular filter box placement.

The placement for the tube shaped concept is found in Figure 5.43. The tube shaped concept was longer than the other flat filter concepts. However, the tube shaped concept needed to be placed further down to create space for the duct bellow.

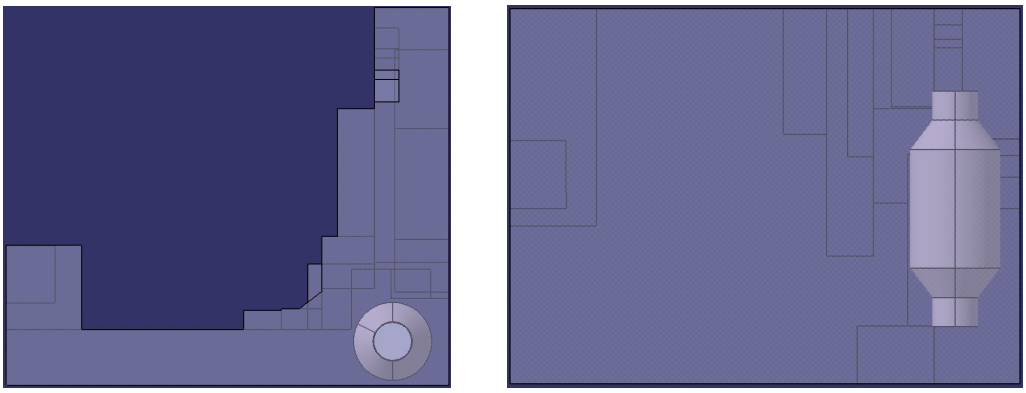

(a) Top view tube concept.

(b) Side view tube concept.

Figure 5.43: Tube filter box placement.

The placement for the half tube shaped is found in Figure 5.44. The half tube shaped concept could be placed further up than the tube concept since the outlet was placed on the side. However, it had the same width and was shorter compared to the tube shaped concept.

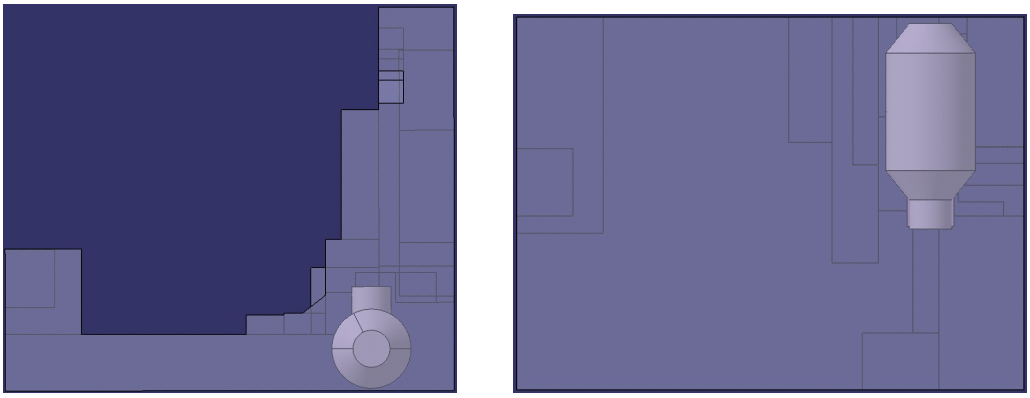

(a) Top view half tube concept.

(b) Side view half tube concept.

Figure 5.44: Half tube filter box placement.

5.9.6 Simulations of duct bellow

Simulations were conducted for the duct bellow to find values for the different design parameters, which can be found in Table 5.43. The baseline for the simulation is represented by the orange cells. Parameters were investigated individually, with the investigated parameter varying based on the values presented in Table 5.43, while the other parameters maintained their respective orange-highlighted values.

Table 5.43: Duct bellow parameters.

Parameter	Value 1	Value 2	Value 3
Height [mm]	8	10	12
Width of bellow [mm]	2	4	6
Angle of bellow [deg]	30	45	60
Number of bellows	8	12	16
Number of sections	1	2	
Space between bellows [mm]	0	1	2

Figure 5.45 shows an illustration of the orange cell values. The shape of the duct bellow remained the same across all tests to make a fair comparison.

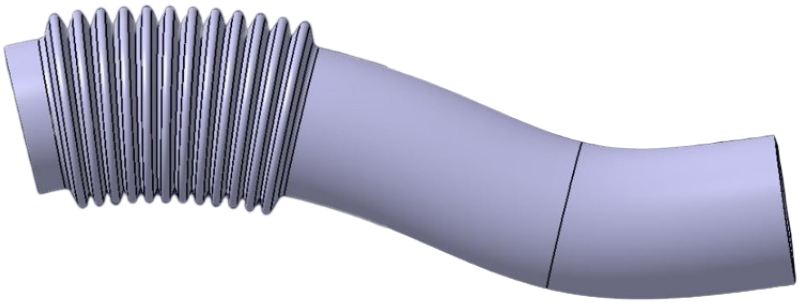

Control Parameters	
A	Height [mm]
B	Width of bellow [mm]
C	Space between bellows [mm]
D	Angle of bellow [deg]
E	Number of bellows
F	Number of section

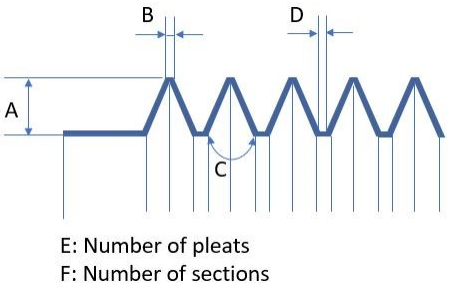

(a) Illustrated parameters for the duct bellow

Figure 5.45: Investigated parameters for the duct bellow.

The initial simulations for the duct bellow investigated the height of the bellows. Three different heights were tested: 8 mm, 10 mm, and 12 mm. The output values examined were the UI over the outlet and the pressure drop. The results showed that the height of 8 mm both had the lowest pressure drop and the greatest UI over outlet compared to the other output values, while the height of 12 mm had the greatest pressure drop and lowest UI over the outlet. All the values can be found in Table 5.44.

Table 5.44: Test of heights for duct bellow.

Parameter	Test 1	Test 2	Test 3
Height [mm]	**8**	**10**	**12**
Max. Velocity [m/s]	62.5	65.8	67.6
Avg Static Pressure [Pa]	560	729	891
Vel. UI Outlet	0.906	0.896	0.891
Pressure drop [Pa]	497	643	785

The results from the test with different widths for the bellows can be found in Table 5.45. The output values showed that the narrowest width had the lowest pressure drop and greatest UI over the outlet. As the width increased, the output values had a higher pressure drop and a lower UI over the outlet.

Table 5.45: Test of widths of bellow.

Parameter	Test 1	Test 2	Test 3
Width of bellow [mm]	**2**	**4**	**6**
Max. Velocity [m/s]	65.8	68.9	70.1
Avg Static Pressure [Pa]	729	924	1010
Vel. UI Outlet	0.896	0.879	0.878
Pressure drop [Pa]	643	814	880

The angle of the bellows also had an affect on the output values. A lower angle resulted in a greater UI over the outlet and a lower pressure drop. Among the tested angles, 30 degrees had the lowest pressure drop and the greatest UI over the outlet. Conversely, an angle of 60 degrees, the largest tested angle, had the highest pressure drop and the lowest UI over the outlet. All values can be found in Table 5.46.

Table 5.46: Test of angle of bellows for duct.

Parameter	Test 1	Test 2	Test 3
Angle of pleat [deg]	**30**	**45**	**60**
Max. Velocity [m/s]	63	65.8	68.6
Avg Static Pressure [Pa]	562	729	908
Vel. UI Outlet	0.901	0.896	0.884
Pressure drop [Pa]	498	643	794

The test for the number of bellows was conducted with 8, 12, and 16 bellows. When using 8 bellows, the pressure drop was the lowest and the UI over the outlet was the greatest. Conversely, when using 16 bellows, the results were the opposite. The pressure drop exhibited the most significant change, almost halving when comparing the values from using 16 to 8 bellows. The values for all different numbers of bellows can be found in Table 5.47.

Table 5.47: Test of the number of bellows for duct.

Parameter	Test 1	Test 2	Test 3
Number of pleats	**8**	**12**	**16**
Max. Velocity [m/s]	61.5	65.8	68.4
Avg Static Pressure [Pa]	498	729	925
Vel. UI Outlet	0.911	0.896	0.887
Pressure drop [Pa]	442	643	816

The test for the number of sections was conducted by dividing the 12 bellows into either one or two sections. In the case of two sections, the bellows were placed six bellows at the beginning of the duct and six at the end. Both the pressure drop was lower and the UI over the outlet was greater when the bellows were placed in a single section compared to two sections.

Table 5.48: Test of the number of sections for duct bellow.

Parameter	Test 1	Test 2
Number of sections	**1**	**2**
Max. Velocity [m/s]	65.8	73.9
Avg Static Pressure [Pa]	729	2030
Vel. UI Outlet	0.896	0.77
Pressure drop [Pa]	643	1600

The final test aimed to determine how the distance between the bellows impacted the outcome for UI over the outlet and the pressure drop. The result from the test, presented in Table 5.49, showed that a distance of 1 mm had the lowest pressure drop. However, a distance of 2 mm had the greatest UI over the outlet.

Table 5.49: Test of the space between bellows.

Parameter	Test 1	Test 2	Test 3
Space between bellows [mm]	**0**	**1**	**2**
Max. Velocity [m/s]	65.8	64.7	64.3
Avg Static Pressure [Pa]	729	696	701
Vel. UI Outlet	0.896	0.901	0,903
Pressure drop [Pa]	643	617	622

A color scheme was created to visualize the impact of different parameters on the outcome, shown in Table 5.50. Every parameter except the space between bellows had a large impact on the pressure drop. The UI over the outlet was less affected by the parameters. The parameter that affected the UI the most was the number of sections for the bellows and the number of bellows. All other parameters that were tested had an impact of approximately 1% or less.

Table 5.50: Color-scheme of the impact of different parameters for the duct bellow.

Duct bellow		
Tested parameters	**Pressure drop**	**UI outlet**
Height		
Angle of bellows		
Width on bellows		
Number of bellows		
Number of sections		
Space between bellow		

Scale	**1.15**	**1.1**	**1.05**	**1.01**
Color				

After evaluating each parameter one by one, the values shown in Table 5.51 were selected. These values were all used in a final simulation of the duct bellow and

the output values are shown in Table 5.51. The output values outperformed all the previous tests for the duct bellow. These values for the parameters are going to be used in future duct bellows when they are designed for the different air filter boxes.

Table 5.51: Chosen values for the parameters of the duct bellow.

Parameter	Value
Height [mm]	8
Width of bellow [mm]	2
Angle of bellow [deg]	30
Number of bellows	8
Number of sections	1
Space between bellows [mm]	1
Max. Velocity [m/s]	57.3
Avg Static Pressure [Pa]	325
Vel. UI Outlet	0.918
Pressure drop [Pa]	285

5.9.7 Simulation of combinations of duct bellow and air filter box

The duct bellow needed to be modified depending on where the air filter box was placed. Therefore, specific duct bellows were designed to fit within the space constraint and connect with the resonator for each air filter box, as mentioned in Section 5.6. All the duct bellows used the values presented in Table 5.51. Simulations were then performed for the whole "unit", consisting of the air filter, air filter box, and duct bellow.

5.9.7.1 Round air filter box & duct bellow

In Figure 5.46 the round concept with the duct bellow is shown. The duct bellow in this concept needed to have a sharp turn in the beginning to fit in the space constraint.

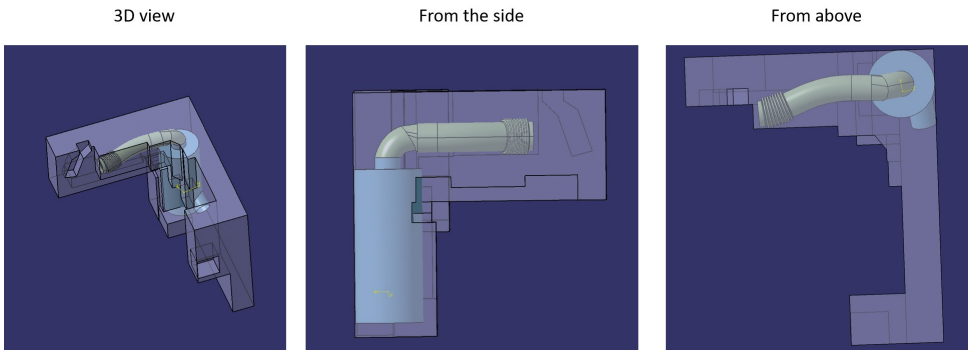

Figure 5.46: Round filter & duct bellow.

This was then simulated, and the results and a velocity graph are shown in Figure 5.47. The result that was most affected by combining the air filter box and duct bellow was the UI over the MAF sensor. The combined version resulted in a UI of 0.898, while the UI for the MAF with only the air filter box was approximately

0.96-0.97, shown in Table 5.23. The sharp turn makes the airflow faster in the inner curve compared to the outer curve which creates a lower UI before the turn.

Max. Velocity [m/s]	66
Avg Static Pressure [Pa]	2380
UI filter	0.633
Vel. UI Outlet	0.887
Pressure drop [Pa]	2190
UI MAF	0.898

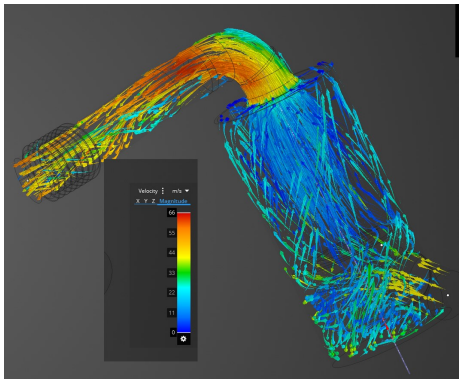

(a) Velocity graph for the round concept.

Figure 5.47: Round air filter box & duct bellow simulation.

To improve the UI over the MAF sensor, the UI was examined at different distances from the air filter box. In this concept, it was 30 mm between the air filter box and the start of the turn. Therefore, a test was conducted to see how the UI changes depending on the distance between the MAF sensor placement and the turn. The test showed that the UI increases when the distance from the turn increases. The values from the test are shown in Table 5.52.

Table 5.52: Test of UI for possible MAF positions.

UI right before turn	0.898
UI middle (15 mm from turn)	0.916
UI right after air filter box (30 mm from the turn)	0.959

To improve the UI even further, the length of the straight duct was increased from 30 mm to 60 mm. The space constraint allowed this change, 60 mm was the maximum length with the current air filter box. This change resulted in an increase of the UI over the MAF sensor for all the positions from the original concepts shown in Table 5.52. With a longer straight duct, the UI of the MAF sensor was not as sensitive to where it was placed. The UI right before the turn improved from 0,898 to 0,946 and the UI right after the air filter box improved from 0,959 to 0,982. The pressure drop between the two different straight duct lengths was also affected, improving from 2190 with a 30 mm duct to 1890 with a 60 mm duct. UI for both the filter and outlet of the duct bellow remained unaffected between the two straight duct lengths. All the results are shown in Figure 5.48.

Max. Velocity [m/s]	73.7
Avg Static Pressure [Pa]	2070
UI filter	0.634
Vel. UI Outlet	0.873
Pressure drop [Pa]	1890
UI MAF before turn	0.946
UI middle (30 mm from turn)	0.963
UI right after air filter box (60 mm from the turn)	0.982

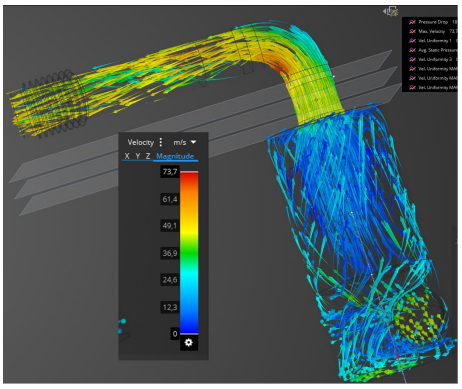

(a) Velocity graph for round concept with a longer straight duct.

Figure 5.48: Round air filter box & duct bellow simulation with longer straight duct.

In the final test for the circular shaped air filter box, the duct was modified by having an angle at the beginning of the duct. By setting an angle that early in the duct, the steepness of the turn was reduced compared to the previous ducts. However, the UI result for the MAF sensor positions became worse in all positions compared to the straight ducts. The results are shown in Figure 5.49.

Max. Velocity [m/s]	65.1
Avg Static Pressure [Pa]	2450
UI filter	0.637
Vel. UI Outlet	0.882
Pressure drop [Pa]	2240
UI right after air filter box (40 mm from the steep turn)	0.913
UI MAF middle (20 mm from the steep turn)	0.882
UI MAF before turn	0.879

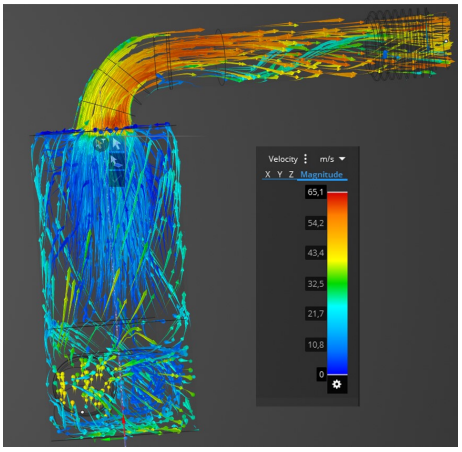

(a) Velocity graph for round concept with an angled duct.

Figure 5.49: Round air filter box & duct bellow simulation with angled duct.

Comparing the second simulation, shown in Figure 5.48, to the final simulation of the air filter box, the "Chosen parameters" are shown in Table 5.23, the pressure drop went from 1260 Pa to 1890 Pa. The UI for the filter was 0,683 for the "Chosen parameters" and decreased to 0,634 when the duct bellow was added. With the change in length of the straight duct out from the air filter box, the UI went from 0.966, in "Chosen parameters" to 0.963 with the duct bellow which was nearly identical. Both these values were measured 30 mm from the air filter box.

5.9.7.2 Oval air filter box & duct bellow

Figure 5.50 shows the oval shaped concept and the duct bellow that was developed for it. The oval shape created a possibility to place it higher in the engine compared to the round air filter box. The same values for the tested design parameters were used for the oval shaped air filter box as the round air filter box. The duct bellow was much shorter compared to the duct bellow used for the round air filter box. There were not any sharp turns needed for the bellow to reach the resonator.

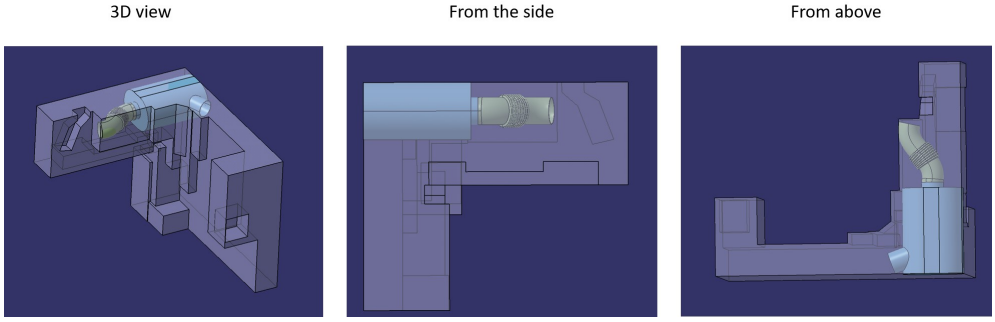

Figure 5.50: Oval filter & duct bellow.

Figure 5.51 shows the result from the CFD simulation. The UI for the MAF sensor, for all positions, were very even, ranging between 0.966 and 0.953. The pressure drop was 2240 Pa which was slightly higher compared to the round air filter box. UI for the outlet to the resonator was 0.893 and UI for the filter was 0.627.

Max. Velocity [m/s]	67.8
Avg Static Pressure [Pa]	2510
UI filter	0.627
Vel. UI Outlet	0.893
Pressure drop [Pa]	2240
UI MAF right after air filter box(30 mm from turn)	0.966
UI MAF Middle (15 mm from turn)	0.961
UI MAF right before turn	0.953

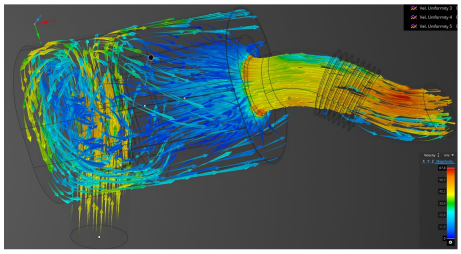

(a) Velocity graph for the oval concept.

Figure 5.51: Oval air filter box & duct bellow simulation.

5.9.7.3 Rectangular air filter box & duct bellow

The configuration of the rectangular concept is shown in Figure 5.52 along with the duct bellow. As shown, the duct bellow for this concept was relatively short. This made the placement of bellows limited for this design. It was also decided to not put the bellows in any curve since the benchmarking of other duct bellows, Section 5.1, had no bellows directly on a curvature. From the literature review, Section 4.2.1.1, the angle of the duct should be around 30 degrees to give less restriction of airflow if the duct can not be straight, which served as a guideline for the duct design for this concept.

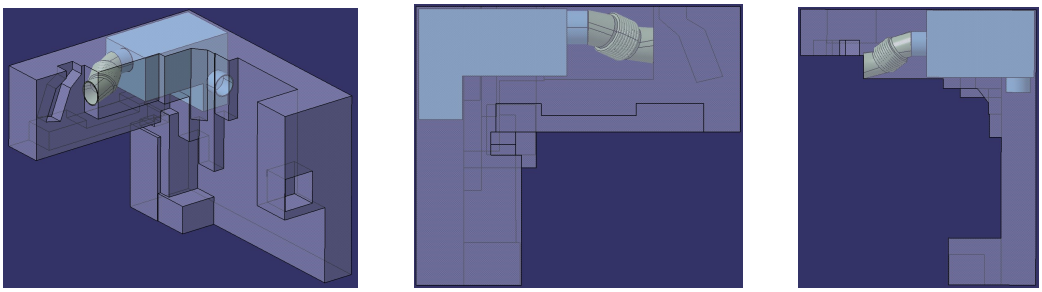

(a) 3D view rectangular concept.

(b) Side view rectangular concept.

(c) Top view rectangular concept.

Figure 5.52: Rectangular filter box & duct bellow.

It was noticeable that the values changed when conducting the simulation with and without the duct bellow. The values from the simulation without the duct bellow can be found in Table 5.53a and the values including the duct bellow can be found in Table 5.54a. The UI for the outlet and MAF sensor were slightly higher for the concept without the duct bellow compared to when the duct bellow was included. The UI over the filter was higher when including the duct bellow but the pressure drop increased. By comparing the presented velocity graphs in Figure 5.53 and Figure 5.54b it is shown that the velocity graphs were similar. As soon as the air goes through the duct bellow, the velocity drastically increases.

(a) Values without duct bellow.

Max. Velocity [m/s]	66.7
Avg Static Pressure [Pa]	1290
Vel. UI Outlet	0.974
UI filter	0.638
Pressure drop [Pa]	1200
UI MAF	0.967

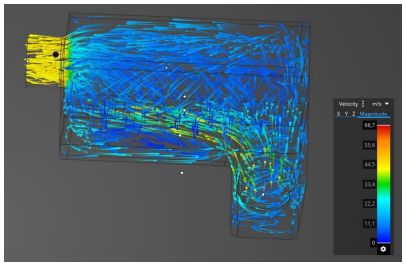

(b) Velocity graph for tube concept.

Figure 5.53: Tube air filter box & duct bellow simulation.

(a) Values with duct bellow.

Max. Velocity [m/s]	71.2
Avg Static Pressure [Pa]	2160
Vel. UI Outlet	0.878
UI filter	0.647
Pressure drop [Pa]	1760
UI MAF	0.955

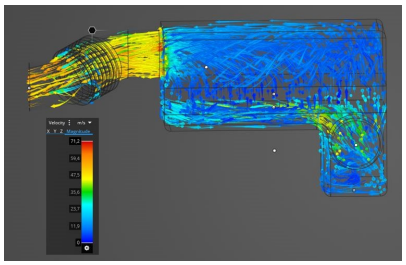

(b) Velocity graph for tube concept.

Figure 5.54: Tube air filter box & duct bellow simulation.

5.9.7.4 Tube air filter box & duct bellow

The design of the duct bellow for the tube shaped concept was significantly longer than for the rectangular shaped concept. It also needed a steeper turn to stay inside the design space. The bellow was placed on the straight path a distance away from the curve since the curve could lead to airflow restriction. There is also a long straight path before the curvature. This decision was influenced by the test conducted for the round air filter box, which indicated that placing the MAF sensor further from the curve would result in a higher UI. The placement and shape are shown in Figure 5.55.

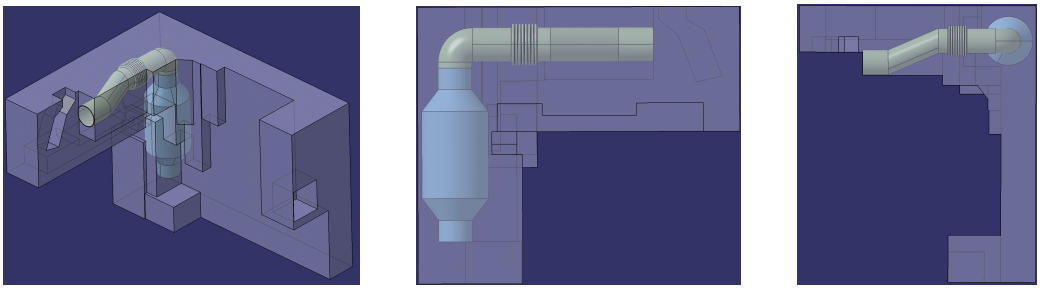

(a) 3D view rectangular concept.

(b) Side view rectangular concept.

(c) Top view rectangular concept.

Figure 5.55: Tube filter box & duct bellow.

A comparison was also made between the tube shaped concept with and without the duct bellow. The differences when adding the duct bellow were that the pressure drop increased and the UI for the MAF sensor increased as well. This is shown in Table 5.56a and Table 5.57a. The velocity is shown in Figure 5.60 and Figure 5.57. It showed that the highest velocity when not using a duct bellow occurred near the rounded corners close to the outlet. When using the duct bellow the highest velocity occurred in the curve instead.

(a) Values without duct bellow.

Max. Velocity [m/s]	52.2
Avg Static Pressure [Pa]	1470
Vel. UI Outlet	0.983
UI filter	0.897
Pressure drop [Pa]	1470

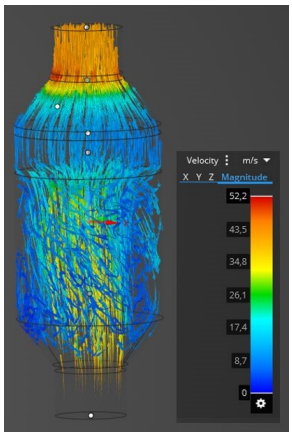

(b) Velocity graph for tube concept.

Figure 5.56: Tube air filter box & duct bellow simulation.

(a) Values with duct bellow.

Max. Velocity [m/s]	86.2
Avg Static Pressure [Pa]	2380
Vel. UI Outlet	0.903
UI filter	0.907
Pressure drop [Pa]	2300
UI MAF	0.963

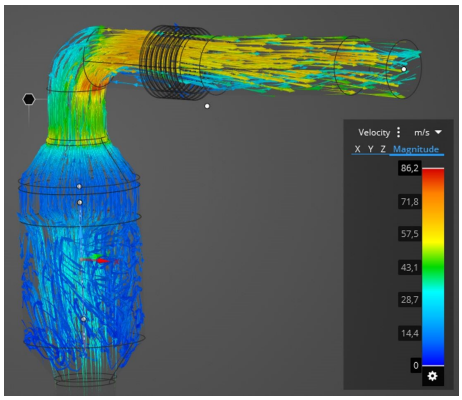

(b) Velocity graph for tube concept.

Figure 5.57: Tube air filter box & duct bellow simulation.

5.9.7.5 Half tube air filter box & duct bellow

The half tube shaped duct bellow had a rise in the z-direction and also a small angle to reach the resonator. Otherwise, the duct bellow was relatively straight with a slight curvature. The placement and shape can be found in Figure 5.58.

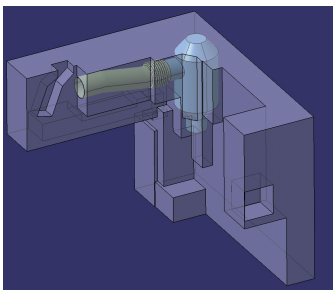

(a) 3D view half tube concept.

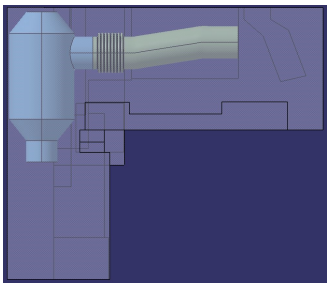

(b) Side view half tube concept.

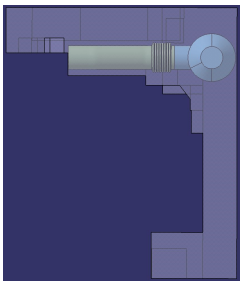

(c) Top view half tube concept.

Figure 5.58: Half tube filter box & duct bellow.

For this concept, the placement of the bellows was tested in two locations, to assess the impact on the outcome. One bellow set was placed near the box and one further away. The one near the box is shown in Figure 5.60b and the one away from the box is shown in Figure 5.61b. The half tube concept without duct had the highest velocity near the inlet and outlet, shown in Figure 5.59b, which also was the case when adding the duct. The pressure drop was higher for the concept that had the bellows near the box compared to the concept with the bellows away from the box.

(a) Values with duct bellow near the box.

Max. Velocity [m/s]	57.8
Avg Static Pressure [Pa]	1840
UI filter	0.839
Vel. UI Outlet	0.973
Pressure drop [Pa]	1800
UI MAF	0.978

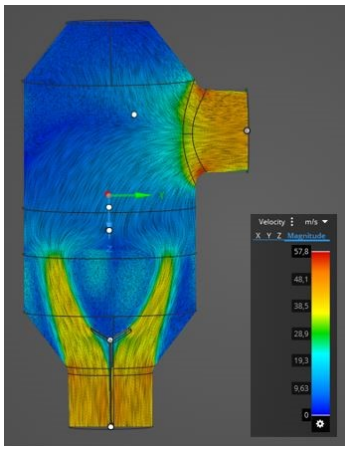

(b) Velocity graph for half tube concept.

Figure 5.59: Half tube air filter box & duct bellow simulation.

When comparing the bellow placement, it was noticed that having the bellows further away from the outlet would create less pressure drop, however, the UI over the outlet got lower. While the UI over filter was nearly the same.

(a) Values for half tube air filter box with duct bellow near the box.

Max. Velocity [m/s]	58
Avg Static Pressure [Pa]	2150
Vel. UI Outlet	0.947
UI filter	0.833
Pressure drop [Pa]	2150
UI MAF	0.976

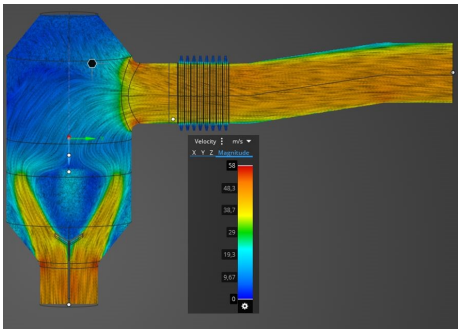

(b) Velocity graph for half tube concept with duct bellow near the box.

Figure 5.60: Half tube air filter box & duct bellow near the box simulation.

(a) Values for half tube air filter box with duct bellow away from the box.

Max. Velocity [m/s]	55.6
Avg Static Pressure [Pa]	2010
UI filter	0.84
Vel. UI Outlet	0.922
Pressure drop [Pa]	1960
UI MAF	0.977

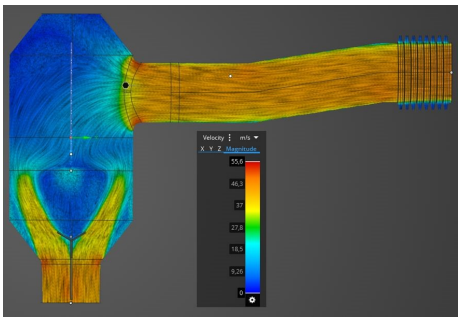

(b) Velocity graph for half tube concept with duct bellow away from the box.

Figure 5.61: Half tube air filter box & duct bellow away from box simulation.

5.10 Pugh matrix

To evaluate the concepts against each other, Pugh matrices were conducted. The Pugh matrices were divided into one matrix for the round/oval air filter boxes and one matrix for the flat air filter boxes. The reason for two separate Pugh matrices were that the coordination system in the CFD software differed between the round/oval filter type compared to the flat filter type. To be able to have a fair comparison, they were split into two matrices.

5.10.1 Pugh matrix round and oval filters

The Pugh matrix of the comparison between the round concept and the oval concept can be found in Table 5.53. The UI values for both the MAF sensor and the filter for the round concept are shown in Figure 5.48, and for the oval concept, in Figure 5.51. For the round concept, the UI for the MAF was 0.963 and UI for the filter was 0.634. For the oval concept, the UI for the MAF sensor was 0.966 and the UI for the filter was 0.627. The oval concept had a better performance in terms of the UI over the MAF sensor and the round concept performed better in terms of the UI over the filter.

The placement of the dirty side duct had a higher score on the oval concept. The reason for this was that the dirty side duct needs to start in a high position to be over the water wading line, the height that a vehicle can drive underwater. The inlet in the air filter box for the oval concept is placed higher which means that the dirty side duct could be shorter compared to the round concept.

The drainage possibilities for the round concept was better than for the oval concept. This was due to that the round concept was placed vertically and the oval filter was placed horizontally. The water is affected by gravity and therefore would a vertical placement of the air filter box perform better for drainage.

The cost for the two concepts has been estimated by comparing the volume for the concepts, as the material choice was out of the scope of the project. Therefore, the oval concept performed better because it had a lower volume compared to the round concept.

The filter volume was better for the round concept. The volume for the round concept was 0.0051 m^3 compared to the oval concept which had a filter volume of 0.0031 m^3.

Pressure drop for the round concept can be found in Figure 5.48 and for the oval concept in Figure 5.51. The pressure drop for the round concept was 1890 Pa and for the oval concept 2240 Pa. The round concept was therefore outperforming the oval concept in terms of pressure drop.

The changeability, the manufacturability and the attachment points were considered equal for both the round concept and the oval concept. The reason was that it was not any distinct advantages or disadvantages between the concepts in these criteria. The changeability, which refers to the ease of changing the filter, was considered equal for both concepts as they both required an attachment point in the middle of the air filter box. The manufacturability was also considered equal since the shapes of the two concepts were similar, suggesting a similar level of difficulty in manufacturing. In terms of attachment points, The air filter box needed to have attachment points on the long side parallel to the duct bellow. Both concepts had their longest surface towards that attachment side which made the concepts equal in the comparison.

The last criterion was the volume of the air filter box. The round concept had a volume of 0.01211 m^3 and the volume for the oval concept was 0.00823 m^3. This means that the round concept had a higher volume compared to the oval concept.

The result from the Pugh matrix was that the round concept had a better score than the oval concept. The round concept also was better in important criteria, such as the filter volume, drainage possibilities and pressure drop. The criteria that the oval concept performed better in such as UI over the MAF sensor, there was only a slight difference. Therefore, the concept that was chosen to be continued with for further development was the round concept.

Table 5.53: Pugh matrix round and oval concepts.

Criteria	Round Concept	Oval concept
UI over MAF	0	+
UI over filter	0	-
Placement of dirty side duct	0	+
Drainage possibilities	0	-
Cost	0	+
Filter volume	0	-
Pressure drop	0	-
Changability of filter	0	**0**
Manufacturability	0	**0**
Attachment points	0	**0**
Air filter box volume	0	-
Result	**0**	**-2**

5.10.2 Pugh matrix rectangular, tube, and half tube concepts

The Pugh matrix and the comparison between the rectangular, tube, and half tube concepts are shown in Table 5.54. The rectangular concept was set as the baseline. As shown in Section 5.9.7.3 the UI over the MAF sensor for the rectangular shape was 0.955, while the tube shaped and half tube shaped concepts were 0.963 and 0.977, respectively. Furthermore, the tube shaped concepts both outperformed the rectangular concept in terms of UI over the filter, with values of 0.907 and 0.84 compared to the rectangular concept which had 0.647.

However, the placement of the dirty side duct would preferably be mounted as far up as possible such that dirt and snow do not enter the system. The tube formed concepts performed poorly since it require a longer dirty side duct to connect with the air filter boxes. The placement for the rectangular concept would result in a shorter dirty side duct since the inlet for the concept was placed higher. The drainage possibilities were also inferior for the tube shaped concepts since the dirty side duct needs to be connected from the bottom of the air filter box. In the case of the rectangular shaped concept, the drainage possibilities were easier since the inlet was placed on the side of the air filter box.

The cost would be lower for the tube shaped concepts, as they have smaller volumes compared to the rectangular concept. The rectangular shape had a volume of 0.01243 m^3, while the other concepts had a volume of 0.004748 m^3 and 0,004903 m^3.

The filter area was almost four times higher for the rectangular shaped concept compared to the other two. The tube concepts had an area of 0.000707 m^3 compared to the rectangular shape which had an area of 0.002731 m^3. The tube shaped concepts also were inferior in terms of pressure drop, 2300 Pa and 1960 Pa compared to 1760 Pa for the rectangular concept.

The same reasoning is applied here as for the round and oval filter concepts in terms of the changeability, manufacturability and attachment points. No clear distinction between the concepts was found.

The air filter box volume was larger for the rectangular shaped concept which had a volume of 0.0124 m^3, while the other concepts had a volume of 0.004748 m^3 and 0.004903 m^3.

The result from the Pugh matrix was that the rectangular concept had a better score than the tubed shaped concepts. The rectangular concept also was better in important criteria, such as the filter volume, drainage possibilities and pressure drop. The criteria that the tube shaped concept performed better in was UI over the MAF sensor, but only slightly. Therefore, the concept that was chosen to be continued with for further development was the rectangular concept.

Table 5.54: Pugh matrix for rectangular, tube, and half tube concepts.

Criteria	Rectangular concept	Tube concept (flat filter)	Half tube concept (flat filter)
UI over MAF	0	+	+
UI over filter	0	+	+
Placement of dirty side duct	0	-	-
Drainage possibilities	0	-	-
Cost	0	+	+
Filter area	0	-	-
Pressure drop	0	-	-
Changability of filter	0	**0**	**0**
Manufacturability	0	**0**	-
Attachment points	0	**0**	**0**
Air filter box volume	0	-	-
Result	0	**-2**	**-3**

5.11 CFD simulations by Aurobay

To compare the last two concepts, the CAD models were sent to the simulation department at Aurobay. They used Siemens The reason for this was that they could perform more accurate simulations that made the comparison fairer. The simulation for the round concept is presented in Section 5.11.1 and the rectangular concept is presented in Section 5.11.2.

5.11.1 Round concept CFD simulation

The simulation for the round concept had a better performance overall compared to the simulation for the same concept presented in Section 5.9.7.1. The velocity distribution from the simulation is shown in Figure 5.62. It can be observed that the velocity distribution in the air filter box was even, with a reduced velocity as the air enters the filter.

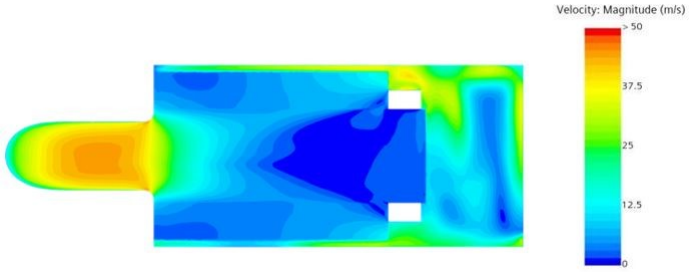

Figure 5.62: Round filter velocity distribution.

Figure 5.63 shows the velocity over the air filter. The UI over the air filter was 0.866 compared to 0.634, which was the result of the simulation conducted by the project team.

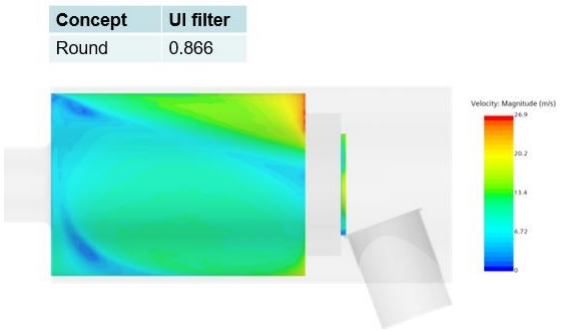

Figure 5.63: Round filter velocity distribution and UI over the air filter.

The UI over the MAF sensor was similar to the CFD simulation performed by the project team, 0.963, and the simulation department at Aurobay, 0.964. The velocity distribution over the MAF sensor from the simulation department at Aurobay is shown in Figure 5.65.

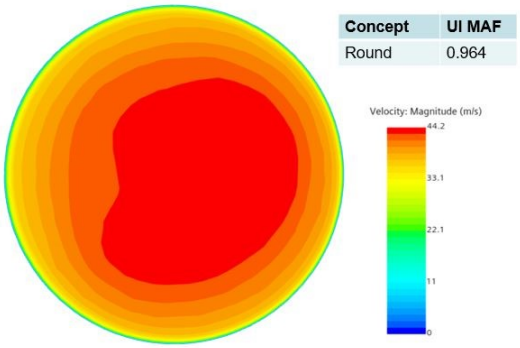

Figure 5.64: Round filter velocity distribution and UI over MAF.

The pressure drop is shown in Figure 5.65. The total pressure drop was 1640 Pa which is lower than the pressure drop that the project team got which was 1890 Pa. The filter itself did not create much pressure drop compared to the way from the inlet to the filter and from the filter to the outlet of the duct bellow.

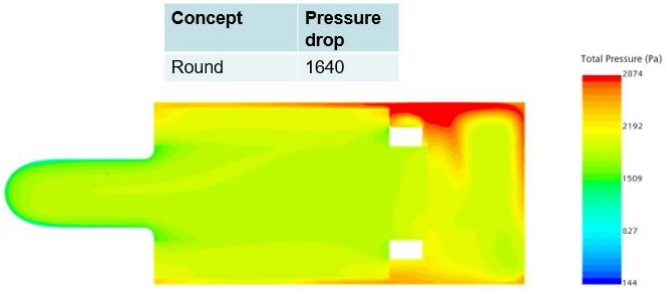

Figure 5.65: Round concept pressure distribution and total pressure.

The results between the project teams' CFD simulations and those performed by the simulations department at Aurobay differed significantly for UI over the filter. The simulation department at Aurobay used a circular coordinate system for the filter while the project team used a Cartesian coordinate system, with X, Y and Z axis. The simulation department at Aurobay also used finer mesh. Both these affected the output values.

5.11.2 Rectangular concept CFD simulation

The project team and Aurobay team got some differences in the values for the rectangular concept presented in Section 5.9.7.3. The velocity distribution when conducted by the Aurobay team is illustrated in Figure 5.66.

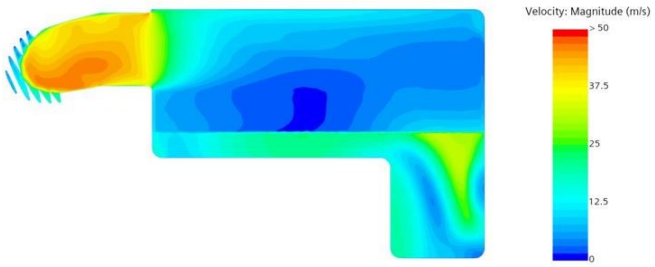

Figure 5.66: Rectangular filter velocity distribution.

The rectangular concept had a higher value in terms of UI over filter. The value for UI over filter from the CFD done by the project team was 0.647 and the result from Aurobay's team was 0.823. The velocity distribution over the filter is shown in Figure 5.67.

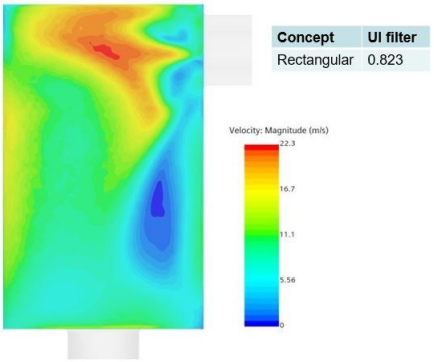

Figure 5.67: Rectangular filter velocity distribution and UI over the air filter.

The value for UI over MAF was also a bit higher when the simulations were performed by Aurobay's team. The project team got the UI over MAF to be 0.955 while Aurobay's team got 0.967. The velocity distribution over the MAF position is shown in Figure 5.68.

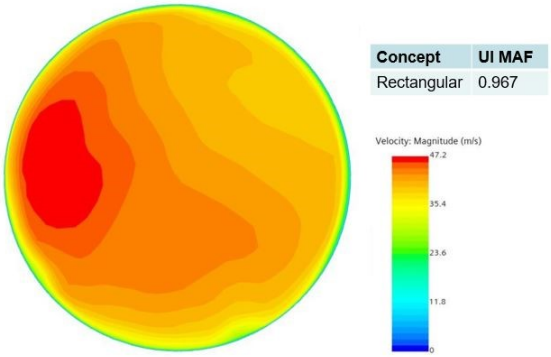

Figure 5.68: Rectangular filter velocity distribution and UI over MAF.

The pressure drop was lower for the simulation from the project team compared the simulation from the Aurobay simulation department. The pressure drop from the simulation of the project team was 1760 Pa and the pressure drop from Aurobay's team was 1643 Pa. The rectangular concepts pressure distribution can be found in Figure 5.69.

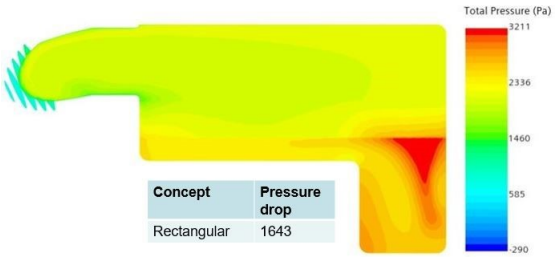

Figure 5.69: Rectangular concept pressure distribution and total pressure.

The results differ between the simulations from the project team and the simulation

department at Aurobay. The simulation department used a finer mesh compared to the project team.

5.12 Kesselring matrix

The final two concepts were evaluated using a Kesselring matrix. The scale for each desire is shown in Table 5.55. Specific values on the scale are not provided due to confidentiality reasons. For desires such as UI, filter area, pressure drop and air filter box volume, the scale was based on the current air filter box, which was used as a reference point. For desires such as attachment points, cost, drainage possibilities, manufacturability and changeability of the filter, an arbitrary scale was used for evaluation. In the case of the placement of the dirty side duct, the distance from the top of the engine to the inlet of the air filter box was used as the grading scale. The reason was that the distance determines the length of the dirty side duct.

Table 5.55: Kesselring value scale.

UI over MAF	
Value	Grade
Reaches the requirment	1
Value exceeds requirement slightly	2
Value exceeds requirement moderate	3
Value exceeds requirement significatly	4
Value exceeds requirement dramatically	5

UI over filter	
Value	Grade
Significantly below todays solution	1
Sligthly below todays solution	2
Same as todays solution	3
Sligthly above todays solution	4
Significantly above todays solution	5

Placement of dirty side duct	
Value	Grade
Inlet placed at the bottom of the available space	1
Inlet placed slightly below middle of the available space	2
Inlet placed in the middle of the available space	3
Inlet placed slighly above middle of the available space	4
Inlet placed at the top of the available space	5

Filter area	
Value	Grade
Significantly below todays solution	1
Slightly below todays solution	2
Same as todays solution	3
Slightly above todays solution	4
Significantly above todays solution	5

Pressure drop	
Value	Grade
Reaches the requirment	1
Value exceeds requirement slightly	2
Value exceeds requirement moderate	3
Value exceeds requirement significantly	4
Value exceeds requirement dramatically	5

Changability of filter	
Value	Grade
Very difficult	1
Difficult	2
Acceptable	3
Easy	4
Very easy	5

Air filter box volume	
Value	Grade
Significantly below todays solution	1
Slightly below todays solution	2
Same as todays solution	3
Slightly above todays solution	4
Significantly above todays solution	5

Cost	
Value	Grade
Very high	1
High	2
Moderate	3
Low	4
Very low	5

Attachment points	
Value	Grade
Very difficult	1
Difficult	2
Acceptible	3
Easy	4
Very easy	5

Drainage possibilities	
Value	Grade
Poor	1
Acceptable	2
Good	3
Great	4
Excellent	5

Manufacturability	
Value	Grade
Very difficult	1
Difficult	2
Acceptable	3
Easy	4
Very easy	5

Both concepts received a score of two out of five on the UI over the MAF, indicating that they both fulfilled the requirement but did not exceed expectations. For the UI over the filter, there was a difference between the two concepts. The round concept had a UI over the filter of 0.866 and the rectangular had 0.823. Based on these results, the round concept received a score of four and the rectangular received a score of three.

For the placement of the dirty side duct, the round concept received a score of two and the rectangular received a score of three. The inlet of the round concept was slightly below the middle of the available space which means that the dirty side duct needs to be longer. Therefore, it could create a higher pressure drop before entering the air filter box. The rectangular concept is placed higher, slightly above the middle, and received a score of four.

The drainage possibilities were considered good for both concepts. They were both placed vertically and had a sufficient distance up to the filter. Therefore, they both received a score of four. Furthermore, the cost for a round filter is approximately twice as expensive as a flat filter, according to "Supplier 2". Therefore, the round concept received a score of two and the rectangular concept received a score of four. The filter area of the rectangular concept was similar to today's solution resulting in a score of three. The round concept had double the filter area compared to today's solution which resulted in a score of five.

Both the rectangular concept and the round concept had similar pressure drop which exceeded the requirement significantly. Therefore, both concepts received a score of four. Furthermore, the changeability for the rectangular concept received a score of five since it worked the same way as today's solution. The air filter box was divided into to two halves, a bottom part and a lid. The filter was placed between those parts, an illustration is shown in Figure 5.7. The round concept received a score of three. The filter could not be placed in the same way as the rectangular because it would block the airflow. Instead, the filter needs to be attached on both ends to prevent leakage.

The filter for the round concept required additional manufacturing steps compared to a flat air filter, according to "Supplier 2". However, both concepts were considered to have acceptable manufacturability, resulting in a score of three for each concept. In terms of attachment points, both concepts received a score of three. The only opportunity to attach the air filter box was the long side parallel to the duct bellow. Both concepts had equal opportunities to attach the air filter box to that side. Furthermore, the air filter box volume was compared to that of today's solution. Both concepts were significantly below the air filter box of today which resulted in a score of one out of five.

Table 5.56: Kesselring matrix.

Criteria	Weight	Ideal		Round		Rectangular	
		v	t	v	t	v	t
UI over MAF	3	5	15	2	6	2	6
UI over filter	4	5	20	4	16	3	12
Placement of dirty side duct	3	5	15	2	6	4	12
Drainage possibilities	4	5	20	4	16	4	16
Cost	4	5	20	2	8	4	16
Filter area	4	5	20	5	20	3	12
Pressure drop	4	5	20	4	16	4	16
Changability of filter	4	5	20	4	16	5	20
Manufacturability	4	5	20	3	12	3	12
Attachment points	5	5	25	3	15	3	15
Air filter box volume	2	5	10	1	2	1	2
Result	**41**	**55**	**205**	**34**	**133**	**36**	**139**

The result from the Kesselring matrix became even between the two final concepts. The round concept received a final score of 133 and the rectangular concept received a final score of 139. This indicated that the rectangular concept was slightly better than the round concept.

There was a trade-off to be considered when selecting the final concept. The round concept had advantages such as a greater filter area and UI over the filter, which would result in a longer service life of the air filter. On the other hand, the rectangular concept offered advantages such as lower cost, both for the filter itself and for the dirty side duct. If the length of the dirty side duct could be low, that would mean that the leftover space could be used for other components. With these trade offs in mind and the score from the Kesselring matrix, the rectangular concept was selected as the winning concept.

5.13 Further development

The rectangular concept was chosen to be the final concept. The further development consisted of attachment points, ribs to strengthen the design, a trail to place the air filter, attachments between the ducts and the air filter box, adding a drainage hole and a detailed design including radius across the box.

5.13.1 Attachment points

The attachment points were an important aspect to make the box able to absorb vibrations. The only possible attachment area was the side parallel with the duct bellow, shown at the top of Figure 5.52b and shown in Figure 5.52c. This side corresponds to the engine frame to which the air filter box needs to be attached. The frame is illustrated in green in Figure 5.70. The air filter box had to be capable of movement due to the vibrations generated by the engine. Therefore, the solution investigated in Section 5.4 was implemented in three different locations of the bottom of the air filter box, shown in Figure 5.70. To achieve a stable mounting, two connections were placed near the engine and the third was located close to the frame, these are marked in orange in Figure 5.70a. To connect these connections to

the frame, two brackets are utilized which were mounted onto the frame, shown in Figure 5.70a circled in blue. The air filter box was connected to the brackets with a snap mechanism. Holes were placed on the frame and a plug shaped connections was placed on the box. The mounting process of this involves inserting the plugs into the holes as illustrated in Figure 5.70b, circled in red.

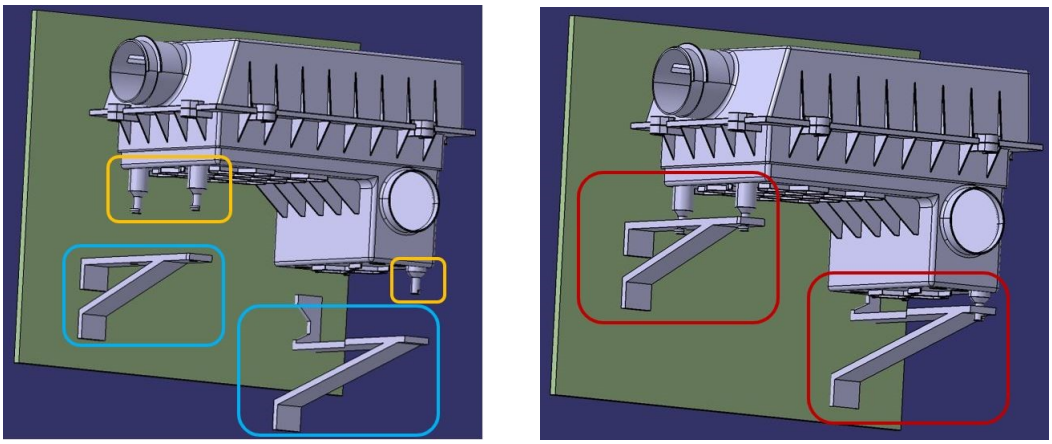

(a) Not assembled attachment points. **(b)** Assembled attachment points.

Figure 5.70: Attachment points for the air filter box.

When the air filter box has been mounted, the protruding part of the plug prevents the box from detaching from the bracket, circled in green in Figure 5.71 ensuring secure attachment on the frame.

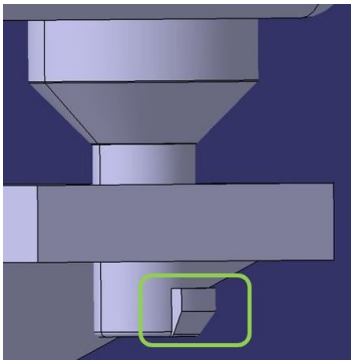

Figure 5.71: Close-up image of one of the attachments.

5.13.2 Drainage

To determine the size of the drainage hole, a physical test was conducted. A bucket filled with two liters was used, and the time required to drain the water was measured. The test started with a hole size of ∅6 mm, and the largest hole size tested was ∅10 mm. To increase the hole area, the number of holes with the size of ∅10 mm was increased. The test showed a linear correlation between the hole area and the

drainage time, whereby doubling the hole area resulted in halving the drainage time. The test showed that an area of XX mm^2 would be needed to fulfill the requirement.

It was decided to incorporate four equally sized drainage holes in the final concept. Two of these holes were positioned near the inlet, while the remaining two were located on the opposite side. This arrangement was intended to prevent water from getting trapped inside the box. The drainage holes are highlighted in Figure 5.72, circled in orange.

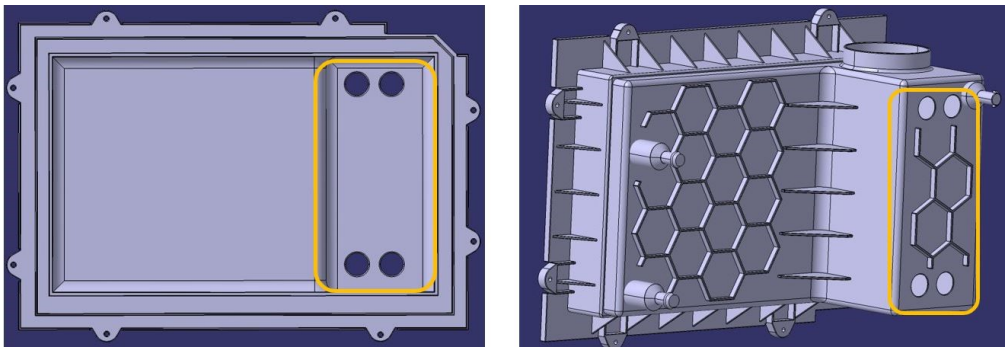

Figure 5.72: Four holes for drainage on the air filter box.

5.13.3 Enhanced Structural Integrity and Safety

To enhance the structural integrity of the air filter box, a hexagonal pattern of ribs was incorporated on the top lid and outer surface of the bottom part, illustrated in Figure 5.73. This design choice utilized the strength-to-density ratio of honeycomb structures, allowing for a lightweight yet robust construction [50]. Furthermore, rounded corners and edges were integrated into the design to promote safety and minimize the risk of accidents. These smooth contours help prevent sharp edges that could potentially cause harm during handling or maintenance. In terms of manufacturing convenience, the top lid was angled inward by two degrees. This slight angle facilitates the manufacturing processes.

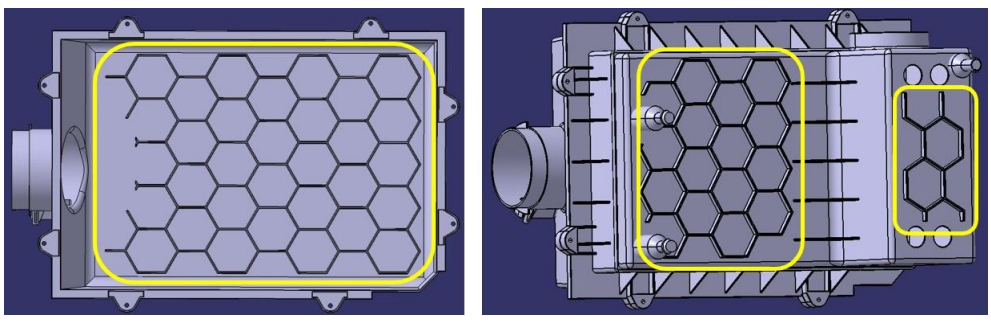

Figure 5.73: Honeycomb structure on the air filter box.

5.13.4 Carry over from Volvo's Air Filter Box

The final design of the air filter box incorporates design parameters discussed in Section 5.4. One parameter taken into consideration was the design of the MAF sensor holder. It was crucial to maintain compatibility with the existing sensor, so the same holder design was retained to ensure a proper fit. The placement for the MAF sensor is indicated by a green circle in Figure 5.74a. Another aspect carried over from the previous design was the connection between the air filter box and the duct bellow, which is shown in Figure 5.74b and highlighted by an orange circle. The outlet of the box has an elevation at the end, which a groove placed in the duct bellow fits into. This allows the parts to fit horizontally, then a hose clamp will be used on top of the duct bellow to securely join the two parts. This connection method was chosen due to its proven performance for the airflow characteristics. To facilitate proper placement of the air filter within the box, a hole was included in the design, marked by a blue circle in Figure 5.74c. The air filter box also used screws to connect the bottom part with the top part of the box. This was used since clips could break and screws would be more durable in the long term.

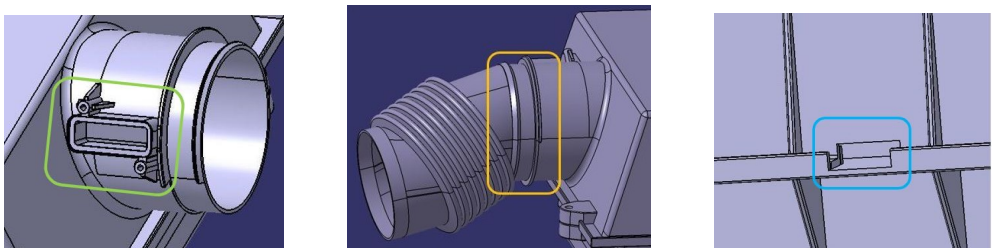

(a) The holder for MAF sensor.

(b) Connection between air filter box and duct bellow.

(c) Hole on the side of the filter box to see the air filter.

Figure 5.74: Carry over parts from the current air filter box.

5.14 The final concept

The recommended final concept, shown in Figure 5.75, was a rectangular air filter box with a flat-shaped filter. It included all the design factors explained in Section 5.13. Furthermore, it incorporated a short duct bellow for cost optimization and the inlet is positioned near the top of the engine to create a shorter path for a dirty side duct. Most importantly, the design fulfilled the requirements set up in Section 5.6.

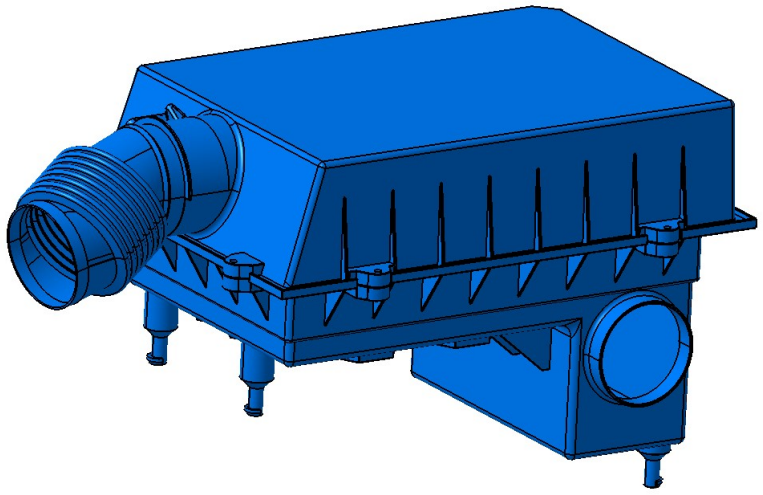

Figure 5.75: Final concept.

5.14.1 Manufacturing and cost estimation of final concept

The analysis of the manufacturability and cost estimation for the final concept was made with an experienced tool developer and cost estimator, "Expert 2". The hole of the MAF sensor holder was not placed in the tooling direction, according to "Expert 2". It creates a need for a slider, an additional tooling part needed for certain shapes, for the hole to be possible to manufacture. Sliders are also needed for the connections in the bottom of the air filter box, shown in Figure 5.71. Furthermore, the radius on the inlet and outlet, shown in Figure 5.33, will be extremely difficult to manufacture. The inlet radius is not possible for the tool to access. The outlet radius can be accessed halfway due to that the wall is angled. However, since this information was discovered late in the project, there was no time to fix these factors to reduce the price.

The cost estimation was made under the assumption that the manufacturing will be in Sweden. Two tools are needed, one for the bottom part and one for the top part. In the tools, an injection mold, robot gripper and control fixture are included. The two tools together were estimated to cost 2.64 million SEK. The tooling cost could be divided equally to all parts manufactured, an assumed volume of 5000-10.000 per year has been used in this example. The material cost was calculated by multiplying the purchasing price of the material with the weight of the part. The material cost for the air filter box was calculated to be 29.97 SEK. The manufacturing cost included the machine cost, 9.15 SEK, labor cost, 6.54 SEK, and overhead costs, 3.14 SEK. This is summarized as 19.02 SEK of manufacturing cost per air filter box. The values can be found in Table 5.57

Table 5.57: Cost estimation air filter box.

Material cost	**29.97**
Direct labor cost	6.54
Machine cost	9.15
Manufacuring overhead cost	3.14
Total Manufacturing cost	**19.02**
Sales and administration costs	**9.8**
Profit	**3.3**
Total cost per part	**62.1**
Tooling cost	**2 640 000**

5.15 Verification of requirements

In this section, the verification methods are presented. The numerical values from the requirements, shown in Table 5.3, were not presented, due to confidentiality reasons.

The CFD simulations performed by the simulation department at Aurobay were utilized to verify a few requirements. These simulations, which are shown in Section 5.11.2, verified the requirements for pressure drop, UI over MAF and airflow.

The requirement for the maximum dimensions of the air filter box and duct bellow were verified by placing the final design in the installation space, shown in Figure 5.11.

The requirement for easy installation was fulfilled by utilizing the attachment points presented in Section 5.13. This was because there was no need for tools during the installation of the air filter box, as only body force would be required.

The drainage requirement was verified through a physical test conducted to determine the needed size of the drainage hole. The test is shown in Section 5.13.2.

There were some requirements that the thesis did not verify. These consisted of the service life of the air filter and the filter efficiency. This was due to that the data required to verify the requirements were not obtained. The strength requirements for the air filter box were also not verified. This was due to uncertainties regarding the loads.

6
Discussion

This section starts with a discussion of the CFD analysis and continues with a discussion about the fulfillment of research question from Section 1.3.

6.1 Discussion of CFD simulations

In this section, the CFD simulations are discussed. This includes the simulations for both the air filter box and the duct bellow.

6.1.1 CFD simulations for round and oval air filter boxes

The simulations for the round and oval filters had a source of error, that the resistance for the filter was the same in all three directions. This should not be the case to get outcome values that are trustworthy. Therefore, the simulations were only to compare the concepts to each other and not to verify that requirements were met. The findings presented in Section 5.9.2 are discussed below.

- The airflow had a smoother path when the inlet was placed on the edge as shown on the right in Table 5.20. This was due to that the inlet placement helped the air into a swirling movement which decreased the pressure drop and increased the UI for both outlet and filter. The round shape keeps the airflow more even across the whole air filter box. It did not lose speed as fast as when the inlet was placed in the middle.

- The angle had a big impact on how the airflow distributed across the air filter box and the pressure drop. An angle close to 90 degrees created a large pressure drop. On the other hand, a low angle had a low pressure drop but also a low UI over the filter. This was due to that a low angle resulted in most of the air passed through the end of the filter. At the angle of 70 degrees, the best output values for UI were found while still having a good pressure drop.

- Placing a guide close to the inlet could improve the UI for the filter and the outlet. However, a guide "pushes" the air in a certain way which increased the pressure drop significantly. A guide could be included in the design if the pressure drop requirement allows it.

- The placement of the inlet on the inside of the filter, shown in Table 5.17,

proved to cause problems. Firstly, the air needed to be guided, otherwise the airflow only passed through the filter on one side. Secondly, if a guide was placed on the inlet, the pressure drop rose significantly. Additionally, DHC decreases by 15% if the airflow enters on the inside of the filter compared to the outside, according to "Supplier 1".

- The distance between the wall of the air filter box and the air filter had a better UI over the filter when the distance was increased. However, increasing the distance also led to a reduction in the filter area. The UI was only slightly better which means that a lower distance would still have a larger DHC.

- Increasing the filter thickness had a positive impact on the UI values but a negative impact on the pressure drop. If the space and pressure drop allows the thickness of the filter to be high, it would have a great benefit to the DHC and service life.

- Adding a radius on the air filter outlet had a great impact on UI for the outlet and pressure drop. This could be due to that the air do not need the same "detour" as with sharp edges. When the outlet edge was sharp the airflow went towards the middle of the outlet.

- The simulations showed that an angle on the outlet affected both the UI on the outlet and the pressure drop negatively. If the requirement for the UI over the MAF still would be fulfilled, an angle could be placed on the outlet to decrease the pressure drop from the duct bellow and the whole system. An angle on the outlet could be used to decrease the sharpness of the angle of the duct bellow.

6.1.2 Rectangular, tube, and half tube shaped air filter boxes with flat filter

It was discovered that the filter sizes analyzed in the initial CFD analysis were much smaller than those commonly employed. Thus, a size of 40mm was adopted as it was deemed more realistic. While changing the size had little impact on the results for round and oval air filters, the outcomes for flat filters were considerably affected by the air filter size utilized. Therefore, more tests ought to have been conducted with the new filter size to assess the earlier concepts tested at the outset. The conclusions outlined in Section 5.9.4 are discussed further below.

6.1.2.1 Rectangular filter box with flat rectangular filter

The results from the tests on the rectangular filter box with a flat filter provide useful insights into how different design parameters impact on filter performance.

- The results from the first test suggest that the position of the outlet had a significant impact on the airflow characteristics. Placing the outlet further from

the inlet allowed for a more uniform airflow distribution, leading to higher UI over the filter and outlet and lower pressure drop. The change in inlet position on the z-axis had some impact on pressure drop and a slight impact on UI over the outlet. This indicates that the inlet position may not be as critical as other factors in achieving optimal airflow characteristics.

- Placing the filter in the middle was found to be the most effective placement, likely due to that it allowed for a more uniform airflow distribution over the filter, resulting in higher UI over the filter, higher UI over the outlet, and lower pressure drop. Placing the filter near the outlet resulted in the worst performance, with poor UI over the filter and high pressure drop.

- The results also suggest that filter thickness plays an important role in the performance of the system. The UI over the filter varied the most with the filter thickness, smaller filters resulted in higher UI over the filter. This could be due to that smaller filters allow for a more uniform airflow distribution over the filter surface.

- Finally, the rounded corners on the inlet and outlet had a significant impact on pressure drop, with rounded corners on the outlet resulting in less pressure drop. This may be due to that rounded corners reduce turbulence and allow for a smoother airflow pattern, resulting in more efficiency overall.

6.1.2.2 Tube filter box with flat circular filter

- The tube shaped concepts without ramps gave higher UI and lower pressure drop. This could be due to that without a ramp, the airflow was not obstructed or redirected, allowing for a more uniform airflow distribution over the outlet. The absence of a ramp also resulted in a more streamlined airflow pattern, reducing the pressure drop.

- A middle placement of the filter resulted in the highest UI over the filter. Placing the filter in the middle resulted in a more uniform airflow distribution over the filter, leading to higher UI. The UI over outlet and pressure drop did not change significantly as they were less affected by the filter placement.

- A longer box resulted in higher UI over the filter and lower pressure drop. It allowed for a more gradual change in airflow direction, reducing turbulence and resulting in a more uniform airflow distribution. This led to a higher UI over the filter and a lower pressure drop.

- Increasing the length of the angle resulted in higher UI over the filter and outlet. As the length of the angle increased, the airflow has more time to adjust to the change in direction, resulting in a more uniform airflow distribution over the filter and outlet. The pressure drop did not have a clear correlation with length because other factors, such as the shape and roughness of the surfaces,

may be affecting it as well.

- Including a ramp resulted in higher pressure drop and higher UI over the filter. The ramp likely causes a redirection of flow, leading to increased turbulence and pressure drop. However, the higher length of the angle allows for a more gradual change in direction, reducing turbulence and resulting in a more uniform airflow distribution over the filter. This led to a higher UI over the filter and a lower pressure drop.

6.1.2.3 Half tube filter box with flat circular filter

- In the initial test, placing the ramp along the z-axis gave high results on the UI over outlet compared to placing it along the x-axis. This could be because placing the ramp along the z-axis allowed for a more streamlined airflow pattern, reducing turbulence and resulting in more uniform flow distribution over the outlet.

- Having a longer part with an angle near the outlet resulted in small improvements in all values. This could be because the longer part allows for a more gradual change in airflow direction, reducing turbulence and resulting in a more uniform airflow distribution.

- When the ramp had rounded corners compared to non-rounded corners, the values of UI over the outlet and filter increased, while the pressure drop decreased. This could be due to that having rounded corners on the ramp reduces turbulence and allows for a more streamlined airflow pattern, resulting in more uniform airflow distribution and lower pressure drop. The increased UI over outlet and filter could be due to that the rounded corners may have reduced the formation of dead zones or eddies, allowing more air to pass through the filter and increasing the UI values.

6.1.3 CFD simulations for the duct bellow

For the height, width, angle of the bellows and the number of bellows all had the best performance when they had the lowest value. This would indicate that lower values would create even better performance on pressure drop and UI over the duct bellow. This could be because the volume of the bellows disturb the airflow and therefore affect the pressure drop and UI over the duct outlet negatively. When the airflow encountered disturbance, the turbulence increases and the pressure drop increases.

The pressure drop and UI over the outlet of the duct bellow were not everything to consider. The NVH performance should also be considered. With the simulations that were conducted, NVH could not be evaluated. Therefore, the article from Jung et al was used to evaluate the same parameters for NVH performance [42]. Jung et al tests did show some differences compared to the tests that were conducted for this

project. It could be that small bellows do not affect the airflow as much as larger does, while larger bellows can absorb vibrations and sound better. For example, a larger width creates better NVH performance but a worse UI and pressure drop. Although NVH is important, the priority in this project was on pressure drop which made the choices mostly dependent on how that was affected.

The simulations for the distance between the bellows showed that 2 mm was the best for the UI for the outlet. However, 1 mm was the best for pressure drop. For the AIS, there exists a requirement on how much pressure drop is allowed. There is no requirement for the UI for the outlet here, which is the inlet to the resonator. Therefore, the distance between the bellows was decided to be 1 mm, which had the lowest pressure drop. The difference for both the pressure drop and UI over the outlet was small.

The results from the simulations were also compared to Song et al which tested how pressure drop was affected by the width and number of bellows [43]. The results from their article showed similar results to the simulations for this project. These were that increasing the width and number of bellows affected the pressure drop negatively.

The selected values for the parameters of the duct bellow can be found in Table 5.51. These values were used for all five concepts. The bellows were placed away from turns based on A2MAC1 findings, which showed that other manufacturers had placed their bellows on straight paths, as mentioned in Section 5.1. The placement of the duct bellow was also tested, and it was discovered that having the bellows placed further away from the outlet of the box resulted in a lower pressure drop. However, the UI over the outlet decreased because the bellows disturb the airflow and made it turbulent close to the outlet. It was also found that the UI over the MAF sensor changed depending on how close the bellows were placed before the turn of the duct. The MAF sensor should be placed away from the turn because turns create uneven airflow, as the air tends to take the closest path to the outlet. Furthermore, adding a duct bellow to the concepts increased resistance to the airflow, due to the longer air path and the turns in the duct.

6.2 Current designs

- **RQ1: What designs and different filters are currently used in the automotive industry?**

To answer the first question, a literature review, benchmarking, study visit and study of Volvo Cars' air filter box were conducted.

Based on the findings from the literature review, it was recommended to use V-pleated shapes for the air filter. This shape allows for a uniform deposition of particles which increases the longevity of the filter. Additionally, it was discovered during an interview that the curved-pleated filter are more expensive to manufac-

ture and are not as efficient as initially suggested. To support the pleats, it was recommended to use glue on the pleats, since it helps to keep the DHC. Furthermore, the literature review found that the air filter could be harmed if its cleaned. This risk should therefore be avoided. The information about the air filter media and configuration can be used in future work to design the filter suitable for the air filter box in this project.

The benchmarking study was conducted to provide a guideline for how the AIS:s usually are designed. Additionally, Table 5.1 was conducted to highlight the most common design similarities for the benchmarked vehicles. However, this research had some limitations that should be addressed. Firstly, the benchmark only examined items from a limited number of manufacturers, which may not be indicative of the entire sector. Secondly, the study did not consider the cost or environmental impact of various air filtration systems, which are key factors for manufacturers and customers.

The study visit to Volvo Cars facility helped in the design and assembly process of the air filter box, air filter, and duct bellow. The main focus of the study visit was understanding the mounting and the connection between the different components in the assembly process. However, there was only one type of each component that was studied in the mounting process. The mounting and connections can vary between various air filter boxes, air filters, and duct bellows. Therefore, it would have been beneficial to study more variants of components and connections. There would have been beneficial to make more study visits to multiple manufacturers to see various solutions on the mounting and connections. In this case, Volvo's facility was the only insight into the mounting possibilities, which could have made other possible solutions disregarded.

Studying Volvo Cars' air filter box and air filter provided an understanding of the design parameters and offered a physical component that could be examined across the whole project. However, the only air filter investigated was a flat filter. It would have been valuable to also look at an air filter box and air filter for a round shape. This could have led to other design factors being considered. It would have been beneficial to investigate more physical air filter boxes as it gave a better practical understanding compared to digital benchmarking.

6.3 Technical requirements

- **RQ2: What are the technical requirements for the designs of the air filter box and duct bellow?**

To answer the second research question, a literature review, interviews, function-means tree and requirement specification were conducted.

The literature review showed the importance of considering NVH levels for the de-

sign of the air filter box and duct bellow. Furthermore, the literature also highlighted the significance of filter efficiency which was considered when the requirement specification was conducted. As mentioned in the literature review in Section 4.4, the duct bellow could either be designed to minimize the NVH level or to minimize the pressure drop. This creates a trade off between these factors.

Internal interviews and meetings with the project team for the REX engine provided some requirements. These were requirements for airflow, service life and installation space. Interviews with the turbo department at Aurobay were conducted to determine the requirements for pressure drop and filter efficiency. The majority of the requirements were gathered through internal interviews and meeting at Aurobay, as the air filter system is a part of the larger AIS. This indicates that other parts of the AIS decides what is required of the air filter system.

The interview with "Expert 1" had a significant impact on the requirements, presented in Table 5.3. The requirement for the water drainage was a "carry over" that "Expert 1" provided. "Expert 1" also explained today's design solutions and the reason for the design decisions. This interview took place at the start of the project which provided valuable insight into what needs to be considered when designing an air filter box. Additionally, interviews were conducted with employees at "Supplier 1", who produce air filters and air filter boxes. They presented an idea to improve the efficiency of air filters, such as using nanofibers or a pre filter. The interviews with "Expert 1" and "Supplier 1" were semi-structured which suited these interviews. More interviews would have been beneficial to get more perspectives. The risk with doing a limited number of interviews externally is that opinions and thoughts could be biased towards their own designs.

The function-means tree was developed with the knowledge acquired from benchmarking, interviews and the study of Volvo's air filter box. The function-means tree served as a visual representation of different components within the air filter system and the functions that needed to be fulfilled by each part. Creating the function-means tree provided an early understanding of the air filter system which later led to the requirement specification. This was the first step of organizing the information gathered in the early phase of the project.

Most of the requirements were gathered through interviews conducted internally at Aurobay, and it was discovered that some of these requirements were "carry over" from previous tests and projects. Therefore, to get more realistic requirements, tests specifically for the REX engine would be necessary to assess the impact of factors such as vibration. The requirement for the NVH level could not be verified in this project, since there was no physical testing that could be conducted in this project. Furthermore, the installation space could also be varied due to how near the air filter box could be placed to other components such as pipes. This was not considered in this project as the exact position of these components was still uncertain.

The design FMEA helped in identifying design factors that could be critical for

the new design. As mentioned in Section 3.3.3, the design FMEA could be more accurate if people with more experience in various fields were involved in conducting it. Therefore, some critical aspects might have been given a lower number compared to a person with experience. There could also be areas that have been missed or overlooked in the FMEA.

6.4 Design possibilities

- **RQ3: What design possibilities exists for the available space?**

The CAD modelling began by drawing the available space that could be used for the air filter system. Knowledge from the information gathering was used to create basic shapes such as round, oval and rectangular, shown in Figure 5.12. Most of the shapes that were drawn had been found in similar designs in the literature review and benchmarking. The concepts were drawn to maximize the volume of the air filter box with the different shapes, while still being within the available space.

The design of the air filter box was explored first. This was done by conducting CFD simulations on and various concepts and then screening. Thereafter, the duct bellow had to be designed specific to each concept of the air filter box. The best performing concepts for the air filter box got a design for a duct bellow that fitted, and connected to the resonator.

Concepts with other shapes could have been created, however, due to time constraints, the focus had to be limited to a few shapes. By doing this, the design space was not fully explored. The generated concepts used as much of the available space as possible, positioned specifically for each shape. There is a risk of overlooking potentially good concepts when not exploring the entire design space. This limitation applies to the air filter box, duct bellow and the combination of them. The design parameters may have yielded different results in the simulations with other shapes and dimensions, compared to the concepts that were created.

6.5 Requirements and desires

- **RQ4: How can the new designs fulfill the requirements and exceed the desires?**

Studying Volvo Cars' air filter box and air filter also served as a valuable source of inspiration during the design stage of the new concepts. It provided insight into various design parameters, including the number of screws and the hole size, ribs, filter support and the connection between the duct bellow and the air filter box. Some of the components, for example, the MAF sensor, were "carry over" which made it crucial to have the measurements for it.

CFD simulations were conducted to gain an understanding of how the airflow behaved depending on input parameters. The simulations performed by the project team were only to compare the concepts to each other rather than to verify that requirements were met. The CFD simulations were performed by changing one parameter at a time. This helped to identify the single effects on different parameters. It may be possible that the parameters would have interacted differently when tested together. Thus, selecting the best performing parameter in all tests would not provide an objective conclusion. To address this, a Design of Experiment (DEO) could also be conducted. However, since this would need more simulations and the time of the project was limited, this was not possible.

The Pugh matrix for the round/oval filters had only a slight difference in score, two points in favour of the round concept. However, the filter area for the round concept was almost twice the size of the oval concept. The filter area is a very important criterion for an air filter system. Pressure drop is also an important criterion, in which the round concept had better performance. Both UI criteria had similar results, it will not affect the performance of the air filter system significantly. An important criterion that the oval filter performed better in was the placement of the dirty side duct. The dirty side duct for the round concept needed to be longer compared to the oval concept. This will probably create a larger pressure drop in the dirty side duct and occupy more space in the engine. With all this in mind, the round concept had still an overall better performance in important areas.

In case of flat filters, the rectangular concept was clearly outperforming the other two concepts in the Pugh matrix. It had a larger surface area compared to the other concepts. However, the UI over the filter was lower, which could result in the filter could need to be changed more often. The UI over MAF was also lower but the difference was not significant. Furthermore, the tube shaped concepts was performing worse in terms of the placement of the dirty side duct, however, there are possibilities to change the inlet to the side instead of having it placed at the bottom of the box. Subsequently, tube shapes performed much worse in pressure drop which is a key factor. However, the rectangular concept would still be seen as superior. Pugh matrices were a great tool to use for this part of the project. The reason for this is that the simulations performed by the project team were conducted to compare the concepts and parameters to each other, which made the Pugh matrix a suitable way to assess the performance.

The simulation performed by the simulation department was used to verify the requirements, as they are more experienced in the field. To determine the value scales for the Kesselring matrix, certain criteria were compared to the current solution for the air filter box. This allowed the assessment of grades to be in relation to the existing solution when grading how the concept performed. However, for some criteria, arbitrary scales were used as there was not enough information to have values on the scale. It is critical to recognize and address potential errors in the evaluation process. One possible error is that people interpret and score things differently, which can lead to differences and biases. To reduce this problem, clear guidelines

and definitions for the criteria are needed, such as comparing the concepts to the current solution. This could however be an issue for the grading the arbitrary scales. Involving more individuals or having independent reviews could also helped in minimizing the individual biases.

Furthermore, it is important to mention that the specific values used for the grading scale in the Kesselring matrix are not disclosed because it is confidential information. It is necessary, but it also limits the evaluation process in terms of lack of transparency and reproducibility. External stakeholders or researchers who want to validate or replicate the evaluation would not have access to the exact scale values used, which makes it difficult. The results from the Kesselring matrix showed that the two concepts were very similar, making it difficult to decide which one was better. This means that the evaluation process did not give a clear answer about which concept was superior. If more experienced people had been involved in the evaluation, the outcome might have been different. Their knowledge and ideas could have given more perspectives, which could have led to a different result. However, the rectangular concept received a better score compared to the round concept, even if the difference only was six points (4.5%). The rectangular concept outperformed the round concepts in terms of the space needed for both the dirty side duct and the duct bellow. This could benefit other components that could require more space. Additionally, the rectangular concept was the cheaper alternative, and the cost is always an important aspect to consider. Even if the service life of the filter was shorter compared to the round concept, the rectangular concept was selected as the winning concept. As usual, a trade-off was needed to select which concept to continue with further development. In this case, it was either to prioritize service life or cost and space, the latter was prioritized. This choice was supported by the score in the Kesselring matrix.

All attachment points had to originate from the frame which only was accessible from one side. Therefore, brackets from the frame were created to be able to stabilize the air filter box. The attachment points in the brackets followed the same principle as the investigated air filter box mentioned in Section 5.4. These attachments were chosen because the principal has been proven to absorb the vibrations from the previous engine. Furthermore, the drainage test consisted of a plastic can and holes in the bottom of it. The time it took for the drainage was measured which started when the water started to drain and ended when all the water had been drained. This approach includes the human factor which could affect the result. However, the test followed a rather linear result, for the time and hole area, which made the test feel valid.

The hexagonal pattern on the ribs was chosen for its strength while still being lightweight, which makes the design more robust. The ribs were placed on the outside of the bottom part of the air filter box due to that it does not affect the airflow. However, the ribs were put on the inside of the top part due to a lack of available space and aesthetics. This placement could affect the airflow. Ribs were placed throughout the whole available air filter box space. This maximized the robustness

of the design, considering that vibration tests could not be conducted.

Several design aspects were carried over from the current design, investigated in Section 5.4. The MAF sensor hole was carried over to secure the positioning of the MAF, as it remains the same as in the current air filter box. The hole on the side of the filter box used to see that the filter is placed in the box, shown in Figure 5.74c, was also carried over. The air filter for the new design needs the same frame as the current design, therefore, the hole was to verify the existence of the filter. The connection between the duct bellow and the air filter box was also carried over. The reason for this was that it has been proven to not affect the airflow significantly. The time constraint for the project limited further investigation on the connection as well.

During discussions with "Expert 2", it became evident that the design needed some changes for it to be ready for manufacturing. The inlet radius needed to be removed, which would have an effect on the airflow. It was discussed that a similar solution as the current one could be applied, shown in Figure 5.6. This solution entailed incorporating a separate part as the inlet which would be placed a bit inside the air filter box. For the outlet radius, only half of it could be included in the final design. Both these changes would affect the airflow negatively. These changes would be beneficial to incorporate in the future. Furthermore, the cost for the manufacturing of the air filter box had a relatively high tooling cost due to that the volume used in the example was low. If a larger production volume would have been set, the cost could have became lower. This is significantly lower than other produced engines at Aurobay. If the engine was to be produced for five years, the price per air filter box in tooling would be between 52.8-105.6 SEK. The higher number would mean that the tooling cost would be 48.5% of the total cost, and with the lower number, it would be 32% of the total cost. The volume produced, directly affects the total cost of the air filter box.

As discussed in Section 5.7 on FMEA, drainage is important when it comes to preventing water from reaching the air filter and potentially damaging the engine. The drainage is also important since snow and water can block the airflow. Additionally, the design FMEA highlighted the importance of ensuring a leak-free connection between the duct bellow and the air filter box. Since leakage testing was not feasible for this project, the existing connection method used in the current air filter box was retained. Another aspect addressed in the FMEA was the placement of the MAF sensor. As outlined in Section 5.14.1, the ideal manufacturing placement would have been on top of the outlet, since the tool has more reach in that direction. However, due to space constraints, this placement was not feasible. Vibration was also identified as a significant factor in the FMEA. To mitigate this issue, it was decided to utilize three attachment points: two near the engine and a third near the frame, shown in Figure 5.70.

6.6 Verification of requirements

Most of the requirements were verified by using the CFD simulations that the simulation department conducted. The reason for this was that most requirements had a connection to the airflow, the main function of the air filter box and duct bellow. These requirements were verified before the Kesselring matrix. This was used because the inner design did not change much at all in the further development. The drainage requirement was verified by doing a physical test described in Section 5.13.2. The needed drainage diameter is not shown due to that it would disclose the requirement for the drainage. The available space was considered from the start when the concepts were developed. Therefore, that requirement was always fulfilled for all the concepts including the final concept, the rectangular concept.

One of the requirements presented in Table 5.3, DHC for the filter, could not be explored in the way that was intended. DHC was intended to be used to calculate the service life of the air filter and to evaluate the different concepts. The reason for this was that to perform a good estimation, previous tests are used. Unfortunately, test data could not be provided by either the interviewed participants or the literature research. This made it impossible to conduct good estimations for the DHC of filters. The initial and overall filter efficiency could not be evaluated either since this information also needed confidential data to be estimated. This made it difficult to determine the filter thickness and size needed for the air filter for this project.

Most of the requirements have been verified in a simulation environment. That was the case due to the time was too limited to make tests with a physical prototype. All the requirements that were verified in a simulation environment need to be verified with a physical prototype in future.

7

Conclusions and Future work

In this chapter, conclusions from the project will be presented along with recommendations for future work.

7.1 Conclusions

In conclusion, this study has focused on the design of an air filter box for REX engine applications in medium/heavy trucks. By comparing existing designs, establishing technical requirements, and exploring design possibilities, the research has provided a solution that answers the research questions and fulfils the requirements stated in this master thesis. The study involved a literature review, comparative benchmarking, CAD modelling and analysis of design parameters through CFD simulations. Furthermore, a cost analysis was performed for the air filter box and an assessment of manufacturing feasibility.

Technical requirements, including factors like NVH levels and filter efficiency, were determined through interviews and meetings. The research employed CAD modelling and CFD simulations to explore different design shapes, with both round and rectangular concepts. Ultimately, the rectangular shape was selected due to its advantages in terms of ease of filter replacement and cost-effectiveness.

The final air filter box design is rectangular and includes attachment points, strengthening ribs, a trail for the air filter, attachments to the ducts, a drainage hole, and other design considerations. The attachment points absorb vibrations and are located on the side parallel to the duct below, connecting to the engine frame. To allow for movement, three locations at the bottom of the box were implemented. Plates on the frame connect to the box using a snap mechanism with plugs and holes. A physical test determined the drainage hole size by measuring water drainage time. Doubling the hole area halved the drainage time, leading to the incorporation of four equally sized drainage holes in the final concept to prevent water from getting trapped. To improve structural integrity, a hexagonal pattern of ribs was added to the top lid and outer surface of the bottom part. Rounded corners and edges enhance safety, while a slight inward angle on the top lid aids manufacturing convenience. The design used for the final concept carried over the same MAF sensor holder as the current air filter box since the same MAF sensor will be used. Furthermore, the connection between the air filter box and duct bellow is also the same as the existing air filter box. A hole was included for the proper placement of the

air filter. In summary, the recommended final concept is a rectangular air filter box with a flat-shaped filter that fulfils all requirements.

7.2 Future work

As stated in delimitations, Section 1.4, and in the design FMEA, Section 5.7, physical testing was out of scope for the thesis. This is a critical part of the development of a product, which makes it important to include it in future work. The test could be made in a flow rig to test the air filter box, duct bellow and that the connections do not leak. Other requirements that need to be tested in a flow rig are pressure drop and flow over the MAF sensor, UI from the CFD simulations.

Future work could also consist of the design of an air filter. Firstly, data from previous DHC tests would be needed to be able to design an air filter with knowledge about the service life. Secondly, a design for pleat height, pleat width etc. could be developed and tested to verify that the requirements are fulfilled. The information from the literature study could be used to help design the air filter.

Future work could also include tests to assess the strength of the air filter box in terms of force and NVH. These tests could involve both simulations and physical testing. This could be made to verify that the air filter box and duct bellow can handle the vibrations from the engine and absorb enough noise and vibrations. These tests/simulations could include a test of how the bellow placement on the duct bellow affects the absorption of vibrations.

The filter box needs some adjustments before it could be produced, presented in Section 5.14.1. These are the radius of the inlet and outlet. It could be beneficial to incorporate separate parts that could include a radius. This is an important factor to be able to fulfill the requirements for pressure drop and UI over the MAF sensor. Finally, the dirty side duct was out of scope for the thesis. Therefore, it needs to be designed in the future. The design needs to be custom made for the placement of the engine in the vehicle.

References

[1] Mann-hummel. (2021). Air cleaners for passenger cars. Mann-hummel.com. https://oem.mann-hummel.com/en/oem-products/air-cleaners/car-air-cleaners.html

[2] Utkarsh Choudhary, Shubham Shinde, Rajat Gupta & Hemant Deore. (2016). Design and Analysis of Snorkel Intake System for an LCV. Researchgate.net. https://www.researchgate.net/publication/303246716_Design_and_Analysis_of_Snorkel_Intake_System_for_an_LCV

[3] Richard van Basshuysen and Fred Schäfer, R. (2016). Internal combustion engine handbook, 2nd English edition. https://www.sae.org/publications/books/content/r-434/

[4] Dziubak, T., & Boruta, G. (2021). Experimental and theoretical research on pressure drop changes in a two-stage air filter used in tracked vehicle engine. Separations, 8(6), 71. https://doi.org/10.3390/separations8060071

[5] Karthikayan, S., Raju, B. N., Sankaranarayanan, G., & Purushothaman, M. (2010). Study of air intake system of turbo charged diesel engines. Frontiers in Automobile and Mechanical Engineering -2010, 175–178.

[6] Vaidya, V. & Hujare, P. P. (2014)., Optimization of sound pressure level of air intake system by using GT-Power. Psu.edu. Retrieved January 31, 2023, from https://citeseerx.ist.psu.edu/document?repid=rep1&type=pdf&doi=0a819884b3bffb8e8a5af51c9fdfc8d711e5deec

[7] Industrial Quick Search. (2023). Mass Flow Meter: What is it? How It Works, Types, Accuracy. Iqsdirectory.com. https://www.iqsdirectory.com/articles/flow-meter/mass-flow-meter.html

[8] Cummins. (2023). HOW A TURBOCHARGER WORKS. Cummins.com. https://www.cummins.com/components/turbo-technologies/turbochargers/how-a-turbocharger-works

[9] A2MAC1. (2023). A2MAC1.

[10] Snyder, H. (2019). Literature review as a research methodology: An overview and guidelines. Journal of Business Research, 104, 333–339. https://doi.org/10.1016/j.jbusres.2019.07.039

[11] Ulrich, K. & Eppinger, S. 2012 Product design and development [5:th ed]. New York: McGraw-Hill.

[12] How to use benchmarking to improve your product? (2022, July 5). Infinitia Industrial Consulting. https://www.infinitiaresearch.com/en/sin-categoria-en/how-to-use-benchmarking-to-improve-your-product/

[13] Lucienne T.M. Blessing, Amaresh Chakrabarti. (2009). DRM, a Design Research Methodology. Springer London. https://doi-org.proxy.lib.chalmers.se/10.1007/978-1-84882-587-1

[14] Robertson, S., & Robertson, J. (2012). Mastering the Requirements Process. Edu.My. http://www.pkt.edu.my/pdf_sys/home/pdf/145

[15] Fakhravar, H. (2020). Application of Failure Modes and Effects Analysis in the Engineering Design Process, 1-7.

[16] Leigh Thompson, & Leo F. Brajkovich. (2003). Improving the creativity of organizational work groups [and executive commentary]. The Academy of Management Executive, 17(1), 96–111. http://www.jstor.org/stable/4165931

[17] Johannesson, H., Persson, J.-G., & Pettersson, D. (2013). Produktutveckling effektiva metoder för konstruktion och design. Stockholm: Liber.

[18] Dassault Systèmes. (2019). Catia V5.

[19] Howard H. Hu (2012) Fluid Mechanics (Fifth Edition), Academic Press, Pages 421-472, https://doi.org/10.1016/B978-0-12-382100-3.10010-1.

[20] ANSYS. (2022). Ansys Discovery.

[21] Cho, H. S. A. (2021). Flow characteristics and noise reduction effects of air cleaners of automobile intake systems with built-in resonators with space efficiency.

[22] Donaldson. (2023). Filter performance & energy savings. Donaldson Filtration Solutions. https://www.donaldson.com/en-us/compressed-air-process/technical-articles/ensuring-effective-filtration-performance-energy-savings/

[23] Iqsdirectory. (2023). Air Filters. Iqsdirectory.com. https://www.iqsdirectory.com/articles/air-filter.html

[24] Dziubak, T & Karczewski, M. (2022). Experimental Study of the Effect of Air Filter Pressure Drop on Internal Combustion Engine Performance. Energies 2022, 15, 3285. https://doi.org/10.3390/en15093285

[25] Filters, A. (2019). Heavy Facts. Volvotrucks.In. https://www.volvotrucks.in/content/dam/volvo-trucks/markets/india/services/sales-tool/heavy-facts-air-filters.pdf

[26] Birkland, C. (2014, October 14). Clearing the (engine) air: Getting the most of your engine air filters. Fleetequipmentmag.com; Fleet Equipment Magazine. https://www.fleetequipmentmag.com/clearing-engine-air/

[27] Toma, M., & Fileru, I. (2015). Research on the Air Filters' Maintenance for Diesel Engines. Researchgate.net. https://www.researchgate.net/publication/295084393_Research_on_the_Air_Filters'_Maintenance_for_Diesel_Engines

[28] Toma, M., Stan, C., & Fileru, I. (2018). The restriction produced by the air filtration system versus the restriction produced by the air filter. Matec-conferences.org. https://www.matecconferences.org/articles/matecconf/pdf/2018/37/matecconf_imanee2018_09002.pdf

[29] Pall Corporation. (2021). Mechanisms of Air and Gas Filtration. Mechanisms of Air and Gas Filtration.

[30] Karandish, M. (2020). Hydraulics and Filtration. Ladanq.com. https://ladanq.com/en/wp-content/uploads/sites/2/2022/01/hydraulics-filtration_EN.pdf

[31] FSutherland, K., & Chase, G. (2008). Filters and Filtration Handbook (5th ed.). Elsevier Science.

[32] Kyle. (2019). Types of air filters for cars. COBB Tuning. https://www.cobbtuning.com/types-of-air-filters-for-cars/

[33] Light, F., & Heavy Dust Conditions. (2022). Engine Air Filtration. Donaldson.com. https://www.donaldson.com/content/dam/donaldson/engine-hydraulics-bulk/catalogs/air-intake/north-america/F110027-ENG/Air-Intake-Systems-Product-Guide.pdf

[34] Karande, V. D., & Dharmarao, S. S. (2018). Selection of air filter for automobile engines. Iosrjournals.org. https://www.iosrjournals.org/iosr-jmce/papers/NCRIME-2018/Volume-2/4.%2023-26.pdf

[35] Dziubak, T. (2018). Performance characteristics of air intake pleated panel filters for internal combustion engines in a two-stage configuration. Aerosol Science and Technology: The Journal of the American Association for Aerosol Research, 52(11), 1293–1307. https://doi.org/10.1080/02786826.2018.1512744

[36] Pleated vs. Non-pleated air filters: Which are best? (n.d.). Filterking.com. Retrieved February 16, 2023, from https://filterking.com/hvac-filters/pleated-air-filters-vs-non-pleated

[37] Wikipedia contributors. (2023, March 17). HEPA. Wikipedia, The Free Encyclopedia. https://en.wikipedia.org/w/index.php?title=HEPAoldid=1145154142

[38] PremiumGuard. (2018, May 8). Three types of engine air filters. Premium Guard Filters -; Premium Guard Filters. https://www.pgfilters.com/air-filters/three-types-engine-air-filters/

[39] Allam, S., & Elsaid, A. M. (2020). Parametric study on vehicle fuel economy and optimization criteria of the pleated air filter designs to improve the performance of an I.C diesel engine: Experimental and CFD approaches. Separation and Purification Technology, 241(116680), 116680. https://doi.org/10.1016/j.seppur.2020.116680

[40] Teng, G., Shi, G., & Zhu, J. (2022). Influence of pleated geometry on the pressure drop of filters during dust loading process: experimental and modelling study. Scientific Reports, 12(1), 20331. https://doi.org/10.1038/s41598-022-24838-7

[41] Kang, J.-H., & Ih, J.-G (2018). Acoustical characteristics of the air filter in the engine intake air cleaner. International Journal of Automotive Technology, 19(6), 981–991. https://doi.org/10.1007/s12239-018-0095-z

[42] Jung, H., Jin, J., Park, J.M., Jin, Y.S.(S.) et al. (2019). "A Study on NVH Performance Improvement of TPE Air Intake Hose Based on Optimization of Design and Material," SAE Technical Paper 2019-01-1491. https://saemobilus-sae-org.proxy.lib.chalmers.se/content/2019-01-1491/. doi:10.4271/2019-01-1491.

[43] Hoseop Song, Haengmuk Cho and Byungmo Yang. (2018). "Air Flow Characteristics For The Geometry Modification of Bellows Pipe On Intake System of Automobile," International Journal of Mechanical Engineering and Technology. pp. 1064-1071. http://iaeme.com/Home/issue/IJMET?Volume=9&Issue=5

[44] Song, X.; Cao, F.; Rao, W.; Huang, P. (2022). Simulation Optimization of an Industrial Heavy-Duty Truck Based on Fluid–Structure Coupling. Sustainability 2022, 14, 14519. https://doi.org/10.3390/su142114519

[45] Dziubak, T., Bąkała, L., Karczewski, M., & Tomaszewski, M. (2020). Numerical research on vortex tube separator for special vehicle engine inlet air filter. Separation and Purification Technology, 237. https://doi.org/10.1016/j.seppur.2019.116463

[46] Saleh, A. M., Tafreshi, H. V., & Pourdeyhimi, B. (2015). Service life of circular pleated filters vs. that of their flat counterpart. Separation and Purification Technology, 156, 881–888. https://doi.org/10.1016/j.seppur.2015.09.041

[47] Ajay Kumar Maddineni, Dipayan Das, Ravi Mohan Damodaran. (2019). Numerical investigation of pressure and flow characteristics of pleated air filter system for automotive engine intake application. eparation and Purification Technology, Volume 212, 2019, Pages 126-134. https://doi.org/10.1016/j.seppur.2018.11.014

[48] Rieger, M.; Hettkamp, P.; Lhl, T.; Madeira, P. (2019). Efficient Engine Air Filter for Tight Installation Spaces. ATZ Heavy Duty Worldwide 2019, 12, 56–59. https://doi.org/10.1007/s41321-019-0023-9

[49] Bensch, L. (2007). Designing the “Perfect” Filter - Revolutionary New Pleat Shape Optimizes Filter Performance. Pall Corporation.
[50] (N.d.). Edu.My. Retrieved May 31, 2023, from http://umpir.ump.edu.my/id/eprint/3446/1/cd6247_111.pdf
[51] Mann-Hummel (2023). MANN+HUMMEL Air Cleaners, 156. https://oem.mann-hummel.com/en/oem-products/air-cleaners/iqoron-series.html

Appendix

A

Interviews

Questions to "Expert 1"

- **What should be considered when it comes to the volume of the air filter box?** According to "Expert 1", the volume of the air filter box depends on the noise level, gets an even flow over the air filter and is able to remove snow without the air filter getting wet. An air filter box with a larger volume could cancel out some of the noise, which could result in more or fewer resonators needed. The air should go into the air filter box on the bottom half due to protect the air filter from water and snow. The lid of the air filter box should have a big volume to get an even flow.

- **How should you place the dirty side duct?** To reduce the amount of water that gets in the air filter box, the dirty side duct should be placed as high as possible. There is also more dust close to the ground.

- **Why does Volvo have a flat filter instead of for example cylindrical filter boxes?** The cylindrical filters are usually more effective but also more expensive. It is mostly dependent on what space you working with.

- **How do you secure that the air filter box does not leak?** For our design, there are six screws, and for our flat filter, it should not be fewer.

- **The inlet into the air filter box has a "funnel" shape, why is that?** This shape is to get better airflow and lower pressure drop.

- **Why do you place the MAF sensor so close to the outlet of the air filter?** Some tests have been made and it shows that the distance does not matter too much. However, the placement in the duct, how central the duct is placed, is important.

- **What requirements exist for the drainage of water and snow?** You should be able to drive in the rain without the water getting to the "clean side". The requirement for water drainage is XXXX. The snow accumulation rate must be lower than XXXX per liter filter box area on the "dirty side".

- **What dust holding capacity do you have in today's air filter?** In today's air filter, the maximum dust holding is XXX and we use a dust called SAE fine to verify the dust holding capacity and service life.

Questions to "Supplier 1"

- **What determines the size of the air filter?** It is the dust holding capacity and the airflow requirements.

- **How can you increase the service life of the air filter?** One possibility is to use a pre filter which uses a cyclone principle to remove the majority of dust before the actual air filter.

- **On cylindrical filters, does the air flow always go from the outside of the cylinder to the inside or could it go in the opposite direction?** It could go both directions, however, the outside of the air filter has a greater area which implies that it is more common. It depends on the space where the air filter box is placed but the dust holding capacity is lower with around 15%.

- **How can you estimate dust holding capacity without testing?** "Supplier 1" is using test data from the previous test there they measure when maximum pressure drop is reached. For those tests the filter is weighed before the test starts and when the test is finished to compare the weight and find the dust holding capacity.

- **What is the dust concentration in different environments?** The different environments are presented in a "Supplier 1" catalogue and shown in Table A.1

Table A.1: Dust concentrations in different environments. [51]

Mean dust concentration in	$[mg/m^3]$
Trucks in normal European road traffic	0.6
Trucks in road traffic outside Europe	3
Off-highway trucks (concentration site use)	8
Construction machines (front-end loaders, track vehicles, mobile compressors)	35
Agricultural machines in central Europe (agriculture without periods of drought)	5
Agricultural machines in areas outside Europe in single operation	15
Agricultural machines used in fleets	50
Quick-moving track vehicles	100

- **The filtering efficiency is lower in the beginning, can you do something to increase that?** In some applications, mostly trucks, do we use nanofiber above the cellulose filter (the usual pleated filter). This increases the efficiency of the filter, making it more waterproof and flameproof.

B

Function-means tree

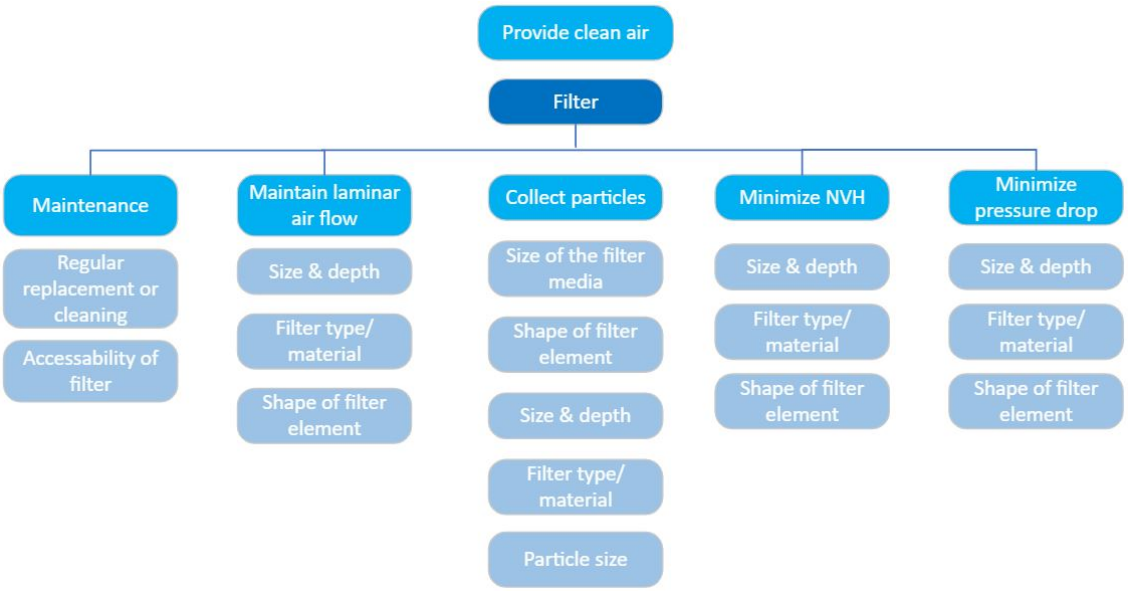

Figure B.1: Function analysis for the air filter.

Figure B.2: Function analysis for the air filter box.

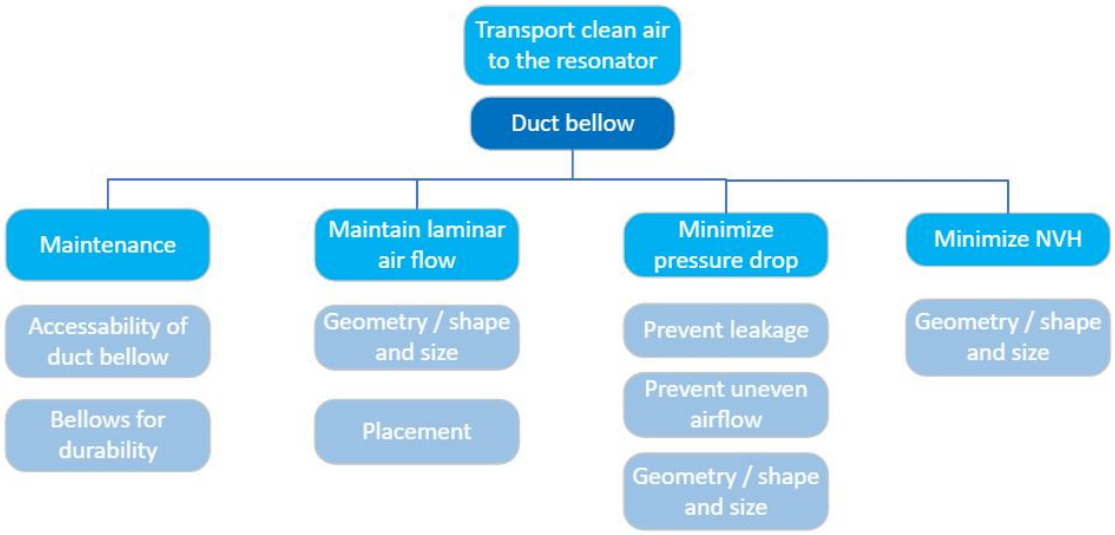

Figure B.3: Function analysis for the duct bellow.

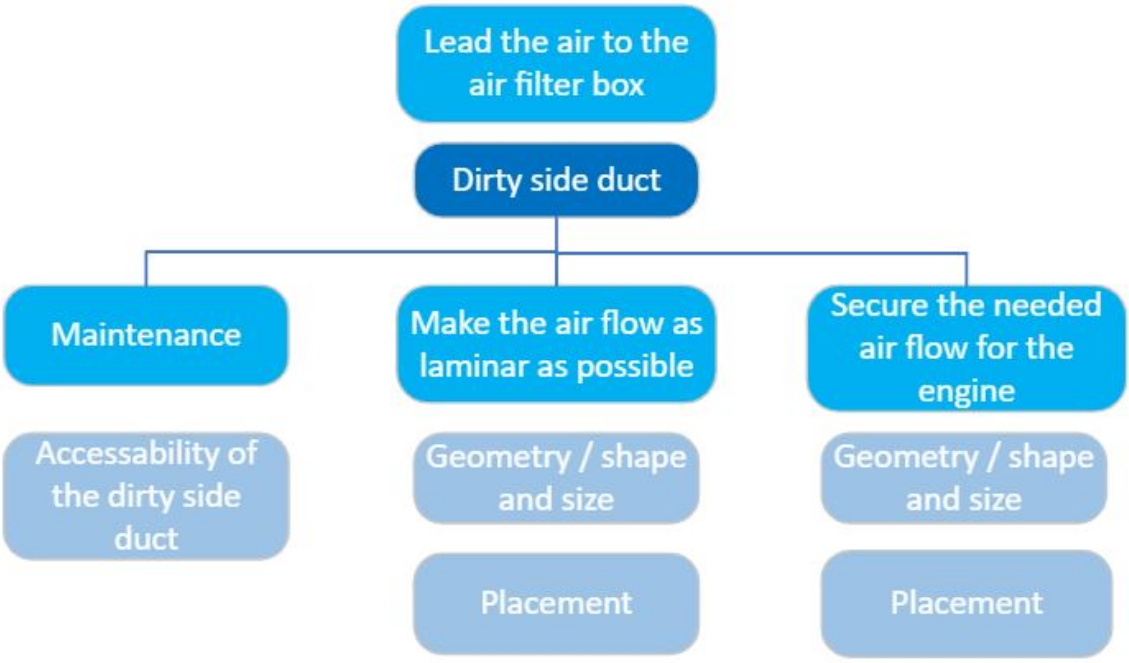

Figure B.4: Function analysis for the dirty side duct.

C

Scale for FMEA

Table C.1: Scale of Severity, Occurrence, and Detection for FMEA.

SEVERITY			OCCURRENCE				DETECTION			
Effect	**Criteria: Severity of Effect on Product (Customer Effect)**	**Rank**	**Likelihood of Failure**	**Criteria: Occurrence of cause Design life/reliability of item/vehicle**	**Criteria: Occurrence of Cause – DFMEA (Incidents per item/vehicle)**	**Rank**	**Opportunity for Detection**	**Criteria: Likelihood of Detection by Design Control**	**Rank**	**Likelihood of Detection**
-2*Failure to Meet Safety and/ or Regulatory Requirements	Potential failure mode affects safe vehicle operation and/or involves noncompliance with government regulation without warning.	10	Very High	New technology/new design with no history.	100 per thousand 1 in 10	10	No detection opportunity	No current design control; Cannot detect or is not analyzed	10	Almost Impossible
	Potential failure mode affects safe vehicle operation and/or involves noncompliance with government regulation with warning.	9	-3*High	Failure is inevitable with new design, new application, or change in duty cycle/operating conditions.	50 per thousand 1 in 20	9	Not likely to detect at any stage	Design analysis/detection controls have a weak detection capability; Virtual Analysis (e.g., CAE, FEA, etc.) is not correlated to expected actual operation conditions.	9	Very Remote
-2*Loss or Degradation of Primary Function	Loss of primary function (vehicle inoperable, does not affect safe vehicle operation).	8		Failure is likely with new design, new application, or change in duty cycle/operating conditions.	20 per thousand 1 in 50	8	-3*Post Design Freeze and prior to launch	Product verification/validation after design freeze and prior to launch with pass/fail testing (Subsystem or system testing with acceptance criteria such as ride and handling, shipping evaluation, etc.).	8	Remote
	Degradation of primary function (vehicle operable, but at reduced level of performance).	7		Failure is uncertain with new design, new application, or change in duty cycle/operating conditions.	10 per thousand 1 in 100	7		Product verification/validation after design freeze and prior to launch with test to failure testing (Subsystem or system testing until failure occurs, testing of system interactions, etc.).	7	Very Low
-2*Loss or Degradation of Secondary Function	Loss of secondary function (vehicle operable, but comfort / convenience functions inoperable).	6		Frequent failures associated with similar designs or in design simulation and testing.	2 per thousand 1 in 500	6		Product verification/validation after design freeze and prior to launch with degradation testing (Subsystem or system testing after durability test, e.g., function check).	6	Low
	Degradation of secondary function (vehicle operable, but comfort / convenience functions at reduced level of performance).	5		Occasional failures associated with similar designs or in design simulation and testing.	.5 per thousand 1 in 2,000	5	-3*Prior to Design Freeze	Product validation (reliability testing, development validation tests) prior to design freeze using pass/fail testing (e.g., acceptance criteria for performance, function checks, etc.).	5	Moderate
-3*Annoyance	Appearance or Audible Noise, vehicle operable, item does not conform and noticed by most customers (>75%).	4	-3*Moderate	Isolated failures associated with similar designs or in design simulation and testing.	.1 per thousand 1 in 10,000	4		Product validation (reliability testing, development validation tests) prior to design freeze using test to failure (e.g., until leaks, yields, cracks, etc.).	4	Moderately High
	Appearance or Audible Noise, vehicle operable, item does not conform and noticed by many customers (50%).	3	-2*Low	Only isolated failures associated with almost identical design or in design simulation and testing.	.01 per thousand 1 in 100,000	3		Product validation (reliability testing, development validation tests) prior to design freeze using degradation testing (e.g., data trends, before/after values, etc.).	3	High
	Appearance or Audible Noise, vehicle operable, item does not conform and noticed by discriminating customers (<25%).	2		No observed failures associated with almost identical design or in design simulation and testing.	.001 per thousand 1 in 1,000,000	2	Virtual Analysis – Correlated	Design analysis/detection controls have a strong detection capability. Virtual analysis (e.g., CAE, FEA, etc.) is highly correlated with actual or expected operating conditions prior to design freeze.	2	Very High
No effect	No discernible effect	1	Very Low	Failure is eliminated through preventive control.	Failure is eliminated through preventive control.	1	Detection not applicable; Failure Prevention	Failure cause or failure mode can not occur because it is fully prevented through design solutions (e.g., proven design standards, best practice or common material, etc.).	1	Almost Certain

DEPARTMENT OF INDUSTRIAL AND MATERIALS SCIENCE
CHALMERS UNIVERSITY OF TECHNOLOGY
Gothenburg, Sweden
www.chalmers.se

CHALMERS
UNIVERSITY OF TECHNOLOGY